Stimulus-responsive hydrogels: Theory, modern advances, and applications

Michael C. Koetting[a,d,1], **Jonathan T. Peters**[a,d,2], **Stephanie D. Steichen**[b,d,3], and **Nicholas A. Peppas**[a,b,c,d,*]

[a]McKetta Department of Chemical Engineering, The University of Texas at Austin, Austin, TX 78712, United States

[b]Department of Biomedical Engineering, The University of Texas at Austin, Austin, TX 78712, United States

[c]College of Pharmacy, The University of Texas at Austin, Austin, TX 78712, United States

[d]Institute for Biomaterials, Drug Delivery, and Regenerative Medicine, The University of Texas at Austin, Austin, TX 78712, United States

Abstract

Over the past century, hydrogels have emerged as effective materials for an immense variety of applications. The unique network structure of hydrogels enables very high levels of hydrophilicity and biocompatibility, while at the same time exhibiting the soft physical properties associated with living tissue, making them ideal biomaterials. Stimulus-responsive hydrogels have been especially impactful, allowing for unprecedented levels of control over material properties in response to external cues. This enhanced control has enabled groundbreaking advances in healthcare, allowing for more effective treatment of a vast array of diseases and improved approaches for tissue engineering and wound healing. In this extensive review, we identify and discuss the multitude of response modalities that have been developed, including temperature, pH, chemical, light, electro, and shear-sensitive hydrogels. We discuss the theoretical analysis of hydrogel properties and the mechanisms used to create these responses, highlighting both the pioneering and most recent work in all of these fields. Finally, we review the many current and proposed applications of these hydrogels in medicine and industry.

Keywords

Hydrogels; Polymers; Stimulus-responsive; Smart materials; Swelling; Drug delivery; pH responsive; Temperature responsive; Chemically-responsive; Molecularly imprinted polymers; Photo-responsive; Electrically-responsive; Shear stress; Scaffolds; Tissue engineering; Biosensors

[*]Corresponding author at: Department of Biomedical Engineering, The University of Texas at Austin, 107W Dean Keeton Street, Stop C0800, Austin, TX 78712, United States. Tel.: +1 512 471 6644; fax: +1 512 471 8227.
[1]Tel.: +1 512 471 6910.
[2]Tel.: +1 512 471 4757.
[3]Tel.: +1 512 472 5681.

Hydrogels are three dimensional network structures consisting of polymeric chains joined by tie points or joints and swollen in water up to thermodynamic equilibrium. This is a simple and quite accurate definition of these materials, which have become so popular in numerous applications over the past 50 years. While this general definition has been used to present and analyze swollen crosslinked hydrogels, especially as defined in our 1986–1987 books on "Hydrogels in Medicine and Pharmacy," there have been variations of this basic definition and deviations from the basic thermodynamic and structural equations that define their performance.

While Paul Flory set the basic theories for hydrogel analysis, it is interesting to note that hydrogels had been prepared long before his original theoretical treatments were established. Indeed, early work on crosslinked polymers and networks first appeared in German literature in the mid-1930s. Meanwhile significant work on the behavior of "natural hydrocolloids" appeared in the late 1930s, but without structural insight. In addition, work in that period and in the 1940s concentrated mostly on reaction kinetics and mechanical properties of the ensuing networks.

PJ Flory (1944–1952; Nobel prize 1974) set the main framework of analysis of gels with his thermodynamic theories, statistical mechanical analysis, and the first analysis of critical miscibility characteristics of hydrogels. At the same time, pioneering work was also done in the Soviet Union (Kargin, 1945–1960, Ushakov, 1943–1953, Korshak 1952–1973), and in Japan (Sakurada, 1948–1965).

Hydrogels possess numerous properties that make them ideal candidates for use as biomaterials, finding significant use in the fields of drug delivery, tissue engineering, implants, and more. The main feature of hydrogels is their "soft" material nature, owing to their highly hydrophilic nature that encourages uptake of water, leading to hydrated yet solid materials, much like cells in the body. Their hydrophilic and crosslinked nature also imparts excellent biocompatibility, and many common hydrogels have found wide use both in laboratory studies and clinical uses. Some of the most commonly used hydrogels include synthetics like poly(ethylene glycol) (PEG), poly(vinyl alcohol) (PVA), or poly(2-hydroxyethyl methacrylate) (PHEMA), as well as naturally occurring hydrogels like agarose, alginate, chitosan, collagen, fibrin, and hyaluronan.

Hydrogels become especially useful when they are used as "smart" materials that can respond to changes in their environment. In this extensive review, we discuss multiple responsive modalities—including responses to pH, temperature, chemicals, light, electric fields, and shear stress—and discuss recent advances both in tailoring these responses and applying them. As the diverse work reviewed herein attests, responsive hydrogels are currently transforming our world by improving healthcare and finding novel benefits in industrial applications.

1. General hydrogel theory

1.1. Physical structure

Hydrogels are characterized by hydrophilic polymers that are crosslinked into an insoluble, but highly hydrophilic structure. As suggested by such a basic definition, hydrogels are a broad class of materials that can be prepared in many different ways and can exhibit significantly different behaviors. For instance, the crosslinks that form the hydrogel network may take on many forms, such as covalent chemical links, ionic bonds, weak physical entanglements, hydrogen bonds, or other dipolar interactions [1]. Chemical crosslinking can be achieved through many methods. For example, use of dimethacrylates as monomers in a chain polymerization leads to crosslinking as both methacrylate functionalities are incorporated into the polymer backbone at two different locations, leading to crosslinking. Glutaraldehyde, on the other hand, has been widely used as a post-polymerization reagent to promote crosslinking after the polymer chains have already been formed. Regardless of the strategy used, however, hydrogels take many forms, including copolymers, blends, or interpenetrating networks (IPNs). IPNs are often prepared by polymerization and crosslinking of one complete polymer network, followed by polymerization and crosslinking of a second in the presence of the first network. If the two polymerizations occur by significantly disparate methods, the network formation may be performed simultaneously.

In addition to the variety of crosslinking methods used, hydrogels may adopt significantly different final morphologies. Hydrogels may be amorphous, semiscrystalline, supramolecular, or colloidally aggregated [1]. The variance in morphology reflects the wide range of monomers that can comprise a hydrogel: monomers may be natural or synthetic; copolymers of both natural and synthetic components may be used; and the final characteristics are highly dependent on the ratios of monomers incorporated into the network and their spatial ordering. As such, the structure of hydrogels becomes strongly dependent on the synthesis procedures followed, solvent used, monomers and their ratios, and even the degradative and mechanical history of the polymer [2].

Depending on the monomers incorporated into the hydrogel and the conditions of the surrounding medium, hydrogels can exhibit a full range of charge properties, being neutral, cationic, anionic, or ampholytic. Much like other macromolecules, such as proteins or nucleic acids, hydrogels' network charge depends strongly on pH of the surrounding medium, as this determines the protonation status of the incorporated pendant groups. Most ionic gels exhibit some degree of charge in aqueous solvents. Carboxylic acid pendant groups are commonly used to impart anionic properties to a hydrogel, while amine pendant groups are commonly used for imparting cationic properties.

The physical structure of hydrogels can be characterized by standard mechanical testing methods. In addition to mechanical properties such as the Young's modulus (E), storage modulus (G'), and loss modulus (G'') [3], the hydrogel structure can be quantitatively modeled using several parameters: $v_{2,s}$ is the polymer volume fraction in the swollen state, which describes the hydrogel's hydration level; $\overline{M_C}$ is the average molecular weight between crosslinks, which describes the overall density of crosslinks in the hydrogel; and ξ is the mesh size of the hydrogel, which reflects the porosity of the gel (and is dependent on

the hydration level and the crosslinking density). These parameters can be used to model the behavior of both nonionic [4] and ionic [5] hydrogels through equilibrium swelling theory and rubber elasticity theory [6].

1.2. Equilibrium swelling theory and network characteristics

Flory–Rehner theory may be utilized for quantitative analysis of nonionic hydrogels [7]. Flory–Rehner theory posits that hydrogel equilibrium is attained through a balance of enthalpic mixing, which promotes swelling, and the elastic forces imposed by the crosslinked hydrogel chains, which promotes contraction. Using Gibbs free energy, the theory's basis may be stated as presented in Eq. (1).

$$\Delta G_{\text{total}} = \Delta G_{\text{elastic}} + \Delta G_{\text{mixing}} \quad (1)$$

Direct application of Flory–Rehner theory to ionic hydrogels is incorrect, as additional forces result from ionic interactions within the hydrogel and with the surrounding medium that shift the hydrogel's swelling equilibrium. This additional contribution is incorporated in an additional term, G_{ionic}, as shown in Eq. (2).

$$\Delta G_{\text{total}} = \Delta G_{\text{elastic}} + \Delta G_{\text{mixing}} + \Delta G_{\text{ionic}} \quad (2)$$

Beyond simply resulting in additional energy terms, ionic properties in the hydrogel also complicate analysis through the mixing term, G_{mixing}. The mixing term describes the thermodynamic interactions occurring between the polymer and the solvent, and is typically expressed through use of an empirical polymer–solvent interaction parameter, χ_1. However, this parameter is explicitly defined for nonionic systems, and use with ionic systems yields approximate results, with potential for error of 30–40% from the correct values.

Application of Eq. (1) to nonionic hydrogel systems prepared in the absence of solvent yields an expression for determining the average molecular weight between crosslinks, $\overline{M_C}$, as shown in Eq. (3). Theoretical treatment of hydrogels prepared in solvent required additional modification by Peppas and Merrill that considered modifications to the elastic potential caused by interaction with the solvent, leading to the expression shown in Eq. (4) [4].

$$\frac{1}{\overline{M_C}} = \frac{2}{\overline{M_N}} - \frac{(\overline{v}/V_1)[\ln(1 - v_{2,s}) + v_{2,s} + \chi_1 v_{2,s}^2]}{[v_{2,s}^{1/3} - (v_{2,s}/2)]} \quad (3)$$

$$\frac{1}{\overline{M_C}} = \frac{2}{\overline{M_N}} - \frac{(\overline{v}/V_1)[\ln(1 - v_{2,s}) + v_{2,s} + \chi_1 v_{2,s}^2]}{v_{2,r}[(v_{2,s}/v_{2,r})^{1/3} - (v_{2,s}/2v_{2,r})]} \quad (4)$$

In these expressions, $\overline{M_N}$ represents the average molecular weight of polymer chains as formed without crosslinks, V_1 is the molar volume of the solvent, $\overline{v}$ is the specific volume of the polymer in the amorphous state, $v_{2,r}$ and $v_{2,s}$ represent the polymer volume fractions in the "relaxed" and "swollen" states, respectively, and χ_1 is the Flory polymer–solvent

interaction parameter. The "swollen" state refers to the equilibrium state of the polymer after exposure to the solvent. The "relaxed" state is the state of the polymer immediately following polymerization but before any swelling has occurred. In the event that the polymer is formed in the absence of solvent, no solvent is incorporated in the newly formed network, causing $\upsilon_{2,r}$ to a value of approximately 1, thus leading to equivalence between Eqs. (3) and (4).

It is also important to note that the term $\upsilon_{2,s}/2$ appearing in the preceding equations effectively incorporates the functionality of the crosslinks—the number of bonds monomers may make. A more rigorous treatment would replace $\upsilon_{2,s}/2$ with $2\upsilon_{2,s}/\varphi$, where φ is the functionality of the crosslinks, assumed to be 4 for most crosslinked networks. Thus, the forms of Eqs. (3) and (4) are only explicitly valid for tetrafunctional crosslinks. Therefore, in the case of mixed multifunctional crosslinks, this analysis is again approximate.

Hydrogel porosity is quantified through the mesh size parameter, ξ. Porosity is a very important characteristic of the hydrogel's structure, as it determines the ability of solute to diffuse through the hydrogel matrix at various conditions—a phenomenon that is widely exploited in the many hydrogels discussed in this review. The mesh size is a measure of the average linear distance between crosslinks, not a diameter or diagonal distance. The mesh size may be determined through either of two possible methods. One method is direct application of Eqs. (5) and (6), in which the term $\left(\overline{r_o^2}\right)^{1/2}$ corresponds to the root-mean-square end-to-end distance of the polymer chains between crosslinks, also termed the unperturbed distance. The term α is known as the extension ratio, which is determined from $\nu_{2,s}$ *via* Eq. (6).

$$\xi = \alpha \left(\overline{r_o^2}\right)^{1/2} \quad (5)$$

$$\alpha = \upsilon_{2,s}^{-1/3} \quad (6)$$

Because of the esoteric nature of the unperturbed distance, it is frequently calculated rather than known directly. The unperturbed distance may be calculated by Eq. (7),

$$\left(\overline{r_o^2}\right)^{1/2} = l \left(\frac{2 C_n \overline{M}_c}{M_r}\right)^{1/2} \quad (7)$$

in which l is the bond length along the polymer backbone (often 1.54 Å for vinyl polymers), C_n is the Flory characteristic ratio—defined as the ratio of the mean square unperturbed distance to the expected end-to-end distance for a freely jointed chain of the same length— which is tabulated for many polymers, $\overline{M}_c$ is again the average molecular weight between crosslinks (calculable using the Peppas–Merrill or Brannon-Peppas equation, as appropriate), and M_r is the molecular weight of the repeat units. Combining this with Eq. (5) leads to a more frequently useful calculation for the mesh size, as shown in Eq. (8) [8,9].

$$\xi = \upsilon_{2,s}^{-1/3} \left(\frac{2C_n \overline{M_C}}{M_r} \right)^{1/2} l \quad (8)$$

In order to accurately characterize the porosity of a hydrogel for use in biomedical applications through the mesh size, $\upsilon_{2,s}$ should be determined experimentally in the end-use solvent, as many parameters such as ionic strength of the solution, pH, and interactions with other molecules may significantly affect the swelling behavior of a hydrogel. Once experimentally deter-mined, quantification of the mesh size may proceed through application of the Peppas–Merrill or Brannon-Peppas expression, as appropriate, for determining $\overline{M_C}$, which is then applied in Eq. (8).

1.3. Dual responsive hydrogels

Interpenetrating polymer networks (IPNs) are composed of two or more polymers in a network and are formed when one polymer network is crosslinked in the presence of another previously crosslinked polymer network [10]. The benefit of IPNs, as compared to standalone polymer networks, is their ability to respond to a multitude of stimuli because each polymer network within the IPN can have a unique environmental responsiveness [11]. However, the modeling of the swelling behavior of these IPNs can be quite complex because of the two or more independent environmentally-sensitive networks involved. Zhang [12] has proposed a model based on three primary assumptions: homogeneous behavior, IPN interaction, and independent network behavior.

1.3.1. Homogeneous behavior assumption—In an IPN, the different polymer compositions and ratios can result in phase separation between the two polymers. Even though phase separation can be avoided by carefully tailoring the polymer composition, it is still an important consideration as any observed phase separating behavior can impact the swelling of the hydrogel networks. When swelling, some minor phase separation occurs in the skin layer of the swollen network; however, none is observed in the bulk. For this reason, during theoretical treatment of IPN swelling, it is assumed that the IPNs are homogeneous single-phase hydrogels. This assumption allows for the determination of the polymer–solvent interaction parameter.

1.3.2. IPN Interactions during the swelling process—The Gibbs total free energy change during the swelling process of a single polymer network under constant temperature and pressure is denoted as follows:

$$\Delta G_{\text{tot}} = \Delta G_{\text{mix}} + \Delta G_{\text{el}} \quad (9)$$

where G_{mix} is the free energy contributions due to mixing, and G_{el} is the free energy contribution due to the elastic retractile forces in the network.

Within an IPN, free energy change due to the swelling of both polymer networks must be considered. The total Gibbs free energy, therefore, has contributions from each polymer system within the IPN, G_2 and G_3. Each polymer network contribution can be broken

down further into both a mixing, G_{mix}, and elastic, G_{el}, contribution. Additional free energy interaction parameters include contributions from the solvent or swelling agent, G_1, and from the ionic interactions of ionizable polymeric networks, G_{ion}. Interestingly, because of the constraints of constant temperature when calculating Gibbs free energy, temperature-responsive networks do not require the inclusion of a separate interaction term. With all of these parameters, the total Gibbs free energy of an IPN can be written as

$$\Delta G_{\text{tot}} = \Delta G_{\text{mix},2} + \Delta G_{\text{mix},3} + \Delta G_{\text{el},2} + \Delta G_{\text{el},3} + \Delta G_{\text{ion}} \quad (10)$$

1.3.3. Independent network assumption—Assuming the networks are completely independent of one another, the Flory–Huggins equation for G_{mix} and the rubber elasticity equation for G_{el} are still acceptable to use for each network. Thus, the derivative of Eq. (10) with respect to the number of moles of swelling agent becomes

$$\begin{aligned} \mu_1 - \mu_1^o = & N\left(\frac{\partial \Delta G_{\text{mix},2}}{\partial n_1}\right)_{T,P} + N\left(\frac{\partial \Delta G_{\text{mix},3}}{\partial n_1}\right) \\ & + N\left(\frac{\partial \Delta G_{\text{el},2}}{\partial \alpha_2}\right)_{T,P}\left(\frac{\partial \alpha_2}{\partial n_1}\right)_{T,P} \\ & + N\left(\frac{\partial \Delta G_{\text{el},3}}{\partial \alpha_3}\right)_{T,P}\left(\frac{\partial \alpha_3}{\partial n_1}\right)_{T,P} + (\Delta \mu_1^*)_{\text{ion}} - (\Delta \mu_1)_{\text{ion}} \end{aligned} \quad (11)$$

There are additional parameters in this equation: N is Avogadro's number; n_1 is the total number of moles of solvent; and α_2 and α_3 are linear chain deformation factors. $(\Delta \mu_1^*)_{\text{ion}} - (\Delta \mu_1)_{\text{ion}}$ represents the difference in chemical potential inside and outside the gel, respectively, due to ionic contributions.

1.3.4. Model development—The final form of the mixing term for single component polymer networks can be determined from the Flory–Huggins theory:

$$\Delta \mu_{\text{mix}} = N\left(\frac{\partial \Delta G_{\text{mix}}}{\partial n_1}\right)_{T,P} = RT(\ln(1 - v) + v + \chi_1 v^2) \quad (11')$$

χ_1 denotes the polymer–solvent interaction parameter, and v is the polymer volume fraction. In an IPN, each polymer has its own volume fraction, denoted v_2 and v_3, and the solvent/swelling agent has a corresponding volume fraction, v_1. All three fractions must therefore be expressed as

$$v_1 + v_2 + v_3 = 1 \quad (12)$$

The individual polymer–solvent interaction parameter, χ, is difficult to obtain for each individual polymer in an IPN. Therefore, the total mixing term can be approximated by considering the two networks as one homogeneous network and including an average χ factor, $\bar{\chi}$. Thus, the total mixing term can be written as follows:

$$N\left(\frac{\partial \Delta G_{\text{mix}}}{\partial n_1}\right)_{T,P} \approx N\left(\frac{\partial \Delta G_{\text{mix},2}}{\partial n_1}\right)_{T,P} + N\left(\frac{\partial \Delta G_{\text{mix},3}}{\partial n_1}\right)_{T,P} \quad (13)$$

or,

$$N\left(\frac{\partial \Delta G_{\text{mix}}}{\partial n_1}\right)_{T,P} = RT[\ln[1-(v_2+v_3)]+(v_2+v_3)+\overline{\chi}(v_2+v_3)^2] = RT[\ln v_1+(1-v_1)+\overline{\chi}(1-v_1)^2] \quad (14)$$

Eq. (11) can be rewritten as follows by using Flory's rubber elasticity theory:

$$\mu_1-\mu_1^o = N\left(\frac{\partial G_{\text{mix}}}{\partial n_1}\right)_{T,P} + N\left(\frac{\partial \Delta G_{\text{el},2}}{\partial \alpha_2}\right)_{T,P}\left(\frac{\partial \alpha_2}{\partial n_1}\right)_{T,P} + N\left(\frac{\partial \Delta G_{\text{el},3}}{\partial \alpha_3}\right)_{T,P}\left(\frac{\partial \alpha_3}{\partial n_1}\right)_{T,P} + (\Delta\mu_1^*)_{\text{ion}} - (\Delta\mu_1)_{\text{ion}} \quad (15)$$

The free energy contributions from the elastic retractile forces of an isotropic network according to rubber elasticity theory are given by Eq. (16).

$$\Delta G_{\text{el},2} = \left(\frac{kTv_{e,2}}{2}\right)(3\alpha_2^2 - 3 - \ln\alpha_2^3) \quad (16)$$

where,

$$\alpha_2^3 = \frac{V}{V_0} = \frac{V_0 + (n_1\overline{v}_1/N) + (n_3\overline{v}_3/N)}{V_0} \quad (17)$$

In this expression, V_0 is the initial unswollen volume of the primary network, V is the total volume of the IPN when swollen, and $v_{e,2}$ is the effective number of chains within the network structure. Upon taking the derivative with respect to number of moles, we obtain Eq. (18):

$$N\left(\frac{\partial \Delta G_{\text{el},2}}{\partial \alpha_2}\right)_{T,P}\left(\frac{\partial \alpha_2}{\partial n_1}\right)_{T,P} = RT\overline{v}_1\left(\frac{v_{e,2}}{V_0}\right)\left(v_2^{1/3} - \frac{v_2}{2}\right) \quad (18)$$

The third term in Eq. (15) represents the contribution to the mixing equation of the second polymeric network in the IPN. It is the polymer that is polymerized in the presence of the first polymerized polymer. Therefore, it cannot be derived in the same way as Eq. (18). The assumption that the networks are elastically independent from one another, however, allows for the treatment of the primary network as a micromolecular diluent that is present during crosslinking of the secondary network. The change of configurational entropy during swelling can be expressed by Eq. (19):

$$\Delta S_{\text{el},3} = kv_e\left(\frac{1}{2}\ln\left(\frac{\alpha_3^3}{\alpha_3^{o3}}\right) - \frac{3}{2}\left[\left(\frac{\alpha_3}{\alpha_3^o}\right)^2 - 1\right]\right) \quad (19)$$

The superscript 0, here, refers to the unswollen IPN, and the corresponding linear deformation factor, α_3^o, is represented as

$$\alpha_3^o \equiv \left(\frac{1}{v_3^o}\right)^{1/3} = \left(\frac{V^o}{V^o - V_o}\right)^{1/3} \quad (20)$$

And the swollen IPN linear deformation factor, α_3, is defined as

$$\alpha_3 \equiv \left(\frac{1}{v_3}\right)^{1/3} = \left(\frac{V}{V^o - V_o}\right)^{1/3} = \left(\frac{V^o + (n_1 \overline{v}_1 / N)}{V^o - V_o}\right) \quad (21)$$

Thermodynamically, it is known that

$$\Delta G_{\text{el}} = T \Delta S_{\text{el},3} \quad (22)$$

Knowing this relationship and expressing $v_{e,3}$ as moles/cm^3, the following expression was derived:

$$N\left(\frac{\partial \Delta G_{\text{el},3}}{\partial \alpha_3}\right)_{T,P} \left(\frac{\partial \alpha_3}{\partial n_1}\right)_{T,P} = -N\left(\frac{\partial T \Delta S_{\text{el},3}}{\partial \alpha_3}\right)_{T,P} \left(\frac{\partial \alpha_3}{\partial n_1}\right)_{T,P} = \frac{RT v_{e,3} v_1}{(V^o - V_o)} \left(v_3^{o2.3} v_3^{1/3} - \frac{v_3}{2}\right) \quad (23)$$

An ionic interaction term has been expressed in terms of various ionic parameters:

$$(\Delta\mu_1^*)_{\text{ion}} - (\Delta\mu_1)_{\text{ion}} = \frac{\overline{v}_1 RT}{4 I M_r} \left(\frac{v_2 + v_3}{\overline{v}}\right)^2 \left(\frac{K_a}{10^{-\text{pH}} + K_a}\right)^2 \quad (24)$$

This expression, developed by Brannon-Peppas and Peppas, will be discussed in more detail later in this review. Briefly, M_r is the molecular weight of the repeat units of the polymer, I is the ionic strength of the solvent/swelling agent, V_1 is the molar volume of the solvent/swelling agent, $\overline{v}$ is the specific volume of the polymer, and the equilibrium constant of the ionizable network is K_a for anionic systems and K_b for cationic systems.

Substituting Eqs. (17), (23) and (24) into Eq. (10) yields

$$\begin{aligned}
\mu_1 - \mu_1^o = RT &\left[\ln[1 - (v_2 + v_3)] + (v_2 + v_3) + \overline{\chi}(v_2 + v_3)^2 \right. \\
&\left. + \left(\frac{\overline{v}_1 v_{e,3}}{V_0}\right)\left(\overline{v}_2^{1/3} - \frac{v_2}{2}\right) + \left(\frac{\overline{v}_1 v_{e,3}}{V^o - V_0}\right)\left(v_3^{o2.3} v_3^{1/3} - \frac{v_3}{2}\right)\right] \\
&+ \frac{\overline{v}_1 RT}{4 I M r}\left(\frac{v_2 + v_3}{\overline{v}}\right)^2 \left(\frac{K_a}{10^{-pH} + K_a}\right)^2
\end{aligned} \quad (25)$$

Eq. (25) describes the chemical potential difference between pure solvent and solvent in the swollen IPN. This is expressed in terms of the volume fractions of the primary, v_2, and secondary, v_3, polymer networks. The term v_e can be written as

$$v_e = \frac{V}{\overline{v} M_c}\left(1 - \frac{2M_c}{M}\right) \quad (26)$$

Substituting Eq. (26) into Eq. (25) yields an expression for overall chemical potential difference describing the swelling behavior of an IPN:

$$
\begin{aligned}
\mu_1 - \mu_1^o = RT &\left[\ln[1-(v_2+v_3)] + (v_2+v_3) + \overline{\chi}(v_2+v_3)^2 \right. \\
&+ \left(\frac{\overline{v}_1}{\overline{v}_2 M_{c,2}} \right) \left(1 - \frac{2M_{c,2}}{M_{n,2}} \right) \left(v_2^{1/3} \frac{v_2}{2} \right) \\
&\left. + \frac{\overline{v}_1}{v_2 M_{c,3}} \left(v_3^{o2.3} v_3^{1/3} - \frac{v_3}{2} \right) \right] \\
&+ \frac{\overline{v}_1 RT}{4IMr} \left(\frac{v_2+v_3}{\overline{v}} \right)^2 \left(\frac{K_a}{10^{-pH}+K_a} \right)^2
\end{aligned}
$$

(27)

In Eq. (27), the parameters $M_{c,2}$ and $M_{c,3}$ are the molecular weight between crosslinks in the primary and secondary networks. When solved, the expression gives insight into the swelling behavior of the IPN hydrogel network. Eq. (27) reduces to the equation for a single ionizable hydrogel network when there is no secondary network present (*i.e.*, $v_3 = 0$).

1.4. Mechanical behavior

The mechanical behavior of hydrogels is crucial in understanding the effect they will have in biomedical applications. Hydrogels have been known to exhibit a variety of physical behaviors, from elastic recovery to the time-dependent recovery associated with viscous behavior. These properties are largely dependent on the crosslinking nature and density, and can be manipulated for different applications. For example, tissue culture substrates often require stiffer hydrogels; whereas intravenously injected particles that exhibit lower stiffness demonstrate better bioavailability and improved circulation [13,14].

The viscoelasticity that is commonly associated with hydrogels used for biomedical applications comes from being used above the glass transition temperature (*Tg*). This viscoelastic behavior comes from the restricted rearrangement of polymer segments due to deformation. The *Tg* of hydrogels is often significantly depressed due to the plasticization caused by the presence of the solvent, meaning the *Tg* of the hydrogels used in biomedical applications is well below physiological temperature when hydrated. In this regime, stress-relaxation, creep, and dynamic loading are important to consider throughout the lifetime of the polymer [15].

Peppas and Merrill [16] modified Flory's original theories on polymer elasticity [17], to account for the presence of solvent in hydrogels. This work is summarized by Eq. (2). Here τ is the applied stress as a function of elongation, ρ is the polymer density, R is the universal gas constant, and T is absolute temperature. This allows for determination of the molecular weight between crosslinks, $\overline{M_C}$, by measuring the applied stress, τ. As with mesh size calculations, the swollen polymer volume fraction refers to the solution in which the gel is swollen.

$$\tau = \frac{\rho RT}{\overline{M}_C} \left(1 - \frac{2\overline{M}_C}{\overline{M}_N}\right) \left(\alpha - \frac{1}{\alpha^2}\right) \left(\frac{\upsilon_{2,s}}{\upsilon_{2,r}}\right)^{1/3} \quad (28)$$

Both equilibrium swelling and elasticity theory can also be applied to non-covalently crosslinked gels. These theories were developed based on the assumptions of tetrafunctional crosslinks and isotropic behavior. This is normally the case with covalent crosslinks. Hydrogels often have physical entanglements, hydrogen-bonded structures, or microcrystallites that have different behaviors.

Equilibrium swelling and elasticity theory have been modified for non-covalently crosslinked systems by treating junctions or entanglements as covalent crosslinks. Normally, the same equations apply, but $\overline{M}_C$ is replaced by either molecular weight between junctions $(\overline{M}_j)$ or entanglements $(\overline{M}_e)$ to indicate the gel is not covalently crosslinked. Applying these theories to semicrystalline networks is more difficult, and is only applicable as an approximation. This is because crystals are a larger size range; on the order of 10 nm, and violates the Gaussian distribution that is assumed in original Flory–Rehner, Peppas–Merrill, and Brannon-Peppas equations.

2. Solute transport in hydrogels

Solute transport in hydrogels is crucial to understand when utilizing them as drug carriers, particularly as many therapeutics have a narrow therapeutic range. In hydrogels, solute transport is governed by Fick's law, shown in vector form below [18]. In Eq. (29), c_i is the concentration of species i and D_{ig} is the diffusion coefficient, which is often a function of c_i. Hydrogels have significant impact on the diffusion of loaded therapeutics, even though they have high water content. Ende et al. examined the effect of various factors, including mesh size, pH, and temperature, and discovered that they all significantly alter solute transport [19]. They concluded that hydrogels could be tailored for the delivery of a specific solute. Brannon-Peppas and Peppas took this a step further by developing pH responsive hydrogels that exhibit near zero-order release [20].

$$\frac{\partial c_i}{\partial t} = \nabla \cdot \left(D_{ig}(c_i) \nabla c_i\right) \quad (29)$$

Renkin's early work into solute diffusion utilized one dimensional Fickian diffusion, Eq. (30), to examine the effects of solute diffusion [21].

$$\frac{\partial N_i}{\partial t} = -DA\frac{\partial c_i}{\partial x} \quad (30)$$

Here N_i/t is the diffusion rate for species i, D is the diffusion coefficient, A is the apparent area, and c_i/x is the concentration gradient across the membrane. In Renkin's experiments, the rate of diffusion of solutes through inert hydrogels was measured. His results were in close agreement with theory proposed by Pappenheimer [22]. This work demonstrated the impact of pore size on the solute transport thorough porous media.

The interactions between solute and polymer play a large role in biological systems. Charge and hydrophobic interactions can lead to partitioning of solutes in hydrogel systems. Gudeman and Peppas studied these effects in ionic systems of IPNs of poly(vinyl alcohol) and poly(acrylic acid). They varied the pH and ionic content of the hydrogel and tested the transport above and below the pK_a of acrylic acid, observing a decrease in the rate of solute transport [23]. They further confirmed that permeation is driven by size exclusion and restrictions on the Brownian motion of solutes through porous substrates [24]. They developed a one-dimensional diffusion-convective theory to define the systems, and even developed equations to account for the impact of the pore wall on solute-solvent drag.

Peppas and Reinhart developed free volume theory based model for a system of water, solute, and polymer [25]. This model predicted the dependence of the diffusion coefficient on solute hydrodynamic radius (r_s), mesh size, and degree of swelling, as well as other structural characteristics of the hydrogels.

$$\frac{D_{SM}}{D_{SW}} = k_1 \left(\frac{\overline{M_C} - \overline{M}_C^*}{\overline{M_N} - \overline{M}_C^*} \right) \exp \left(-\frac{k_2 r_s^2}{Q_M - 1} \right) \quad (31)$$

D_{SM} and D_{SW} are the diffusion coefficients of solutes in the hydrogel and water respectively. This ratio is the normalized diffusion coefficient. k_1 and k_2 are parameters of the polymer–water complex, M_C^* is the average critical molecular weight between crosslinks at which diffusion is precluded, and Q_M is the degree of swelling of the membrane. This theory assumes diffusion in highly swollen membranes. Characterization of the diffusion through amorphous PVA membranes validated this theory [26].

Prausnitz based a theory on the statistical distribution of network chains and used Monte Carlo simulations to develop a modified size exclusion theory [27]. However, this theory does not consider effects of pendant groups or ionic interactions. The intention was to provide a general understanding focusing on chains in free space to be built upon by others.

To describe the effect of ionic interactions, solute diffusion through PAA has been observed as a function of pH. Solute diffusion through PVA/PAA membranes has been demonstrated to be a function of ionic strength and pH of the solvent [23,28–31].

3. pH-responsive hydrogels

pH-responsive hydrogels are a subset of stimuli-responsive systems capable of responding to perturbations in the environmental pH. These responses range from pH-induced deswelling/swelling behavior [32]. Systems that can respond to a dynamic pH environment are of particular interest for biomedical applications as several locations in the body exhibit substantial pH changes during either normal function or as part of a disease state. These pH variations exist within sites such as the gastrointestinal tract [33,34], vagina [35], blood vessels, intracellular vesicles [36–38], inflamed tissue/wounds [39], and the extracellular tumor environment [40,41] which can trigger a pH response. The particular dynamic pH ranges are detailed in Table 1.

3.1. Polymer composition and swelling behavior

The pH responsive behavior of the hydrogel network is imparted by the presence of ionizable pendant groups in the polymer backbone [32]. When exposed to an aqueous solution of an appropriate pH and ionic strength, these pendant groups will ionize and result in the buildup of a fixed charge along the polymer. The generation of electrostatic repulsive forces results in the pH-dependent swelling and deswelling processes as the water is either absorbed or expelled from the hydrogel network [32,42,43].

Two different families of pH-responsive hydrogel exist that differ in their pendant group ionization and subsequent swelling behavior. Anionic hydrogel networks contain pendant groups that are ionized in solutions at a pH greater than their acid dissociation constant, or pK_a. Therefore, the hydrogel swells at $pH > pK_a$ because of the large osmotic pressure generated by the presence of the ions. Conversely, cationic pendant groups are ionized at a pH less than their pK_a and the corresponding hydrogel network is, therefore, swollen at $pH < pK_a$. These swelling behaviors are described in Fig. 1. The most common monomers used to introduce pH-responsive behavior include acrylic acid (AA), methacrylic acid (MAA), dimethylaminoethyl methacrylate (DMAEMA), diethylaminoethyl methacrylate (DEAEMA) and acrylamide (AAm) [44]. Table 2 shows the chemical structures of these common monomers as well as their anionic or cationic behavior.

Natural polymers such as albumin [45], gelatin [46], alginate [47,48], and chitosan [49] can also exhibit pH-responsive behavior. Specifically, proteins such as albumin and gelatin, when in a linear configuration, will form helices stabilized by hydrogen bonding at given pH and temperature conditions. These helices can then act as the crosslinks in the hydrogel network. The isoelectric point, pI, of the protein will then dictate the swelling behavior. When the pH of the solution is either lower or higher than the pI, the protein will accrue surface charge, which will result in electrostatic repulsion and swelling of the network [32]. Polysaccharides such as chitosan and alginate undergo physical crosslinking due to hydrophobic or charge interactions. Swelling occurs as a result of the ionization of groups along the polysaccharide chain resulting in the buildup of charge and subsequent electrostatic repulsion and swelling [50]. The benefit of natural pH-responsive polymers, as compared to their synthetic counterparts is their ability to degrade within the body over time, which is ideal for implanted materials or circulating drug delivery vehicles [51].

3.2. Swelling behavior and theoretical considerations

The swelling behavior of ionic hydrogels is governed by the properties of the polymer, the properties of the swelling medium, and the polymer–solvent interactions. The composition of the swelling medium dictates the pH and ionic strength of the solution, which is governed by the primary counterions in solution and their valency [32,52]. The hydrogel network, in turn, acts as a semipermeable membrane to those counterions. This localization of charge influences the osmotic balance between the hydrogel and external swelling solution and results in water imbibition. The ion exchange that causes this osmotic balance will obviously be impacted by the ionic interactions present in a charged gel, specifically, the ionizable groups and degree of ionization [53–55]. Therefore, the ionic contribution to the overall swelling must be considered and is represented by the ion osmotic swelling pressure, π_{ion}:

$$\pi_{\text{ion}} = RT \sum (C_i - C_i^*) \quad (32)$$

C_i and C_i^* are the counterion concentrations inside and outside the gel, respectively. R is the universal gas constant and T is the absolute temperature [55]. Additionally, the elasticity of the polymer network and its hydrophilicity/hydrophobicity will impacts affinity and ability to imbibe water [55,56]. The crosslinking density is another hydrogel property that has a significant influence on the overall swelling capability of the network as it impacts the extent to which the final hydrogel network can swell.

Brannon-Peppas and Peppas have modeled the overall swelling capacity of an ionic hydrogel network, which includes the dependencies of the swelling behavior on the ionic strength of the surrounding swelling agent and the ions within the gel [54,57]. The expression is a modification of the original Peppas–Merrill equation (Eq. (4)) including the contributions of the ionic moieties to the free energy and chemical potential. The results yield two separate but equivalent expressions for anionic and cationic hydrogels, Eqs. (33) and (34), respectively:

$$\frac{V_1}{4I} \left(\frac{v_{2,s}^2}{\overline{v}^2 M_r^2} \right) \left(\frac{10^{-pKa}}{10^{-pH} + 10^{-pKa}} \right)^2 = \left[\ln(1 - v_{2,s}) + v_{2,s} + \chi_1 v_{2,s}^2 \right] + \left(\frac{V_1}{\overline{v}\,\overline{M_c}} \right) \left(1 - \frac{2\overline{M_c}}{\overline{M_n}} \right) v_{2,r} \left[\left(\frac{v_{2,s}}{v_{2,r}} \right)^{1/3} - \left(\frac{v_{2,s}}{2v_{2,r}} \right) \right] \quad (33)$$

$$\frac{V_1}{4I} \left(\frac{v_{2,s}^2}{\overline{v}^2 M_r^2} \right) \left(\frac{10^{-pK_b}}{10^{-pH} + 10^{-pK_b}} \right)^2 = \left[\ln(1 - v_{2,s}) + v_{2,s} + \chi_1 v_{2,s}^2 \right] + \left(\frac{V_1}{\overline{v}\,\overline{M_c}} \right) \left(1 - \frac{2\overline{M_c}}{\overline{M_n}} \right) v_{2,r} \left[\left(\frac{v_{2,s}}{v_{2,r}} \right)^{1/3} - \left(\frac{v_{2,s}}{2v_{2,r}} \right) \right] \quad (34)$$

Using these equations to calculate the average molecular weight between crosslinks, $\overline{M_C}$, in addition to the previously described parameters, also requires the ionic strength, I, and the dissociation constants, K_a and K_b. M_r is the molecular weight of the repeating unit and $\overline{v}$ is the specific volume of the polymer. This complex expression, although somewhat cumbersome to use, provides important insight into the equilibrium structure and behavior of ionic hydrogel networks at the molecular and macromolecular level [57].

The kinetics of hydrogel swelling is largely determined by mass transfer limitations. Ionic gel swelling kinetics also rely on ion exchange, ion interactions, and Donnan equilibrium considerations [55,58]. The swelling behavior, both equilibrium and dynamic, is clearly dependent on the nature of the surrounding fluid. In the case of drug delivery applications, the swelling medium is biological fluid which has a wide variety of different ionic species and will, therefore, drastically impact not only the swelling behavior but also solute diffusion into and out of the polymer network [56,59,60]. Additionally, the ionic character of the solute/drug will also impact its diffusion into the hydrogel due to the interaction between two charged species. The ionic strength of the solution can shield the charge of the polymer network and decrease either the repulsion or attraction between the solute and the hydrogel, resulting in increased diffusion [61,62]. Therefore, the ionic character and other properties

of the solute, solvent, and network all function together to impact the overall swelling behavior of ionic hydrogels in complex fluids for biomedical applications.

3.3. pH responsive hydrogels for controlled drug delivery

pH-responsive hydrogel systems have been widely used for the controlled drug delivery of a variety of therapeutics ranging from proteins [63], to small molecule drugs [64], chemotherapeutics [65], and genetic material such as RNA and DNA [66]. These therapeutic molecules can be dissolved or encapsulated within the hydrogel network [54], such as in protein loaded hydrogels [67], or electrostatically bound to the charged hydrogel network, as in the case of genetic material [68]. The controlled drug release from these loaded hydrogels are triggered by a change in the surrounding pH, for example, the change in pH during the transit through the GI tract or intracellular trafficking pathways (Table 1) [69]. This pH-response can be tailored for delivery to specific sites around the body by careful and intentional selection of the monomer components. A brief overview of hydrogel formulations and corresponding applications will be provided.

3.3.1. Anionic hydrogel networks—Anionic hydrogel networks, as a reminder, remain collapsed at low pH due to the presence of physical interactions (*i.e.*, hydrogen bonding) that keep the network tightly complexed. Once the pH increases above the pK_a of the polymer, the complexes dissociate due to changes in the ionic character and the polymer swells due to a combination of electrostatic repulsion and water imbibition [44]. This swelling behavior is triggered by an increase in the pH of the surrounding environment, which is observed in systems such as the gastrointestinal tract and the vaginal canal during intercourse.

3.3.1.1. Oral delivery: Anionic hydrogel network swelling is triggered by the substantial pH change in the gastrointestinal tract, ranging from as low as pH 1.0 in the stomach to upwards of 8 in certain segments of the upper small intestine and colon [33,34]. During transit through the GI tract, the anionic hydrogel network remains collapsed when in the stomach, thereby protecting any delicate encapsulated therapeutic cargo from being denatured by the harsh pH conditions and digestive enzymes. Based upon the composition of the polymer network, swelling can be initiated either in the highly absorptive upper small intestine or further down the GI tract, in the colon.

The laboratory of Peppas et al. has focused substantial effort on developing anionic hydrogel networks for the oral delivery of therapeutic proteins to the upper small intestine. The primary network of interest is a copolymer consisting of methacrylic acid (MAA) polymer backbone and grafted poly(ethylene glycol) (PEG) chains. This network, henceforth designated as P(MAA-g-EG), obtains its pH-responsive behavior from the MAA, which has a pendant carboxylic acid that is protonated below its pK_a of 4.8 and deprotonates at pH > pK_a. When MAA is protonated it undergoes hydrogen bonding, or complexation, with the etheric oxygen of the PEG, which maintains the hydrogel in its collapsed configuration. The negative charge present on the pendant carboxylic acid after deprotonation participates in the electrostatic repulsion that initiates the swelling behavior, while the hydrophilic nature of PEG helps to increase the rate of water imbibition [70]. Upon swelling, the porous structure of the P(MAA-g-EG) expands resulting in a corresponding increase of the mesh size, ξ,

from 70 Å during collapse to ~210 Å when swollen [71]. John Klier et al. were the first to investigate the P(MAA-g-EG) complexation hydrogel for the oral delivery of protein therapeutics [72,73]. The swelling properties of this system were successfully tailored by modifying the ratio of hydrogen-bonding groups of MAA to hydrogen-bonding groups of PEG and the molecular weight of the PEG tether. Specifically, when the hydrogen bonding groups of MAA and PEG are equivalent and the molecular weight of the PEG tether is 1000 (corresponding to 23 repeat ethylene glycol units/hydrogen bonding sites), the P(MAA-g-EG) exhibited the highest degree of complexation at low pH and an improved swelling response at high pH [70,71].

The P(MAA-g-EG) systems have been optimized for the delivery of protein therapeutics to the upper small intestine, where the tight junctions of the intestinal epithelial layer are more conducive to the passive transport of bulkier macromolecules. This "absorp-tion window" can be rather narrow as most material passes through the upper small intestine within 2–4 h after exiting the stomach [74]. The incorporation of high molecular weight PEG tethers into the P(MAA-g-EG) network is of utmost importance, not just to allow for swelling, but also because of the mucoadhesive behavior of PEG. The tethers of PEG interact with the mucus lining of the upper small intestine, penetrating into the polysaccharide matrix of the mucus and engaging in physical entanglements and hydrogen bonding [75]. This behavior anchors the hydrogel particle at the intestinal wall where it can remain for longer periods of time to ensure complete diffusion of the therapeutic out of the matrix and also guarantees the close proximity of the therapeutic to the site of delivery for improved overall bioavailability [76,77]. Other mucoadhesive molecules have been incorporated into the P(MAA-g-EG) network including wheat germ agglutinin [78] and dextran (ongoing).

The P(MAA-g-EG) network has shown great promise for the oral delivery of insulin, in particular. Insulin is a small protein with a molecular weight of 5.8 kDa and a pI of 5.3. The insulin is loaded into the hydrogel network in a post-synthesis loading scheme by swelling the hydrogel network, crushed into microparticles and sieved into narrow size ranges (<75 μm, 75–150 μm, >150 μm), in a concentrated protein solution. The insulin was loaded into the hydrogel network at high efficiencies [79]. These insulin-loaded particles were introduced to the gastrointestinal tract of male Sprague-Dawley rats and the overall bioavailability of the insulin was measured by the protein concentration in the bloodstream after time. The insulin-loaded hydrogels were capable of introducing insulin into the bloodstream of these rats at a 4.6–7.2% bioavailability and the transported insulin was able to exert a hypoglycemic effect [79–81]. The insulin-loaded hydrogel carriers were also successful in mitigating the effects of food intake on glucose levels when orally administered three times per day with food [82].

P(MAA-g-EG) has also shown some success for the delivery of additional protein therapeutics, such as interferon-β [83] and calcitonin [83,84]. However, efforts in the lab have shifted toward the optimization of different complexation hydrogel networks for the oral delivery of a variety of protein therapeutics. One such example, developed by Carr et al., is P(MAA-co-NVP), a hydrogel network with a backbone composed of a copolymer of MAA and N-vinyl pyrrolidone (NVP) [85]. N-vinyl pyrrolidone is a highly hydrophilic monomer that can be readily polymerized into the backbone of the hydrogel network and

possesses desirable properties such as mucoadhesion, minimal toxicity, hydrogen bonding groups, and a neutral charge. P(MAA-co-NVP) exhibits the appropriate anionic swelling behavior needed for oral delivery, in fact, remaining more tightly collapsed at low pH than its P(MAA-g-EG) counterpart. High insulin loading efficiencies were observed and the release profile (shown in Fig. 2) shows no insulin release at low pH and complete insulin release within 10 min after exposure to neutral pH [86]. Also promising is the fact that the P(MAA-co-NVP) hydrogel microparticles appear to have no cytotoxic effect on two model cell lines, Caco-2 colon adenocarcinoma cells and HT29-MTX mucus-secreting goblet cells [86].

The hydrogel network was also tested for its ability to load proteins of different isoelectric points and higher molecular weights, such as calcitonin and growth hormone, respectively. While P(MAA-co-NVP) was quite successful in the loading and release of the higher molecular weight growth hormone (MW ~ 22 kDa), even performing better than P(MAA-g-EG), the calcitonin did not mirror that behavior [87]. High isoelectric point proteins, when compared to lower isoelectric point proteins, are positively charged at neutral pH. Therefore, at neutral pH, or the pH during release, the negatively charged hydrogel network and positively charged protein have favorable ionic interactions that limit or completely inhibit release from the network. Koetting et al. has focused on developing alternative anionic hydrogel networks composed of itaconic acid (IA) and NVP copolymer specifically for the treatment and delivery of high isoelectric point proteins [62].

The optimization of P(MAA-g-EG) and other complexation hydrogel networks for the specific therapeutic of interest is incredibly important. Minor variations in the size, isoelectric point, and hydrophobic/hydrophilic composition will drastically affect the loading efficiencies, release kinetics, and overall value of the hydrogel system. Many therapeutic molecules, particularly those used to treat cancer, are incredibly hydrophobic in nature and do not partition well into the very polar, hydrophilic environment within the hydrogel matrix [65]. However, the oral delivery of chemotherapeutic agents, particularly for cases of cancers within the gastrointestinal tract, would be particularly desirable as it has the potential to limit the off-target effects of chemotherapeutics [37,65]. Schoener et al. synthesized hydrophilic P(MAA-g-EG) hydrogels with embedded hydrophobic nanoparticles composed of poly(methyl methacrylate) (PMMA). The hydrophobic chemotherapeutic agents, modeled as fluorescein in these studies, could partition into the hydrophobic or non-polar region of the hydrogel network and associate with the PMMA nanoparticles. The incorporation of hydrophobic moieties did have a detrimental effect on final equilibrium swelling capability of the hydrogel, but drastically improved fluorescein loading and subsequent release and, importantly, did not shift the dynamic pH-response [65]. The customization of synthetic pH-responsive hydrogel networks is clearly a very powerful tool for the oral delivery of sensitive therapeutics such as proteins and hydrophobic chemotherapeutic drugs.

A number of biologically derived polymers, including alginate and chitosan are attractive alternatives to synthetic polymers for pH-responsive applications due to their inherent biocompatibility and physicochemical properties. Alginate is a naturally derived polysaccharide-based biopolymer that is extracted from brown algae (kelp) [88]. When

exposed to calcium ions (Ca^{2+}), the polysaccharide crosslinks and forms a gel [88,89]. These mild gelation conditions are highly favorable for biological applications because sensitive therapeutics, or even cells, could be encapsulated in the hydrogel network during synthesis while still maintaining activity and viability [88]. Alginate exhibits a pH-dependent swelling/deswelling behavior, collapsing at low pH and swelling at neutral pH [90]. When formed into calcium-crosslinked beads, alginate hydrogels have successfully administered both vaccines [91] and small molecule [92,93] drugs *via* the oral route, protecting them throughout their transit in the GI tract and delivering them at the sites of interest. More recently, a pH-responsive hydrogel system composed of a semi-IPN network of a chitosan derivate (NOCC) and alginate has been developed for the oral delivery of protein therapeutics. The NOCC and alginate associate with one another due to favorable charge interactions and are then crosslinked by the presence of the naturally occurring crosslinking agent, genipin [90]. The pH responsiveness of this system is driven by the behavior of the anionic alginate hydrogel, remaining collapsed at gastric pH and swelling at intestinal pH. The encapsulation of a model protein, bovine serum albumin (BSA), was successful with the hydrogel network protecting the cargo during low pH exposure and releasing it only upon triggering by pH change [90].

3.3.1.2. Vaginal delivery: A healthy vagina will have a pH between 4–5 [35]. However, upon the introduction of sperm (pH ~7.5) during intercourse, the pH of the vagina can easily increase to above pH 7. In addition to raising the overall pH of the vaginal environment, the ejaculatory fluid can carry a variety of sexually transmitted diseases, including the HIV virus [94]. Several systems currently exist to locally administer therapeutics designed to prophylactically treat potential STD exposure, for example, vaginal rings for the delivery of the HIV microbicide dapivirine [95] and potential monoclonal antibody therapies [96], thin films administering contraceptive antimicrobial agents [97], and a gel containing tenofovir, an anti-HIV prodrug [98]. pH-responsive nanogels have several unique advantages such as their small size, minimal site irritation, and the ability to protect the loaded drug and both target and control its release into the environment [94]. Unlike the other systems, a pH-responsive nanogel system will only release the therapeutic upon a pH shift induced by the introduction of potentially infectious semen. Additionally, if engineered correctly, the nanoparticles will slowly degrade over time into harmless bioproducts requiring no removal of a spent film or ring. The system proposed by T. Zhang et al. are nano-sized hydrogel particles composed of pH-responsive MAA and degradable poly(lactic-co-glycolic acid) (PLGA) loaded with either Tenofovir, TNF, or its prodrug TDF, tenofovir disoproxil fumarate [94]. Nano-particles were synthesized by either freeze- or spray-drying techniques [94,99]. These systems showed successful incorporation of either TNF or TDF and a clear pH-responsive drug release for most tested polymer formulations. When introduced to different vaginal cell types some minor cytotoxicity was observed, but, more importantly, the nanoparticles were uptaken into the vaginal endothelial cells, which is important for retention within the vaginal canal [94].

3.3.2. Cationic hydrogel networks—Cationic hydrogel networks exhibit opposite swelling behavior to anionic hydrogels. Specifically, the hydrogels exist at a swollen state at

low pH (pH < pK_a) and collapse upon exposure to a higher pH environment (pH > pK_a). The swelling behavior is, therefore, triggered by a decrease in the pH of the surrounding area.

3.3.2.1. Gastrointestinal delivery: Chitosan is a naturally derived polysaccharide obtained from the deacetylation of chitin, an abundant polysaccharide extracted from marine crustacean. It is linear in structure and composed of linear β-(1 → 4)-glycosidic-linked 2-amino-2-deoxy-β-ᴅ-glycan monosaccharide units. The primary amines in the chitosan structure result in the overall polysaccharide being positively charged and, therefore, inherently mucoadhesive [100]. This, coupled with its inherent biocompatibility and mild gelation conditions, makes chitosan an attractive system for a multitude of drug delivery applications [101,102]. The cationic character of the chitosan means that it is insoluble in water at neutral or basic pH due to the free amino groups present. When those amino groups undergo deionization at acidic pH, the structure becomes soluble in water. It retains this inherent pH-responsiveness when crosslinked into a hydrogel network either by modification by synthetic polymer species or by ionic cross-linking with multivalent anions [100].

This pH-responsive behavior of chitosan-based hydrogels can be harnessed for the targeted gastrointestinal delivery of a variety of therapeutics. Without modifying the chitosan hydrogel network, it would remain collapsed at the neutral pH in the mouth and only swell once reaching the acidic environment of the stomach. To achieve this gastric-specific delivery, Patel et al. synthesized a semi-IPN network composed of chitosan and poly(ethylene oxide) [103]. The polymer network swelled approximately 10 times more in the gastric fluid than in the intestinal fluid. When model antibiotics, metronidazole and amoxicillin, were loaded into the hydrogel network and then released at gastric and intestinal pH conditions, both antibiotics were released to a far greater extent at acidic pH than at neutral pH [103]. Upon the inclusion of another ionic moiety, such as alginate, into the hydrogel network, the pH-responsive behavior can be adjusted. Dai et al. crosslinked a chemically modified chitosan, *N*-succinyl chitosan (Suc-Chi), copolymerized with alginate by ionic gelation. The addition of Ca^{2+} ions results in the ionic complexation of the network, providing the tie points for crosslinking. The resulting system remains collapsed at low pH and swells at neutral pH, much like one would expect out of an anionic system. The therapeutic nifedipine was encapsulated within the hydrogel network and its release monitored over different pH conditions. As would be expected, minimal release was observed at low pH when the gel was collapsed and more significant release was seen once the gel was swollen. Interestingly, the *N*-succinyl modification to the chitosan improved its solubility at neutral pH. Although the ionic character of the chitosan was not changed, the pH-response of the network could be manipulated very readily simply by changing the solubility of the chitosan material [104].

3.3.2.2. Intracellular delivery: Intracellular vesicle pH, particularly within those vesicles engaged in intracellular trafficking, decreases rapidly from neutral to acidic conditions [36–38]. Peppas et al. have recently focused on the development of cationic nanogels for the intracellular delivery of siRNA. The cationic nanogels were composed of a copolymer of poly(2-(diethylamino)ethyl-methacrylate) (DEAEMA) and *t*-butyl methacrylate with grafted poly(ethylene glycol) chains (PDBP). These nanogels were approximately 51 nm in

diameter and exhibited the expected pH-responsive swelling/deswelling behavior around the pK_a of the gel (Fig. 3). The swelling response, loading efficiencies for protein, cellular uptake and biocompatibility were all tailored by tuning the crosslinking density, hydrophobic polymer content, and polymer composition [105–107]. To further tune the swelling behavior and to optimize the system for the intracellular delivery of siRNA, Liechty et al. synthesized three separate cationic nanogel formulations: (1) crosslinked 2-(diethylaminoethyl) methacrylate and poly(ethylene glycol) methyl ether methacrylate, P(DEAEMA-g-PEGMA), (2) inclusion of t-butyl methacrylate, P(DEAEMA-co-TBMA-g-PEGMA), and (3) inclusion of t-butylaminoethyl methacrylate P(DEAEMA-co-TBAEMA-g-PEGMA). The increase in hydrophobic content, *i.e.*, the inclusion of TBMA and TBAEMA, resulted in a decreased onset of pH-dependent gel swelling, while the TBMA depressed the critical swelling pH from 7.8 to 7.0 [108]. Forbes et al. were able to exhibit tighter control of final cationic nanogel parameters by switching from a UV-initiated polymerization to ARGET-ATRP initiated polymerization [109,110]. Furthermore, these cationic nanogels were able to be successfully complexed with siRNA, and promote cellular uptake in RAW264.7 macrophages and HEK293T cells [66,110]. It is argued that the pH-triggered swelling of the nanogel in response to the decrease in pH within the endosome results in the so-called proton-sponge effect, which ends in the bursting of the vesicle due to excessive water imbibition due to an osmotic pressure imbalance [111]. Once the vesicle bursts, the siRNA is no longer complexed with the now deionized cationic nanoparticle and is distribution into the cellular cytosol where it can exert therapeutic effect. The particles developed by Forbes et al. do indeed accomplish siRNA-mediated gene silencing, which indicates that the siRNA and associated nanogel undergo some extent of endosomal escape [66,110]. These results have powerful implications for the treatment of a variety of disorders that are caused by gene overexpression including several autoimmune disorders and types of cancer.

3.3.2.3. Intracellular delivery of chemotherapeutics: The ability of cells to preferentially uptake nanoparticles of specific size and surface charge can be taken advantage of for the intracellular delivery of a variety of therapeutics [112]. This is particularly advantageous for the treatment of cancer because nanoparticles containing chemotherapeutic agents can be administered directly into the cancerous tumor cells and initiate apoptosis. If active targeting moieties are included on the surface of the nanoparticle, preferential and specific delivery to tumor cells can be accomplished, which leaves the healthy cells intact and significantly reduces off-target side effects [37].

Both natural and synthetic cationic hydrogels have been developed to deliver chemotherapeutic drugs into cancerous cells. A hydrogel composed of a chitosan derivative, *N*-[(2-hydroxy-3-trimethylammonium)propyl] chitosan chloride (HTCC) was ionically crosslinked by sodium tripolyphosphate to form cationic chitosan-based nanogels [113]. These nanogels were further functionalized by the surface conjugation of Apo-transferrin, an iron shuttling protein that interacts with the overexpressed transferrin receptors on the surface of tumor cells and initiates cell-mediated endocytosis. The cationic pH-dependent swelling behavior results the gel swelling upon uptake into the endosome and releasing its chemotherapeutic payload, methotrexate disodium (MTX). When these systems were added

to the immortalized HeLa cancer cell line, they were uptaken at a higher rate than unmodified nanoparticles and induced a higher rate of apoptosis [113].

A synthetic cationic gel was synthesized *via* an emulsion copolymerization of 2-(*N,N*-diethylamino)ethyl methacrylate with a heterobifunctional PEG with a 4-vinylbenzyl group at the α-end and a carboxylic acid group at the ω-end. The chemotherapeutic agent doxorubicin was loaded into the hydrogel network *via* a solvent evaporation method and incorporated at up to 26 wt%. The pH-responsive moieties within the hydrogel allowed for a burst release of doxorubicin to occur at endosomal pH, which improved its cytotoxic effects on HuH-7 human hepatoma cells compared to naked doxorubicin. The uptake of doxorubicin bearing pH-responsive hydrogels *via* endocytosis results in the accumulation and delivery of the chemotherapeutic agent directly into the cellular cytosol where it can exert its most potent cytotoxic effect [114].

3.4. Concluding remarks

Both anionic and cationic hydrogels have demonstrated utility in pH-responsive drug delivery applications ranging from oral protein delivery to intracellular chemotherapeutic and gene delivery. The wide variety of existing pH-responsive polymers, both of synthetic and natural origin, allow the researcher to fine tune the swelling properties for the application and target of interest. The inherent pH variability within the human body, especially during particular disease states, lends great applicability to these pH-responsive hydrogel systems.

4. Temperature responsive hydrogels

Thermoresponsive materials for medical use have been of great interest due to the relatively universal physiological temperature of 37 °C and the development of a number of mechanisms to manipulate and control temperature *in vivo*. Thermoresponsive hydrogels fall into two primary categories, positively and negatively responsive systems. Normally, these systems are identified by having an upper critical solution temperature (UCST) or a lower critical solution temperature (LCST), respectively. The expansion or collapse that correlates with the critical shift in aqueous solubility has been utilized as a mechanism for drug delivery, membrane separation/cleaning, and recently, *in situ* gelling scaffolds for tissue regeneration [115,116].

4.1. Swelling theory

4.1.1. LCST—The swelling response of reverse thermoresponsive biomaterials has been extensively studied for poly(*N*-isopropylacrylamide) (PNIPAAm) and other alkyl-substituted acrylamides. The LCST response arises from a balance of hydrophobic and hydrophilic groups, and the entropic and enthalpic costs required to solvate these groups. Bae et al. demonstrated the effect of temperature on the aqueous mixing of different *N*-alkyl substituted acrylamide hydrogels, including PNIPAAm and other non-temperature sensitive polymers [117]. By utilizing the following definitions of the polymer interaction parameter, χ, and the enthalpic and entropic contributions to this parameter, χ_H and χ_S respectively, they were able to identify the enthalpic and entropic shifts throughout this critical phase shift.

$$\chi = \frac{\ln(1 - v_{2s}) + v_{2s} + v_e^* V_S^0 v_{2r}\{(v_{2s}/v_{2r})^{1/3} - 1/2(v_{2s}/v_{2r})\}}{v_{2s}^2} \quad (35)$$

$$\chi_H = \frac{1}{T(\partial\chi/\partial(1/T))} = -T(\partial\chi/\partial T) \quad (36)$$

$$\chi_S = \chi - \chi_H \quad (36')$$

The variables v_{2s}, and v_{2r} are the volume fraction of the polymer in the swollen and relaxed state, respectively, v_e^* is the crosslinking density, and V_S^0 is molar volume of the solvent. The results of these studies are seen in Fig. 4. There are two things to note from these studies. First, poly(acrylamide) (PAAm) is the only gel to demonstrate a mild positive swelling response. This is due to the lack of a hydrophobically modified amide group, meaning that the primary interaction is hydrogen bonding, not the hydrophobic interactions that dictate *N*-alky substituted acrylamides. Second is the sharp peaks in the PNIPAAm and poly(*NN*-diethyl acrylamide) (PDEAAm) results. These two polymers are the only two to exhibit a critical phase shift; they are also the two polymers with the most hydrophobic alkyl side-groups, as determined by their inverse volume fraction in ethanol.

This means that the swelling responses exhibited by these LCST polymers are greatly aided by drastic differences in hydrophobicity. The other major note is the large contribution of entropy to the χ parameter. This is due to the fact that the hydration of hydrophobic segments requires the formation of water cages. These water cages balance the insolubility of the hydrophobic backbone in water, allowing the hydration of the polymer. The formation of these cages comes at a steep entropic cost, which is only balanced out by the hydrogen bonds formed by the amide groups. As the temperature increases, the entropic costs become too great, as seen in Fig. 4, coming to a peak at the LCST. This forces the system to react by expelling the water from the hydrogel, resulting in collapse.

4.1.2. UCST—Although UCST systems are less common than LCST, the common UCST hydrogel is an interpenetrating network (IPN) composed of interlocking networks of acrylamide (AAm) and acrylic acid (AA) [118]. The critical responsiveness of these materials is often described by what is commonly referred to as a "zipper" effect, illustrated in Fig. 5. Essentially, hydrogen bonds between the AA and AAm networks force the gel to collapse at low temperatures. As the temperature increases, the enthalpic gains from these bonds are overpowered by the entropic loss of separation of the water and polymer phases. The resulting criticality unzips the networks, allowing the hydration of the polymer networks.

Although this is a relatively simple explanation, it is often a sufficient explanation for most UCST systems, even though the one-to-one alignment of AAm units to AA units is idealized. However, the critical response depends on a number of other factors, in addition to the breaking of hydrogen bonds, to result in some of the drastic transitions observed [119].

Another important factor in the effective swelling of these UCST hydrogels comes in the form of ionic repulsions. Also, due to the presence of AA units, the swelling response can be greatly impacted by the ionic strength and pH of the fluid. Due to the need of protonated acrylic acid groups, the optimal swelling response of the polymers has been shown to be approximately 4.6, about the pK_a of acrylic acid. However, this can be overcome by the use of propyl acrylic acid, which has a pK_a of over 7 [120].

These issues, along with the high degree of sensitivity to ionic species, lead to limitations of these technologies *in vivo* where pH and ionic strength are constantly fluctuating both in and between patients. This is the primary reason why UCST systems have been studied less than their LCST counterparts.

4.2. Common monomers

4.2.1. LCST monomers

4.2.1.1. *N*-alkyl substituted monomers: There are a wide range of synthetic and naturally occurring polymer systems that exhibit LCSTs around physiological temperature [121]. The majority of the work done in LCST systems has centered around hydrogels composed of poly(*N*-isopropylacrylamide) (PNIPAAm) and its copolymers. PNIPAAm exhibits an LCST around 32 °C, close to physiological temperature, making it an ideal target for biomedical applications. The LCST can be and has been modified by a number of comonomers [121]. The inclusion of hydrophilic monomers raises the LCST, while hydrophobic comonomers depress the critical point. However, there are limitations to the shift of the LCST, due primarily to the necessity of contiguous NIPAAm units. Because of this requirement, the lower the NIPAAm content is, the weaker the collapse.

In addition to PNIPAAm, there have been studies to identify other *N*-alkyl substituted acrylamides that display LCST swelling behavior [122]. One common monomer that is looked to in order to shift the LCST above 37 °C is PDEAAm, exhibiting an LCST of approximately 39 °C. However, the work by Plate and Okano has turned up other monomers for these systems with a range of LCSTs. However, they also exhibit different magnitudes of collapse, as the same alterations that shift the critical temperature lead to different hydration levels, both in collapsed and swollen states [117].

4.2.1.2. Polyethylene glycol: PEG is an interesting amphiphilic molecule that, in addition to providing effective stealthing properties, demonstrates negative temperature response in aqueous environments [123]. PEG methacrylate hydrogels decrease in swelling ratio as temperature increases. The temperature response of these gels can be manipulated by changing the length of the PEG chains, as longer chains lead to lower solubility at lower temperatures. Although PEG hydrogels do exhibit a temperature response, it is not a critical response, though their inverse temperature response can be utilized in the backbone of other macromolecular systems.

One popular system is commonly referred to as pluronic F-127. This material is a triblock polymer consisting of poly(propylene oxide) (PPO) sandwiched between two poly(ethylene oxide) blocks that also demonstrates an LCST gelling response. These systems lack covalent

crosslinks, and thus are not standard hydrogel networks containing chemical crosslinks. The gelation of these systems relies heavily on the self-assembly of hydrophobic propyl oxide groups *versus* hydrophilic ethylene oxide units. Because of this, these systems have been investigated less for their effectiveness as large scale gels, and more for particle based drug delivery [124]. The self-assembly of nanoparticles can be controlled by both the block lengths and concentration in water.

4.2.1.3. Other LCST responsive monomers: The LCST response has been observed in polymers of other naturally occurring and synthetic polymers. Chitosan, a naturally occurring cationic polymer, forms gels much in the way PEO-PPO-PEO systems do [125]. When chitosan is dissolved in water, it shifts from a flowing polymer solution to a gel at about 32 °C. Due to its natural properties, it has been included into a PNIPAAm backbone to develop crosslinked structures without impacting the LCST, while still demonstrating the positive biological properties of chitosan [126].

Poly(vinyl methyl ether) also collapses at 32 °C, and responds much in the same way PNIPAAm does [127]. These systems are polymerized and cross-linked by gamma radiation, and thus the degree of crosslinking and the overall swelling response can be controlled by the level of irradiation. No results are present for the impact of copolymers on the swelling response of these systems. This is similar to another vinyl thermoresponsive monomer that has been recently utilized in hydrogel systems, poly(vinyl caprolactone). For this polymer, the lack of study is due to the sensitive nature of the pendant group [128]. The caprolactone side chains are sensitive to changes in pH as they tend to polymerize between the ester groups.

4.2.2. UCST monomers

4.2.2.1. AAm and AA: IPNs and other hydrogels that exhibit UCST behavior generally focus around an acrylic acid based monomer. Some random copolymers of AAm and AAc have also demonstrated some unique UCST properties, though nothing that can be identified as a critical temperature response [129]. Like their LCST counterparts, the AAm and AA networks can be modified with hydrophobic or hydrophilic comonomers to shift the critical temperature, although the magnitude of collapse diminishes with increasing comonomer concentration [118,130].

4.3. Applications

4.3.1. Oral drug delivery—The use of temperature sensitive hydrogels as drug delivery vehicles has been studied since their inception. The significant change between ambient temperature and physiological temperature has been targeted as a mechanism for the delivery of proteins and small molecules, such as ibuprofen [131] and insulin [132]. However, this mechanism of administration was rendered obsolete with the development of pH responsive hydrogels.

4.3.2. Particle based drug delivery—Originally, it was postulated that thermally responsive hydrogel nanoparticles could be actuated by the rise in temperature in the body that accompanies a fever. However, the immune response to the presence of these

nanoparticles would result in a similar localized temperature increase. This problem can be neutralized by the stealthing of these particles with PEG tethers [133]. However, the temperature sensitive particles still fail to respond to the relatively slight temperature changes that often accompany fevers. This required investigation into other uses for temperature responsive hydrogels. One of the largest fields of interest for thermal responsive materials falls into the category of theranostics, or composites designed to deliver both therapeutic and diagnostic capabilities. These systems generally are developed as composites of an external stimulus, thermogenic, and traceable particle, such as iron oxide or gold, coated in a thermally responsive, drug loaded hydrogel [134].

These systems will ideally provide for improved control and localization of therapeutics that are highly toxic when delivered systemically. One treatment where this technology is desperately needed is in chemotherapeutic delivery, as the highly toxic drugs show improved effectiveness when localized and concentrated at the site of a tumor [135]. UCST and LCST hydrogels have been used as the thermally responsive polymer, however no systems have managed to reach clinical trials, primarily due to targeting limitations and the complexity of the treatment.

4.3.3. Tissue culture—Thermally responsive materials, particularly PNIPAAm, have been utilized as cell substrates in an attempt to trap cells in a porous membrane at 37 °C. Galperin et al. [136] developed degradable porous PNIPAAm hydrogels. Porosity was manipulated in two ways: first by the change in crosslink density, and second by the inclusion of degradable micro-particles. The degradable microparticles provide pores large enough to allow NIH 3T3 cells to pervade the hydrogel matrix. They also included a thermally degradable linker that allows for dissolution of the hydrogel matrix. This is crucial for *in vivo* applications, as the matrix needs to initially be a scaffold for tissue generation, while subsequently disappearing as the synthesized tissue incorporates into the target area.

One area where these thermoresponsive substrates have started to stand out *versus* other hydrogel substrates is as *in situ* gelling platforms. These are systems that can be injected into damaged areas, and fill in missing tissue through the precipitation and post-synthesis crosslinking of PNIPAAm based polymers. The Mikos group developed a thermally and chemically gelling system composed of PNIPAAm, AAm, pentaerythritol diacrylate mono-stearate (PEDAS), and 2-hydroxy ethyl acrylate (HEA), as demonstrated in Fig. 6 [137]. These systems non-covalently gel at 37 °C, while providing a mechanism to covalently bond to provide a substantial substrate for tissue growth.

4.3.4. Ocular drug delivery—Thermoresponsive materials are effective for retinal treatment for many of the same reasons that they are effective for tissue engineering. They provide substrate for cell growth, and gel at physiological temperature [138]. Furthermore, the phase transition provides a mechanism for detachment from a cell layer [126]. This allows for the attachment of a hydrogel contact lens, and as the temperature increases, these hydrogels can promote healing and be peeled off after reaching equilibrium above their LCST [139].

Ocular treatments can take the form of either delivering a therapeutic or as a cell substrate loaded with growth promoters. Verestiuc et al. developed and characterized a system for the delivery of pilocarpine hydrochloride and other ocular drugs utilizing AA functionalized chitosan, copolymerized with either NIPAAm or hydroxyethyl methacrylate (HEMA) copolymers [126]. They varied the concentration of ratio of chitosan:HEMA and chitosan:NIPAAm, and measured drug delivery rates and lift off forces. They found that not only did NIPAAm gels have higher adhesive strengths, but there was also a significant drop after heating above the LCST.

Studies performed by Von Recum et al. have investigated the effect of PNIPAAm scaffolds on the enzymatic integrity of donor retinal cells [140]. They discovered that in addition to having no ill effects on the retinoid enzymatic profile, the temperature sensitive material proved one of the least deleterious routes for cell growth and detachment. This and other substrate studies that utilize, at least, a PNIPAAm based coating to remove substrates from retinal cell regeneration have demonstrated the need for the thermal gelling material in the realm of ocular rehabilitation [136].

4.3.5. Membranes, microfluidics, and sensors—Thermally responsive materials also offer a unique mechanism for the actuation of flow channels. The collapse that the LCST materials, specifically PNIPAAm, are capable of has provided sharp on/off switching to control the release of therapeutics. Hoare, et al. developed a magnetic particle loaded membrane for the restricted delivery of fluorescein, represented in the schematic in Fig. 7 [141]. By entrapping microgels of thermally responsive PNIPAAm, they were able to actuate the hydrogel-based valve by alternating magnetic field. Thermally switching polymers offer another interesting characteristic, as the hydrated–dehydrated shift has proven effective as a mechanism to remove fouling from membranes made of the hydrogels [139,142]. This functionality also lends itself to microsensors, providing a mechanism by which adsorbed solutes can be cleared out for reusability [143].

5. Chemically-responsive hydrogels

Another broad class of hydrogels has been designed to exhibit swelling or degradation in response to individual target molecules. Because of the wide array of chemicals which could act as practical stimuli for achieving useful functions, this review focuses on only a few examples of chemically-responsive hydrogels, as an exhaustive review would be a monumental undertaking. Nevertheless, these few examples are demonstrative of the basic mechanism by which many chemically responsive hydrogels have been made. The mechanisms either make use of the activity of the target molecule itself, as with using peptide-based hydrogels that degrade in response to the target enzyme, or use a transduction pathway to convert recognition of the target molecule into a pH, temperature, or electrical charge change that drives swelling, collapse, or degradation.

5.1. Glucose-responsive hydrogels

Glucose-responsive hydrogels respond to the presence of elevated levels of glucose and have obvious uses in the treatment of diabetes. Diabetes affected approximately 171 million people worldwide in 2000, and is expected to affect approximately 366 million by 2030

[144]. Diabetes can be effectively treated with injection of insulin, but the high frequency of injection, the need for frequent testing, and the inconvenience and pain associated with the injection route have led to researchers seeking improved insulin delivery options. Hydrogels that are capable of acting as long-term insulin depots that respond to increased blood glucose levels and automatically release doses of insulin at appropriate times are a promising development, and could obviate the need for frequent injection and therefore provide a more convenient treatment option that would improve treatment efficacy and quality of life for hundreds of millions of people.

5.1.1. Glucose-oxidase gels—Glucose-responsive hydrogels have typically relied on one of three mechanisms for detecting glucose and responding appropriately [145]. The first of these is to use glucose oxidase (GOx) as a detecting enzyme and its reaction with glucose as a transduction pathway for stimulating response. Enzymes entrapped in hydro-gels have been reported and used since 1963 when Bernfeld and Wan reported successful immobilization of enzymes into acrylamide hydrogels [146]. Glucose oxidase was later immobilized in hydrogels comprised of *N,N*-dimethylaminoethyl methacrylate, hydroxyethyl methacrylate, and tetraethylene glycol dimethacrylate, making the first true glucose-responsive hydrogels using glucose oxidase [147–150]. Since then, many studies have been performed seeking to improve upon these original hydrogels using the same GOx pathway.

The basic mechanism by which these GOx-based gels work is by GOx-catalyzed oxidation of glucose followed by pH-responsive swelling or deswelling of the hydrogel. When glucose is present in the blood (or other surrounding medium), it diffuses into the hydrogel matrix, where GOx catalyzes reaction of glucose with oxygen per the following reaction [151]:

$$\text{Glucose} + O_2 + H_2O \xrightarrow{\text{GOx}} \text{Gluconic acid} + H_2O_2$$
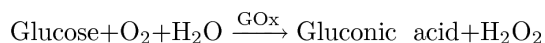
One of the products of the reaction, gluconic acid, reduces the local pH in the hydrogel, which then elicits a pH-dependent response per one of the mechanisms described previously. Therefore, the immobilized GOx acts both as the glucose sensor and the transduction mechanism—the actual response is pH dependent, but the GOx-catalyzed oxidation reaction is responsible for converting glucose detection into the requisite pH shift.

Researchers have expanded on this basic idea in multiple ways. Multiple pH-responsive polymers have been used, such as poly(*N*-isopropylacrylamide-co-methacrylic acid) [152,153], poly(o-phenylenediamine) [154], poly(diethylaminoethyl methacrylate-g-ethylene glycol) [155], and poly(methacrylic acid-g-ethylene glycol) [156]. Additionally, use of hydrogels based on sulfonamide chemistry allowed for a pH transition to occur within a narrow and physiological pH range of 6.5–7.5 [157].

Another important improvement was the introduction of catalase into the hydrogels. Because the GOx-catalyzed reaction is oxygen-dependent and consumes oxygen, the reaction is oxygen limited within the local environment of the hydrogel. To address this issue, catalase has been simultaneously immobilized in the hydrogel, which catalyzes the degradation of the hydrogen peroxide product back into oxygen and water [150,151,157,158]:

$$H_2O_2 \xrightarrow{\text{Catalase}} \frac{1}{2}O_2 + H_2O$$
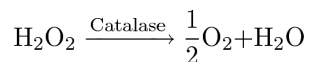
This reaction helps keep oxygen available for the GOx-catalyzed reaction, and also importantly removes the hydrogen peroxide product which can cause degradation of the GOx enzyme. As a result, the rate of swelling and enzyme stability are both improved by introduction of catalase.

5.1.2. Concanavalin A gels—The second main pathway for glucose-responsiveness relies on the use of lectins, primarily concanavalin A (Con A). Hydrogels are comprised of a glycosylated polymer backbone and physically immobilized Con A [159–161]. Con A binds with the glycosylated moieties in the hydrogel, leading to a tightly complexed matrix with small pore sizes, keeping insulin entrapped within the hydrogel. As glucose diffuses into the polymer matrix, the glucose competitively binds with Con A; because Con A has greater affinity for glucose than for the glycosylated moieties, glucose displaces the glycosylated polymer, causing the hydrogel to decomplex and either swell, releasing insulin by diffusion, or exhibit a gel–sol transition, releasing insulin by liberation from the matrix, depending on if the hydrogel is chemically crosslinked or not, respectively. This release mechanism is shown schematically in Fig. 8.

Because the mechanism of these early Con A-based gels relied on competitive displacement of Con A from the glycosylated polymer, they suffered from a relatively slow response time and leakage of Con A from the hydrogel that limited therapeutic potential and repeatability. The stability of the hydrogel system has been improved through alteration of Con A and through alternative linking strategies. Conjugation with poly(ethylene glycol) chains yielded a more hydrophilic, stable Con A that exhibited improved solubility, stability, and affinity toward glucose, which in turn improved sensitivity of the hydrogel and reduced lag time [162,163]. Furthermore, covalent immobilization of Con A into the hydrogel matrix using carbodiimide crosslinking prevents leaching of Con A out of the polymer, increasing stability of the gel and allowing for repeatable swelling behavior [164–166]. In addition to various experiments using modified insulin [167–169], these improvements have led to Con A-based systems for insulin delivery that have significant therapeutic potential.

5.1.3. Phenylboronic acid gels—The last main mechanism for glucose-responsive hydrogels has been based on use of phenylboronic acid (PBA) functionalized hydrogels. PBA has long been known to have ability to bind saccharide, being first reported in 1954 by Kuivila et al. [170]. PBA does this by forming reversible, covalently linked complexes with diols [171,172], as shown in Fig. 9. When glucose, with its diol functionality, enters the hydrogel, the PBA moieties reversibly complex with glucose, shifting equilibrium toward cationically charged boron residues. The phenylborate group ordinarily exists in aqueous environments at equilibrium between uncharged and cationically charged forms. However, reaction with glucose only occurs through the cationically charged form, the product of which is also cationically charged. Therefore, the reaction shifts the overall gel charge density toward cationically charged residues. This increased charge endows the hydrogel

with greater hydrophilicity, which, together with ionic repulsion within the hydrogel, leads to a distinct swelling response.

PBA-based hydrogels have become the most promising candidates for clinical use because they can offer sensitive glucose responsiveness, but do not have the same degradability and stability concerns that adversely affect GOx and Con A-based gels. While GOx and Con A are proteins susceptible to degradation by enzymatic action or simple leakage out of the gel, PBA is a synthetic functional group that is not readily degraded *in vivo* and is incorporated into the polymer directly, thus providing the potential for long acting drug delivery depots while also avoiding extensive chemistry to immobilize proteins in the gel matrix.

PBA-based gels have therefore become the most prominent area of research in glucose-responsive hydrogels. Many researchers have reported unique variations on the basic chemistry that yield suitable drug delivery carriers or glucose sensors [173–181]. Al-though such systems are yet to replace insulin injection or insulin pumps as the primary treatment option for diabetics, the advances in glucose-responsive systems, whether based on glucose oxidase, concanavalin A, or phenylboronic acid, have shown that superior options are available, and further improvements on the technologies will hopefully lead to treatment options that improve the quality of life for the hundreds of millions of people living with diabetes worldwide.

5.2. Enzyme-responsive

In addition to hydrogels like the glucose-responsive hydrogels that respond upon detection of a target molecule, hydrogels can also be made to respond by being directly acted upon by the target molecule. This is most notable in the design and use of enzyme-responsive hydrogels. Among the possible methods for making enzyme-responsive hydrogels, one of the well-studied methods has been to use peptide chains as linkers, either as crosslinks within the hydrogel or as links between the polymer backbone and drug molecules. These peptides are typically made of short sequences chosen to be specifically digestible to certain enzymes, causing degradation of the hydrogel in the presence of the targeted enzyme.

Kopecek and colleagues have for decades developed hydrophilic polymers based on *N*-(2-hydroxypropyl)methacrylamide (HPMA) with drugs attached *via* short oligopeptide sequences [182–191]. The oligopeptide sequence is chosen to target cleavage—and therefore release of the conjugated drug into the target site—to a specific enzyme. For example, the GFLG sequence was selected for cathepsin B-based degradation, thus enabling lysosomal drug delivery [188]. In these studies, the GFLG sequence is used as a side chain link between the drug and the HPMA backbone. The HPMA copolymer with GFLG side chains is made by polymerization of HPMA and methacryloyl-GFLG-nitrophenyl ester monomers, and the drug is conjugated by aminolysis [186,189,192]. Drugs studied have included doxorubicin [185], insulin [193], and ampicillin [190]. The peptide sequence was selected because it is cleavable by cathepsin B, releasing the drug payload into the lysosomal compartment of the target cell, but other peptides could of course be used to target various other enzymes and thus other cell types or compartments of the body using this same basic system.

Peptides have also been incorporated into hydrogels as the chemical crosslinker rather than as a pendant linker, thus causing gel–sol degradation of the hydrogel upon cleavage by the target enzyme. Kim and Healy [194] synthesized poly(*N*-isopropylacrylamide-co-acrylic acid) hydrogels that incorporated QPQGLAK peptides as crosslinkers for use as artificial extracellular matrix in tissue engineering. The QPQGLAK sequence was selected to be specifically degraded by matrix metalloproteinases (MMPs) such as MMP-13 that are produced by osteoblasts. The peptides were incorporated into the hydrogels directly during the polymerization: first the sequence was functionalized to have acrylic end groups by reaction with acryloyl chloride, and then the product was used as a monomer along with *N*-isopropylacrylamide and acrylic acid in a standard chain polymerization reaction. The hydrogel exhibits an LCST temperature response, as described previously, but also is degradable by MMPs. The result is a possible artificial ECM that is degradable in the body, but in response to a biological signal that is found in remodeling bone instead of the random hydrolysis that PLA, PGA, or PLGA hydrogels exhibit, thus allowing the hydrogel to act as a scaffold for bone regeneration that will not remain in the body and impede bone recovery, but will remain sufficiently long for osteoblasts to migrate into the scaffold and begin bone reformation.

The use of peptide crosslinkers has also been extended to drug delivery systems. Glangchai et al. [195] incorporated the GFLGK sequence into nanofabricated hydrogel particles formed through step and flash imprint lithography (S-FIL). GFLGK was functionalized using acrylation by acryloyl chloride and then used in the S-FIL photopolymerization along with poly(ethylene glycol) diacrylate to form shape-specific, highly monodisperse nanoparticles. The GFLGK sequence was chosen to be specifically degraded by cathepsin B, and the resulting nanoparticles proved to be effective at delivering encapsulated plasmid DNA or IgG antibodies upon exposure to the enzyme.

West and Hubbell [196] had previously worked on similar systems also for use as an artificial extracellular matrix. Their system consisted of telechelic block copolymers of the form BAB, where A is a PEG chain and B represents a peptide sequence chosen to be degradable by a particular enzyme—APGL was chosen for degradation by collagenase, and VRN was chosen for degradation by plasmin. The triblock polymers were then acrylated by acryloyl chloride and made into hydrogels by UV-initiated polymerization. The hydrogels were shown to be degradable by the expected enzymes and thus potential candidates for assisting in wound healing and tissue engineering.

One of the primary limitations of using peptides for targeting is the difficulty making large quantities of synthetic peptides, which results in high cost. The use of peptides as crosslinkers, rather than as an integral part of the hydrogel backbone, enables targeted degradability while greatly reducing the amount of peptide required since the bulk of the gel is comprised of some other, cheaper biomaterial. Therefore, because of the limiting cost of peptides, the crosslinking approach is more likely to be clinically relevant since it provides degradation with limited amount of peptide. Furthermore, using other known biomaterials as the hydrogel backbone polymer allows for multiple response modalities, such as temperature or pH-responsiveness along with the degradation pathway.

It is therefore important to note that many other crosslinking chemistries are available. While the above work all utilized acrylation to directly incorporate the peptides in the polymerization reaction, any suitable crosslinking chemistry may be utilized. Michael addition [195], click chemistry, carbodiimide reactions, reductive amination, thiolation and maleimide chemistry, and many other potential crosslinking chemistries will all serve the purpose, although the ideal pathway will be system-specific depending on what unwanted cross-reactions could occur [197].

5.3. Molecularly imprinted polymers

Molecularly imprinted polymers (MIPs) make use of hydrogels formed in the presence of a template molecule in order to produce binding sites that will later recognize the target molecule, much like how antibodies or aptamers are capable of binding target molecules. MIPs are a promising method for yielding similar results as antibodies or aptamers in multiple applications; although they do not currently have as high of specificity and binding capability, because they are formed from synthetic monomers, they do not have the disadvantages of high cost, limited ranges of stability (with respect to pH, temperature, and enzymatic environment), and limited shelf-life that limit anti-bodies and (to a lesser extent) aptamers [198–203]. MIPs therefore bear mention as an important and expanding class of chemically-responsive hydrogels; although the response is at times limited to recognition and binding of the target molecule, this can lead to further responses using transduction pathways, as exemplified in the glucose-responsive hydrogels.

5.3.1. Synthesis—The basic synthesis procedure for MIPs is simply described. The molecule to be recognized is incubated with one or more monomers, chosen to exhibit some form of interaction with the structure of the template molecule, allowing the monomers to bind to the template. The bound monomers are then polymerized and crosslinked into a set polymer, while the monomer units are still bound to the target molecule. Finally, the template is washed out of the polymer, leaving a porous polymer where the functional units of the monomers are bound in such a manner as to form a binding site for the target molecule upon further exposure [204]. This forms the typical "lock and key" pairing often mentioned with regard to antibodies, where the synthetic "lock" is built up around the "key" of the template molecule.

The interaction between the monomer and the template may be covalent or non-covalent in nature. Non-covalent interactions—such as hydrogen bonding, pi-pi stacking, dipolar interactions, ion pairing, and hydrophobic interactions—are more common for imprinting [205–207]. The use of non-covalent interactions offers easy synthesis: no chemical reactions are required, reducing the required amount of knowledge of the target molecule's properties and the required level of control over the synthesis, and a small number of widely-used and inexpensive compounds, such as methacrylic acid, acrylic acid, methacrylamide, acrylamide, vinyl-pyridine, or hydroxyethyl methacrylate, may be used to achieve target recognition. However, because of the same non-specific nature of non-covalent interactions that make synthesis straight-forward, this method also yields MIPs that exhibit significant levels of binding of molecules other than the target, thus limiting selectivity. This issue can be

overcome by using more advanced monomer structures that provide better specificity for the target molecules, although this increases cost slightly [208–211].

Multiple reviews have been published on the detailed synthesis and evaluation of MIPs [204–207,212–218], so this section focuses on applications. However, it should be briefly mentioned that successful retention of the formed binding site generally requires high levels of crosslinking. At low crosslinking density, once the template is removed and the covalent or non-covalent interactions are no longer present, the recognition sites are free to redistribute through entropic mixing as allowed by the hydrogel structure, typically to a point where any observed binding is non-specific due to the loss of the binding-site geometry [219]. High crosslinking density inhibits this entropic mixing and thus keeps the geometric requirements for recognition largely satisfied. Other than this constraint, however, the synthetic procedures for MIPs are widely varied, and many different chemistries can achieve significant target recognition and specificity.

5.3.2. Diagnostics/sensors—The most commonly mentioned application of MIPs is for use as inexpensive diagnostics or sensors. The need for quick and easy detection of biological signals for medicine and dangerous chemicals for security purposes drives an estimated $52 billion diagnostics market [220], which relies largely on use of antibodies for sufficient specificity [221]. However, because of the many current limitations of antibody selection and production, cheaper tests that are easier to make, and therefore quicker to market in response to new health and safety concerns, are in high demand. MIPs may offer exactly that.

Because of their facile synthesis, MIPs can be quickly and inexpensively made for most target molecules. MIPs have been prepared for detection of many targets, such as hemoglobin, trypsin [222], cholesterol [223], uric acid [224,225], Hev b1 latex allergen [226], TNT [227], perfluorooctane sulfonate [228], theophylline [229], diazepam [229], atrazine [230,231], morphine [232], corticosteroid [233], yohimbine [234], methyl-α-glucoside [235], and S-propranolol [236,237], to name a few.

In order to function as a sensor or diagnostic, some transduction mechanism is needed to convert the binding action into a noticeable and/or quantifiable response. There have been multiple proposed mechanisms for achieving this. The transducer may be an added element to polymer matrix or can be incorporated as part of the polymer itself.

Systems with incorporated transducers are capable of reagent-less sensing, which generally results in faster results and simpler assays due to the direct nature of generating a signal. Therefore, integrated transducers are preferable, but unfortunately are currently limited. Available reagentless technologies include electrochemical sensing *via* voltage, current, impedance, or capacitance changes [238–244], fluorescent quenching [245], infrared spectroscopy [246], Raman spectroscopy, and optical or acoustic measurements of changes in mass or refractive index [247–250].

Addition of elements to the polymer can improve sensor sensitivity by providing signal amplification. For electrochemical detection methods, MIP nanoparticles have been attached

to the surface of carbon nanotubes [225,251–253], gold nanoparticles [254], and silver nanoparticles [255], which increases binding surface area and provides better electrical properties for stronger signal with lower levels of analyte. For optical methods, addition of quantum dots has allowed amplification of fluorescent detection, leading to highly sensitive detection assays [256–261]. While these methods require additional synthesis complexity, the enhanced sensitivity they provide will doubtlessly make the addition of transducing elements the primary method of producing sensors and diagnostics.

5.3.3. Drug delivery—Although not yet widely studied in drug delivery systems, some studies have been performed using MIPs to achieve high levels of control over release of drug molecules [262,263]. Norell et al. [264] first studied use of theophylline-imprinted MIPs for drug delivery of theophylline. Using MIPs with pre-bound theophylline at levels up to 50 mg/g polymer, they demonstrated complete release within 6–10 h, but with only small differences between imprinted and non-imprinted polymers. Ciardelli et al. [265] followed up on this work using nanospheres comprised of poly(methylmethacry-late-*co*-methacrylic acid) imprinted with theophylline to create nanoparticles capable of binding up to 1 mg theophylline/g polymer. This system also allowed for sustained release of theophylline— approximately 50% of theophylline was released within 3 h, while 80% was achieved over 7 days. Clearly, the specificity of binding to the target molecule is the main advantage of MIPs; however, in both of these simple, proof-of-concept systems, nothing was demonstrated that could not have been achieved through more traditional drug delivery systems.

More advantageous use of MIPs has been shown in the enantiomeric-specific delivery of drug compounds. The selectivity of MIPs allows for preferential binding of one enantiomeric form of a chiral molecule over the opposing enantiomer, which can be exploited for selective delivery of selected enantiomers from racemic mixtures of compounds [266]. For example, an S-propanolol imprinted MIP made from methacrylic acid crosslinked with ethylene glycol dimethacrylate was able to selectively deliver the S-enantiomer over the R-enantiomer; since the S-isomer has approximately 100-fold greater activity than the R-isomer, this selectivity can be used to deliver the superior medication without requiring upstream separation in the manufacturing process [267].

The true capability of MIPs as drug delivery devices is still yet to be shown. Feedback-controlled devices would be ideal, where highly-selective binding of target molecules would trigger or stop the release of a molecule such that it is delivered only when needed. However, the advantages of MIPs will only be seen when more traditional systems, like those seen in the glucose-responsive hydrogels, are not sufficiently selective. Therefore, MIPs will likely only see commercial use for drug delivery if they can be shown to offer improved delivery capability and/or control over more traditional responsive hydrogels, or in the very select cases where great specificity toward a drug over its structural analogs is needed.

5.3.4. Sorbents—Along with their potential use as inexpensive, portable, and easily storable sensors and diagnostics, MIPs will likely find wide utility as sorbents. The basic purpose of MIPs is to selectively bind a particular molecule (or even cell), so they are inherently useful for selective isolation or removal of particular components from a mixture

or solution. MIPs have already been used, both academically and commercially, for various purposes in solid phase extraction, food processing and purification, biological sample treatment, and environmental analysis [268–272].

The primary benefit of using MIPs as opposed to more traditional sorbents used in solid phase extraction is, once again, the selectivity they show for a particular analyte. Traditional sorbents may be chosen to show some selectivity, but inevitably end up adsorbing at least trace amounts of various other components as well. González-Mariño et al. [273] demonstrated this selectivity by comparing adsorbing capability of a common, commercially-available hydrophilic balance sorbent (Oasis HLB), a mixed-mode sorbent (Oasis MCX), and an MIP sorbent for analysis of five amphetamines from wastewater samples. The hydrophilic balance sorbent performed worst—three of the five analytes could not even be measured by LC–MS following extraction—followed by the mixed-mode sorbent. However, these were significantly outperformed by the MIPs, which gave the cleanest extracts, the lowest matrix effects, the lowest limits of detection, and the greatest precision.

Because of this selectivity, MIPs have seen widespread use through multiple industries [274]. In the field of food processing, MIPs have been made for extraction of a wide variety of analytes: norfloxacin, enrofloxacin, and ciprofloxacine from milk [275,276]; tetracycline from fish [277]; chloramphenicol from milk and shrimp [278]; zeralenone, simazine, atrazine, propazine, fenuron, linuron, metoxuron, clortoluron, isoproturon, metobromuron, and tebuconazole from multiple vegetables [279–282]. Biological uses have focused on primarily on either plasma or urine analysis, for many various analytes: alfuzosin [283,284]; cefathiamidine [202]; enrofloxacine and ciprofloxacine [285]; tamoxifen [286]; amoxicillin [287,288]; and dopamine [289]. Finally, environmental uses have focused almost solely on treatment of water, whether from lakes, rivers, or sewage, and have likewise focused on various analytes: 17-β-estradiol [290]; simazine, atrazine, propazine, and terbutilazine [291]; phenobarbital, cyclobarbital, amobarbital, and phenytoin [292]; diclofenac [293]; and bisphenol A [294].

Although the compounds listed above are quite numerous, that is far from an exhaustive list of the multiple uses of MIPs as sorbents. Clearly, the selectivity and binding capability afforded by MIPs as used in hydrogels makes them a highly useful chemically-responsive material. The ability to bind a particular analyte with high specificity using inexpensive materials that are readily stored for long periods of time enables many practical uses, many of which are yet to be fully realized. There remains much work to be done in advancing the technology of molecularly imprinted polymers, but such work will indubitably lead to widespread commercial use of MIPs in the near future.

6. Photo-responsive hydrogels

The great advantage of photoresponsive polymers is the high level of control that is granted by the stimulus. Photoresponsive polymers, commonly, respond to light energy by way of a reaction. This reaction can be a variety of degradation and bonding reactions. However, they are unanimously governed by the Planck–Einstein relation:

$$E = h\upsilon = \frac{hc}{\lambda}$$

where the energy of the light (E) is equal to Planck's constant (h) multiplied by the frequency (υ). Photo-dependent reaction rates have shown strong correlations to the energy and irradiance of light, with little variation [295]. This, combined with the high degree of dimensional control of light exposure, makes photocatalyzed reactions an attractive mechanism for hydrogel manipulation. The major downfall with photo-induced changes comes in *in vivo* models. Due to the inability of ultraviolet and visual electromagnetic wavelengths to penetrate tissue, these mechanisms are only really viable for *ex vivo* systems and skin level treatments. However, recent advances with near infrared (IR) wavelength sensitive reactions have opened up some possibilities.

6.1. Theory

Photochemical reaction kinetics depends on a number of factors, including standard reaction parameters such as product and reactant concentrations, temperature, *etc.* However, uniquely, they depend on a concept of absorbed intensity (I_{abs}). This is defined by the Beer–Lambert law in Eq. (37), for individual and mixtures of absorbing species, respectively [296].

$$\log \left(\frac{I_0}{I_{\mathrm{abs}}} \right) = \varepsilon C d = \varepsilon_1 C_1 d + \varepsilon_2 C_1 d \dots \quad (37)$$

where C is concentration, d is depth of penetration, and ε is a molar absorptivity constant. It is important to note that the molar absorptivity (ε) is wavelength and, at high levels, concentration dependent. However, this does not account for scattering, meaning at high concentrations the relationship between absorbed and emitted light breaks down. This often translates to ineffectiveness of photoresponsive reactions.

The other major determining factor for photochemical reactions is the overall quantum yield (ϕ). Quantum yield is the measure of efficiency of reaction, essentially measuring the rate of reaction with respect to the absorbed intensity, defined in Eq. (38), where A is the light reactive species. In practice, it is easier to determine it from the kinetic constant (k), energy, emitted light intensity, and proportionality constant of the wavelength of light. However, this breaks down in the rare condition of an absorbance (I_{abs}/I_0) well above 10% [297].

$$\varphi \equiv \frac{-d[A]/dt}{I_{\mathrm{abs}}} = 10^6 \frac{k N_A hc}{\varepsilon \lambda I_0} = 10^6 \frac{k N_A h\upsilon}{\varepsilon I_0} \quad (38)$$

This quantity is compared to primary quantum yield (ϕ_1), essentially the efficiency of reaction assuming no side reactions. A primary quantum yield close to unity means that, ideally, the reactant converts absorbed energy entirely into product. This occurs only when the energy cannot be quenched by fluorescent emission, or converted into other energy forms. The ratio of overall to primary quantum results in a value similar to kinetic chain

length of polymerizations, as it is the ratio of rate of reactant consumption to the rate of initiation.

In the realm of hydrogels, due to the high water content and, inversely, low reactant concentrations, these are rarely issues, unless the gels are collapsed. The relative response of these hydrogels can generally be well characterized and standardized to the intensity of light emitted (I_0). The other simplification that hydrogel systems allow for photoreactive systems is the relatively low diffusion rates of molecules through the system. This becomes important when considering additive photoreactions and reversible systems. When a secondary molecule is involved, the rate of diffusion from the activated location can lead to bleeding over in photochemical reactions. However, when the diffusional timescale is limited by the hydrogel's structure, this effect is limited [298].

6.2. Common monomers

Photoresponsive monomers fall into 3 primary categories: isomerization, degradation, and dimerization. These three mechanisms can be incorporated as crosslinkers and as pendant groups.

6.2.1. Isomerization monomers—These materials can be further classified as either a *cis–trans* shift or cyclization. One of the more common structures that utilize a *cis–trans* shift in order to exhibit drastic differences in polarity and hydrophobicity are azobenzenes. Azobenzenes have been incorporated as both monomers and cross-linkers into hydrogels to induce a photo-sensitive phase shift. The *cis–trans* shift leads to changes in stacking efficiency and, in response to polarized light, can lead to orthogonal bending [299]. The azobenzene systems also bring reversibility to their stacking, shifting from *trans* to *cis* forms and back in response to 360 and 440 nm light, respectively. The wavelength of light that these systems respond to can be altered by manipulation of the end groups attached to the benzene rings [300].

There are other *cis–trans* reactive groups, however very few of them exist as covalently linked hydrogel networks, due to availability of double bonds to radical polymerizations. However, they do exist as sol–gel networks. For example, a modified fumaric amide has been used to trigger a photo-switching from solution to a gel, and has been shown to contain enzymes and substrates separately until UV irradiation [301].

The other form of isomerization often utilized is cyclization. The delicate balance of ring structures caused by ring strain makes these molecules prime targets for low energy photo-irradiation. The common functional group for these reactions is spirobenzopyran [302]. This group is also unique in that, in the non-cyclized form it presents as zwitterionic, with the charged groups being consumed during cyclization. This translates into a hydrophilic linear polymer, and a hydrophobic polymer when cyclized. This functional group is also interesting, because instead of having on/off switching, the light source only acts as a catalyst to cyclization. Since the cyclized product is unstable, the cessation of exposure will naturally reform the linear starting product. However, there has been some success, through modification, of developing a product with a mildly stable cyclized product [303].

6.2.2. Degradation—Degradation depends on the breakdown of covalent bonds. However, this can be utilized in a number of ways to present different functional groups or, in the form of a cross-linker, change the mesh size of a polymer. The most common group utilized for photo-degradable moieties is the *o*-methoxy nitro-benzene family of monomers. The delicate balance of the strong electron draw of the nitro group coupled with the electron-donating effect of the methoxy group makes this a good leaving group, requiring little energy to break down the bridge. This, combined with the ease of functionalization of the benzene ring, has resulted in a large number of monomers and cross-linkers that have been utilized for photodegradable polymers [304]. The wavelength of light that these monomers respond to can also be manipulated by the functionalization of the benzene group, allowing for modification of the photoresponse, attaining a range of reactivity to light with wavelengths from 350 to 450 nm, even going as high as 872 nm for two photon exposure processes [305].

By including two nitrobenzene groups in one monomer, a hydrogel can be designed to respond to multiple wavelengths by the inclusion of a single monomer. In these instances, cleavage of one nitrobenzene group leads to a significant shift of the responsiveness of the second. This allows for, potentially, one wavelength for the degradation of a cross-linker, and another to present a new pendant group with unique properties [304]. A number of different cross-linkers have taken advantage of this, by combining different chemical bridges between the two nitrobenzene groups. These have focused mostly on alkyl and ethylene oxide chains, in order to provide significant space between the two reactive groups. However, some aryl ethers have been utilized in order to combine the two groups. Ethylene oxide chains are the most appealing for biological systems, as they exhibit higher biocompatibilities than their alkyl and ether counterparts [304].

Other degradation reactions that have been developed are less customizable, but still important. They usually deal with the removal of a small side group, such as a hydroxyl. Regardless of size, the removal of these groups has been shown to yield in significant changes to the chemical structure of the hydrogels. One such group that has been demonstrated to have such an effect is triphenylmethane [306]. This group responds to light by the ejection of a hydroxyl group, forming a carbocation.

6.2.3. Dimerization—Dimerization and degradation are often both available in response to different wavelengths of light. In this sense, the previous section was incomplete. Dimerization depends on the conjoining of two units. Occasionally, these reactions require the presence of a third species, as a catalyst. A large number of these reactions depend on cyclization of two double bonds. Coumarin is a common molecule that provides an effective dimerization route. Two coumarin molecules cyclize to form a cyclo-butyl ring, and due to intense ring strain, they readily break up in response to ~350 and ~250 nm light respectively [307]. By polymerizing an acrylate form of this copolymer into a PNIPAAm backbone, He et al. managed to make a photo-crosslinkable and degradable hydrogel system [308]. This is a common mechanism for reversible dimerization; it has also been achieved with other functional groups, such as cinnamylidene acetate [309] and anthracene modified PEG chains [310].

6.3. Applications

6.3.1. Tissue culture—One of the major contributions that photoresponsive hydrogels have made is the exact control they can yield over substrates for cell growth. Due to relative narrow ranges of sensitivity, high conversion percent, and the exact three dimensional control that can be achieved with lasers, they offer precise control for *ex vitro* substrate modification. Since cell differentiation depends greatly on mechanical properties and chemical biomarkers, the high level of control allowed for can drastically change the rate of cell proliferation on a substrate.

One method investigated altering mechanical properties through the degradation of side groups. By copolymerization of 2-nitrobenzyl acrylate and hydroxyethyl acetate, a rigid polymer can be formed [311]. The degradation of the nitrobenzyl group to acrylic acid yields a softer, more wettable polymer that demonstrates a much higher cell population, as can be seen in Fig. 10. This can be used to pattern the cell growth, as the fibroblast cells preferentially proliferate on softer, light exposed, hydrogels.

DeForest and Anseth developed systems with higher control by developing hydrogels with dual photo-responses, in the form of a degradable cross-linker and a side group for conjugation with bioactive groups [295]. The gel was formed with an azidedifluorinated cyclooctyne click reaction. Then, by the careful inclusion of carbon-carbon double bonds and a nitro benzene groups, they were able to pattern in a desired thiolated biomarker while also providing a mechanism to degrade the crosslinked network. The patterning of the thiolated biomarker allows the hydrogel to express cell compatible biomarkers with high levels of control. The degradable nitrobenzene group provided a mechanism for mechanical alteration, giving two mechanisms to control the cell growth in the hydrogel. As seen in Fig. 11, the hydrogel can even be patterned in 3 dimensional space, providing high levels of control over cell growth.

6.3.2. Microfluidics—Another large field for phtoresponsive materials is in micro-fluidics, where the ability to actuate flow channels and switches are necessary for the control of mixing and washing procedures. Photo-reversible hydrogels are crucial for these roles, as they provide a swelling response to plug or open flow channels. Sugiura et al. achieved this by developing spirobenzopyran-functionalized PNIPAAm gels, as described in Fig. 12 [302]. These hydrogel systems allowed for real-time pathway opening, allowing for enhanced flow control based on the irradiated area, as seen in Fig. 13.

6.3.3. Drug delivery—Photo-actuated drug delivery runs into a major issue due to the limited penetration of visible and UV light through skin. However, light controlled degradation does offer an interesting control mechanism for a drug loaded nanoparticle. Azagarsamy et al. demonstrated the high level of on/off control that photo-degradable nanoparticles provide [312]. Griffin and Kasko took this work a step further by including multiple therapeutics that released in response to different wavelengths of light [313]. They included three alternatively modified nitrobenzene linkers that connected the drugs into the backbone of the hydrogel. Although each drug does not exclusively release, there is enough

difference in molar absorptivity, as shown in Table 3, to significantly affect the rate of release of the different therapeutics. The different types of control are described in Fig. 14.

7. Electrically-responsive hydrogels

It has long been known, since work both by and preceding Flory, that many hydrogels also demonstrate stimuli-sensitivity toward electromagnetic fields. Whereas many of the previously-discussed stimulus-responsive gels are quite limited in the number of monomers available for producing the response, responses to an applied electric field can be observed using any polyelectrolyte gel. Hydrogels of poly(2-(acrylamido)-2-methylpropanesulfonic acid) (PAMPS) [314,315], poly(acrylic acid) [316,317], poly(acrylamide) [316], chitosan and poly(2-hydroxyethyl methacrylate) (PHEMA) [318], poly(dimethylsiloxane) (PDMS) with titanium dioxide particles [319], and others have been studied and reported; however, stimuli-sensitivity can be observed in hydrogels based on any ionizable monomer. Neutral hydrogels are unresponsive on their own [314], but can become electromagnetically-responsive if coupled with dielectric liquids or electrically-responsive particles [317,320].

When a polyelectrolyte gel is placed within an electric field exhibiting a potential gradient, such as by placing between two electrodes with an applied voltage, the hydrogel will swell or contract depending on the charge of the hydrogel [314,321]. This responsive behavior occurs through a combination of Coulombic, electrophoretic, piezoelectric, electroosmotic, and electrostrictive interactions. As a result, the magnitude of the response varies based on the charge density of the hydrogel, the degree of crosslinking in the hydrogel, the magnitude of the applied voltage, the dielectric properties of the surrounding medium, and the pH and ionic strength of the surrounding medium, all of which modulate the strength and probability of electric interactions within the hydrogel [321].

The mechanism of the swelling response has been described as follows. Within a polyelectrolyte hydrogel, there are fixed charges on the polymer backbone of the hydrogel that, at equilibrium, attract counterions in the surrounding medium that balance out the charge of the polymer hydrogel. This process is well-described by the Donnan equilibrium effect [322,323]. Upon application of an external electric field, the charged network ions and counterions are attracted in opposite directions by electrophoretic forces. However, the network ions are restricted from individual movement because of the crosslinked nature of the hydrogel. Therefore, although there is some contraction of the hydrogel based on electrophoresis alone, the magnitude of the response is limited because the crosslinking prohibits long-range rearrangement of the network ions into a more compact form. However, the transport of counterions leads to an osmotic potential that in turn leads to electroosmotic movement of water molecules carried along with the counterions [314]. The net result is an electrically-induced contraction of the polyelectrolyte hydrogel with the polymer hydrogel and the water and counterions moving in opposite directions.

Many efforts have been made to model this responsiveness. Gong et al. [314] modeled this contractive behavior in a one-dimensional model using Poisson–Boltzmann and Navier–Stokes equations to describe the transport of counterions and water. The modeling yields

theoretical equations (Eqs. (39) and (40)) for calculating contraction efficiency (u_{av}) and weight swelling ratio (W/W_w):

$$u_{av} = \frac{\left\{ \int_{r_i}^{r_o} [2\pi r / \rho(r)] dr \right\}}{\pi (r_o^2 - r_i^2)} \quad (39)$$

$$\frac{W}{W_w} = \frac{L(t)}{L_0} = 1 - \int_0^t \frac{v_{av}(t) dt}{L_0} \quad (40)$$

where u_{av} [m^3/C] is the average gel contraction efficiency, r_i [m] is the radius of the cylindrically-shaped macroion, r_o [m] is the distance to the midpoint of two adjacent macroions, $\rho(r)$ [C/m^3] is the local charge density in the gel, W is the weight of the gel at time t, W_w is the weight of the gel at $t = 0$, $L(t)$ is the length of the polymer gel at t, L_0 is the length of the gel at $t = 0$, and $v_{av}(t)$ is the average value of the water flow.

The above model was compared against experimental data taken by weight swelling measurements (gravimetry) using poly(2-(acrylamide)-2-methylpropanesulfonic acid) (PAMPS) gels. Upon application of an electric field, a large potential drop is quickly seen due to the formation of a Helmholtz bilayer and the gel responds rapidly. As can be seen in Figs. 15 and 16, the model agrees with experiment in showing that a significant and rapid contraction of the PAMPS gel should occur in response to the electric field, that contraction is faster with higher degree of swelling (q), that the response is approximately linearly proportional to the quantity of electricity, and that the contraction efficiency is inversely proportional to the crosslinking density of the gel. Notable deviations from the model include that there is a "minimum" value of W/W_w at which contraction stops, possibly due to water bound to the macroions by attractive dipole forces at very close distance, and that the magnitude of response is significantly different between experimental and predicted results.

The discrepancy between model and experiment results primarily from the simplifications of one-dimensional modeling, which neglects the full impact that crosslinking has within the hydrogel, and from using free water values for the dielectric constant and viscosity of water, rather than experimentally-determined values that would be more likely to be observed within the charged network. Nevertheless, although using only a one-dimensional transport model, this early work highlighted several salient features of hydrogel response to an electric field, provided support for the proposed mechanisms by which the response was thought to occur, and demonstrated the ability to understand hydrogel swelling dynamics with basic application of electric theory and transport phenomena. Later theoretical studies have used similar theoretical treatments to obtain highly accurate models of the electrical swelling response [324,325].

7.1. Applications

7.1.1. Artificial muscles—Ionized hydrogels which show electrically-responsive behavior have many potential uses. One of the most exciting and frequently studied potential applications is as artificial muscles. Because many hydrogels exhibit high biocompatibility

and similar properties to biological tissues, they are prime candidates for use in tissue replacements. Those that exhibit electrically-stimulated swelling or contraction are especially auspicious for use as muscle, since they can mimic the response seen by muscle fibers in response to the electrical voltage applied by neurons. Of course, for use as artificial muscles, rapid kinetics are necessary, while simultaneously being repeatable, yet exhibiting sufficient material strength to handle high loads and stresses in repeated use. Furthermore, because the range of human movement is varied, at times necessitating large movements and at others subtle ones, a sensitive and tunable response is also needed. A significant amount of work has been published looking to achieve these multiple goals.

Hydrogels have been made that respond to the application of an electric field with angular movements or linear deformation, or a mixture of both. Large ranges of angular movements have been observed, ranging from a few degrees to over 360° [326,327]. The pioneering work on electrochemomechanical systems was per-formed by Osada et al. [315]. Using a PAMPS hydrogel with low crosslinking density of *N,N*-methylene bisacrylamide that was immersed in a surfactant solution (*n*-dodecyl pyridinium chloride), it was demonstrated that the gel could be made to "walk" through a solution by alternately applying and reversing a 20 V potential at 2 s intervals. The mechanism by which this occurred was explained as "a reversible and cooperative complexing of surfactant molecules on the polymer gel in an electric field, causing the gel to shrink" and bend, as shown schematically in Fig. 17 and visually in Fig. 18. The benefits of this system are that it performs work as an actuator in a rapid manner with reversible and tunable response, all while retaining the desirable properties of a "soft" material.

Kim et al. [318] expanded on Osada et al. and reported on a chitosan/P(HEMA) semi-IPN hydrogel system that exhibited controllable angular deformations ranging from 3° to 45°, dependent approximately linearly on voltage applied and non-linearly on ionic strength of the surrounding medium. Further-more, reversing the polarity of the voltage reversed the direction of deformation. Unfortunately, the bending response occurred over a long time period of 20–40 s. While this is sufficiently fast for use as a basic actuator, a faster response would be preferable for use in an artificial muscle application.

Otero and Cortés [327] reported the synthesis and characterization of a polypyrrole film surrounding a non-conducting film that exhibited the ability to angularly deform with application of an electric field while exhibiting tactile sensitivity in measuring the work required. The hydrogel achieved angular deformations of up to 108°, and was capable of moving objects up to 1200 times its weight. The response time was also rapid, with measurements taken after only 10 s of response time. Such systems, including many other systems exhibiting electrically- responsive angular deformation [328–334], show promise as actuators, and the simplicity of the design is promising for application in biological uses.

The other typical response is a linear deformation of the hydrogel—an expansion or contraction as described previously. Although acrylic copolymer elastomers have been reported for such a response, exhibiting strains from 233 up to 380%, these materials require relatively large voltages and often do not have the softness (low Young's modulus) expected of a biomaterial [335,336]. Hydrogels based on poly(vinyl alcohol)/dimethyl sulfoxide

(PVA/DMSO) or poly(vinyl chloride)/di-*n*-butylphthalate have shown the ability to exhibit electrically-induced responses of up to 8% strain, as well as bending of up to 1808 within a time frame of only 90 ms [337–339]. In fact, Hirai et al. [338] were able to utilize a PVA/ DMSO gel to flap a 12.5 cm wing at 2 Hz by periodic application of an electric field, demonstrating the capability of using such gels as artificial muscles. Although the strain observed was just 8% in length, this was hundreds of times greater response than observed in conventional ferroelectric materials. Liang et al. [336] expanded on this by demonstrating use of a PVA/DMSO gel to achieve motility of up to 14.4 mm/s in a path-controlled manner in air by application of a 400 V/mm electric field. Although this is a high potential to be applied, the combination of rapid speed and well-controlled path of the gel shows great promise for use in small bionics.

7.1.2. Drug delivery—As with the multiple other responsive hydrogels discussed in this review, electrically-responsive hydrogels have also been explored for applications in drug delivery. Because of the predictable and highly reproducible contraction, or deswelling, exhibited by electrically-responsive hydrogels, these systems could make auspicious drug carriers that enable highly targeted drug delivery with excellent temporal and spatial control. The application of an electrical field to sites within the body is a bit difficult, however, and is likely an obstacle that will limit the use of such systems. Nevertheless, it is not an impossible problem. Topical electric field application through iontophoresis and electroporation has allowed for transdermal drug delivery, and would enable electric responses of hydrogels implanted subcutaneously, allowing for pulsed drug release over long periods of time [340–343].

As an alternative to external electric field application, Santini et al. [344] prepared a silicon microchip containing 34 separate drug reservoirs sealed with a thin layer of gold that dissolves upon application of a 1.2 V potential. The potential was applied directly in experiments, but could potentially be performed by the device itself with incorporation of a battery and an onboard controller that regulates when each well is released. Because thousands of wells could be incorporated into such a device, regular application of a drug over a long period of time could be achieved without needing an external field. One can imagine multiple potential improvements that could allow this system to be even more application specific: the onboard controller could potentially receive wireless signals from an external device to know when to release drug if irregular intervals are needed, or could incorporate some kind of sensing capability to pulse only in response to some bodily condition. Although this system did not make use of electrically-responsive hydrogels, it demonstrates that electrical responsiveness may still be used within the body; the gold films used for response could easily have been replaced with electrical-ly-responsive hydrogels to enable a different drug release profile. Thus, while application of an external field may be a difficult—though not intractable—challenge, there are potential ways of using cleverly designed implantable systems with batteries to enable regular drug delivery without needing externally-applied electric fields. Further, one can imagine that future advancements in wireless electricity could also enable simpler application of external electric fields, opening up the ability to make use of this well-characterized responsiveness.

The release of drug from electrically-responsive hydrogels can be effected through multiple mechanisms: diffusion out of a hydrogel matrix following electrically-induced swelling, which changes pore size to alter diffusion kinetics; syneresis following electrically-induced contraction of the hydrogel; electrophoresis of charged drugs through the hydrogel; electrostatic partitioning of charged drugs; or erosion of the hydrogel complex stimulated by an electric field [340,345]. In the first of these mechanisms, the porosity of the hydrogel is enhanced in response to the application of the electric field. This behavior has been reported in ultrafiltration membranes by Pasechnik et al. [346], in poly(pyrrole) membranes by Burgmayer and Murray [347], and in liquid crystalline membranes by Bhaskar et al. [348].

More common than drug release by enhanced permeability is the forced convection of drug out of the hydrogel following electrically-induced deswelling. The drug is carried out of the hydrogel with the syneresis of water out of the matrix. Kim and Lee [349] used this behavior to achieve approximately pulsatile release of cefazoline and theophylline from anionic poly(vinyl alcohol)/poly(acrylic acid) interpenetrating polymer networks. The ionic properties of the drug were shown to have significant effect on the release rate, with the ionic cefazoline showing greater release rates and greater responsiveness to the magnitude of the applied electric field than the nonionic theophylline. Therefore, the observed release of the uncharged theophylline indicates that the deswelling of the hydrogel was responsible for drug release, while the greater release of the charged cefazoline shows that electrophoresis and electroosmosis of charged drugs can also be used for or contribute to drug release.

Similar results have been obtained in many other studies. Ramanathan and Block [350] used acetylated chitosan to achieve electrically stimulated delivery of anionic benzoic acid, neutral hydrocortisone, and cationic lidocaine, in order of delivery rate. Sawahata et al. [351] used poly(methacrylic acid) hydrogels to deliver pilocarpine hydrochloride, raffinose, and insulin with well-controlled on-off capability. Importantly, a threshold voltage was observed, below which no drug release was measured; although this value was only about 1.1 V/cm, it will likely prevent small voltages that can occur *in vivo* from causing premature drug release, as sufficient voltage to effect the conformational change must be achieved. Sutani et al. [352] used anionic gels made from acrylamide or HEMA, along with hyaluronic acid, to achieve electrically responsive delivery of the model drug D-chlorpheniramine maleate. Yuk et al. [353] used calcium alginate gels with poly(acrylic acid) to deliver hydrocortisone, observing enhanced release with increased poly(acrylic acid) content, since the ionized carboxylic acid groups allow for enhanced deswelling.

It is commonly observed that increasing the magnitude of the electric field increases the rate of drug release [350,351,354,355]. The trend is generally nonlinear, as can be seen in Fig. 19 [354], owing to the "saturation" of the deswelling response, as repulsive forces in the gel and entropic mixing forces eventually match the applied forces once the gel is sufficiently collapsed.

Another interesting observation is the common occurrence of back-flow of the released drug into the gel after release when attempting pulsatile delivery [351,356]. Typically, the drug is released when an electric field is applied, per the hydrogel's deswelling response and the resulting syneresis of water and drug out of the hydrogel. Once the electric field is turned

off, the hydrogel will return to its equilibrium state. The expansion of the hydrogel creates an osmotic pressure that convectively draws the surrounding medium into the hydrogel until equilibrium is established. During this process, some of the drug present in the surrounding medium, after having previously been released from the hydrogel, is brought in with the water (or other medium) by the convective current. Because the process is convective, it is seen to occur whether the drug concentration inside the hydrogel is greater or lesser than the concentration in the surrounding medium [340,351]. Furthermore, the size of the drug is important in determining to what extent this back-flow occurs. Small molecules are more prone to uptake by the convective force and easily transport through the pores of the hydrogel, while larger molecules require larger forces to move and can be excluded by small pore sizes [356].

Hydrogels that erode in response to an applied electric field have also been synthesized [357,358]. Kwon et al. [357] formed a complex comprised of poly(ethyloxazoline) and poly(methacrylic acid), which exhibit hydrogen bonding between the oxazoline and carboxylic acid groups. Upon application of an electric field, electrolysis of water produces hydroxyl ions at the cathode, increasing the pH near the cathode which in turn causes deprotonation of the carboxylic acid groups and resultant loss of hydrogen bonding capability. The complex therefore disintegrates into two separate water-soluble polymers, releasing any encapsulated drug as the surface dissolves away. Using insulin-loaded complexes formed into disks and applying a 5 mA current in pulses, this system showed the ability to deliver insulin at a constant rate in pulsatile fashion. This zero-order release profile from the disk is characteristic of surface erosion in a slab geometry, which the disks approximate [359]. Therefore, surface erosion of the hydrogel enables well-controlled drug delivery by liberating the encapsulated drug upon erosion.

The benefit of these erodible systems is that the erosion of the hydrogel liberates the drug completely into the surrounding medium, rather than requiring transport by diffusion or convection through hydrogel pores, which can severely limit the rate of release of large molecules. Defects in the gel matrix may make the release rate susceptible to wide variations, however. Nevertheless, such systems show promise as potential drug delivery depots for long-term, pulsatile release of a wide range of both large and small molecule drugs.

In vivo tests of electrically responsive hydrogels have been performed. Kagatani et al. [360] demonstrated a poly(dimethylaminopropylacrylamide) gel loaded with insulin as a subcutaneously implanted drug delivery depot in rats. A schematic of the electrode system used is shown in Fig. 20. The anode was applied to the abdomen of the rats, and consisted of an acrylic casing with silicon gum, stainless foil, and an electrical wire attached to the inner surface and saline filling the casing. The cathode was applied to the back of the rats, and was the same setup as the anode with the addition of a foam rubber sponge and cotton in the casing to ensure contact with the skin to maintain a complete circuit. The drug-loaded gels were inserted under the abdominal skin by surgical incision. Direct current of 1.0 mA was applied for 1 min initially, and for 10 min after 2 h to give pulsed doses of insulin.

The results of Kagatani et al., shown in Fig. 21, showed pulsatile release of insulin only when current was applied which led to a noticeable decrease in plasma glucose concentrations [360]. Release was rapid and well-controlled, with no discernible lag time in response and no observed leakage of insulin between pulses. Furthermore, bioavailability calculations showed that the gel system used in the rats carried sufficient insulin for up to 1670 individual pulses, although this assumes ideal total release, which could be affected by insulin aggregation or binding within the gel. Rats in this experiment did not show any visible skin irritation from the applied electric field, as low current densities were used. The results of this experiment are therefore quite encouraging as implantable drug delivery depots for enabling externally-controlled, pulsatile release of drug compounds over a long time period, especially with more recent improvements to iontophoretic devices.

8. Shear stress responsive hydrogels

Stimulus-responsive hydrogels capable of responding to mechanical perturbations in the environment are classified as shear-responsive hydrogels. Upon exposure to shear-stress these hydrogels undergo some conformational change that imparts either shear-thinning or shear-thickening behaviors to the polymer network [361,362]. These characteristic responses to shear can be harnessed for a wide variety of biomedical applications ranging from injectable hydrogel networks for drug delivery and tissue engineering to wound repair [363–366]. These applications, specific polymer compositions, and the theoretical considerations behind their behaviors will be explored.

8.1. Theoretical considerations

The mechanical properties of the hydrogel networks will dictate their response to applied shear-stress and the applications to which they are suitable [367]. Therefore, a great deal of emphasis has been placed on elucidating the mechanisms behind polymeric and hydrogel network properties and responses to mechanical perturbation [368–371].

Polymeric systems, such as hydrogels, typically exhibit a viscoelastic mechanical behavior upon deformation, *i.e.*, a behavior that is an intermediate between a viscous (liquid) and elastic (solid) material [370]. When stress is applied, viscous materials will strain linearly with time and resist shear flow. Elastic materials will strain with applied stress and return quickly to the original state once that stress is removed [372,373]. Viscoelastic materials, exhibiting a combination of viscous and elastic properties, will strain in a time-dependent manner upon application of a stress. This time-dependency is due to a complex rearrangement of molecules that occurs upon a macroscopic mechanical deformation [368]. In polymeric systems, the application of stress will result in the molecular rearrangement of a portion of the polymer chain. The resultant movement is called creep. The overall polymer network will remain solid even while the polymer chains rearrange, or creep, due to the applied stress. This results in an accumulation of back stress in the material. When the applied stress and internal back stress reach equilibrium, the material will no longer creep. Upon removal of the applied stress, the back stress causes the polymer to recover. This combination of polymer creep, a viscous behavior, and material recovery, an elastic behavior, results in the viscoelastic properties exhibited by polymer networks [368,369].

In addition to the described creep behavior, viscoelastic polymers will also exhibit stress relaxation, wherein the material, upon being subjected to constant strain, will relax and stress will gradually decrease [374]. These viscoelastic behaviors can be modeled using a linear combination of elastic and viscous components, modeled as springs and dashpots, respectively. The Maxwell, Kelvin–Voigt, and Standard Linear Solid models use different combinations of these components to predict the stress and strain interactions and temporal dependencies in response to different loading conditions [369].

The elastic component of the polymer network can be modeled as a spring with the elastic modulus, E. The modulus represents the energy stored in the spring. The corresponding relationship between stress, σ, and strain, ε, can then be described by Eq. (41):

$$\sigma = E\varepsilon \quad (41)$$

The viscous components of the polymer network are modeled as dashpots, or mechanical dampers that resist perturbation due to friction from a viscous force. The dashpot dissipates energy at a rate relative to the viscosity of the modeled system and can be modeled by Eq. (42):

$$\sigma = \eta \frac{d\varepsilon}{dt} \quad (42)$$

where η is the viscosity of the material, σ is the stress, and $d\varepsilon/dt$ is the strain rate.

The Maxwell model is represented by an elastic spring and viscous dashpot connected in series, as shown in Fig. 22 and described by Eq. (43) below:

$$\frac{d\varepsilon_{\text{total}}}{dt} = \frac{\sigma}{\eta} + \frac{1}{E}\frac{d\sigma}{dt} \quad (43)$$

The model, under constant stress, has two strain components. The first is attributed to the elastic behavior of the polymer system and occurs instantaneously upon application of stress. The second is due to the viscous behavior of the polymer, and increases in a time-dependent manner after onset of stress. In constant strain conditions, the model accurately predicts that stress decreases exponentially with time when put under constant strain. However, it does not capture creep behavior accurately, as it incorrectly predicts that strain increases with time instead of the observed trend of strain rate decreasing with time [369,372].

The alternative Voigt model places the viscous dashpot and elastic spring in parallel, instead of in series (Fig. 22), and is described by Eq. (44) below:

$$\sigma(t) = E\varepsilon(t) + \eta\frac{d\varepsilon(t)}{dt} \quad (44)$$

When exposed to constant stress, the model predicts that the strain will tend to a constant value, σ/E, as time approaches infinity. This represents the material deforming at a

decreasing rate and reaching a steady-state strain. The material will recover to its original undeformed state once the stress is removed. This model, while capable of accurately describing creep, is much less accurate at predicting stress relaxation [368,369].

The standard linear solid model is a combination of the Maxwell model and a spring in parallel. The schematic is shown in Fig. 22 and described by Eq. (45) below:

$$\frac{d\varepsilon}{dt} = \frac{(E_2/\eta)((\eta/E_2)(d\sigma/dt) + \sigma - E_1\varepsilon)}{E_1 + E_2} \quad (45)$$

Upon application of a stress, the material will deform instantaneously due to the elastic portion of the strain. After this initial response, deformation will continue and approach a steady-state strain, which represents the viscous portion of the strain. This model, although more accurate than both the Maxwell and Voigt models, inadequately predicts the strain under certain loading conditions. Furthermore, it is much more difficult to handle mathematically than the other models [369,374].

Experimental determination of the creep and stress relaxation moduli can be readily obtained. For creep determination, the material of interest is exposed to steady uniaxial stress σ_0 and the time-dependent strain $\varepsilon(t) = \delta(t)/L_0$ is measured [375]. The ratio of time-varying strain to applied constant stress provides the creep compliance:

$$C_{crp}(t) = \frac{\varepsilon(t)}{\sigma_0} \quad (46)$$

For stress relaxation determination, a steady strain is applied to the material and the time-dependent stress is measured [375]. The relaxation modulus is the ratio of time-varying stress to the applied constant strain as described below:

$$E_{\text{rel}}(t) = \frac{\sigma(t)}{\varepsilon_0} \quad (47)$$

While insights into the creep and stress relaxation of polymeric species are incredibly important, the limitation is on the time scale of analysis. Creep and stress relaxation tests study the material responses at longer time scales, ranging from minutes to days. Dynamic tests, which assess the response of the polymeric network to sinusoidally applied stress or strain, allow for elucidation of material responses at much shorter time scales [375]. This experimental method, known as small amplitude oscillatory shear (SAOS), is a small deformation rheological technique carried out within the linear region of a polymer network [376]. In this linear viscoelastic region, the hydrogel properties are independent of the magnitude of applied stress or strain [371,377,378].

In practice, either a sinusoidal shear strain or shear stress is applied at an angular frequency, ω, and described by $\gamma(t) = \gamma_0(\sin(\omega t + \delta))$ or $\tau(t) = \tau_0(\sin(\omega t + \delta))$, respectively. The measured shear stress or shear strain is a phase-shifted sine wave, described by either $\tau(t) = \tau_0(\sin(\omega t + \delta))$ or $\gamma(t) = \gamma_0(\sin(\omega t + \delta))$. In a purely elastic material, the stress and strain

curves are completely in-phase with one another, *i.e.*, the phase angle, δ, is zero. Conversely, in a purely viscous material, the two curves are out of phase by 90°. As expected, a viscoelastic material, having intermediate properties between a purely elastic and viscous material, will result in an observed phase angle somewhere between 0° and 90° [367,370,371,377].

The relationship between the oscillating stress and strain can be described by the complex modulus, *G*, which can be resolved into two components, *G′* and *G″*,

$$G = G' + iG'' \quad (48)$$

G′, the storage modulus, is the real or in-phase component of the complex modulus. It measures the stored deformation energy during applied shear and, therefore, represents the stiffness or elastic contribution of the material. The loss modulus, *G″*, is the imaginary or out-of-phase component of the complex modulus. This modulus captures the energy dissipation during applied shear, *i.e.*, the liquid-flow or viscous response. The magnitudes of *G′* and *G″*, and the ratio between them, describe the elastic *versus* viscous character of a viscoelastic material. Specifically, if $G' > G''$ the material behaves more like an elastic solid. Conversely, if $G'' > G'$, the material will behave more like a viscous liquid [370,371,374,378].

The gelation kinetics of hydrogel systems can be determined by monitoring the temporal dependence of *G′* and *G″*. For most systems, the curves for *G′* and *G″* intersect as time increases and the magnitude of *G′* surpasses that of *G″*. This indicates the transition of the material into a robust gel from an initial liquid-like state [367,379]. This so-called "cross-over" point can also be observed for temperature-responsive gels, where the sol–gel transition is captured at the temperature, not time, where the *G′* and *G″* curves intersect [380].

After gelation, gel stiffness can be observed over long and short timescales by modulating the frequency of the oscillating shear stress or strain and measuring the corresponding *G′* and *G″* values. The gel may act very differently at high frequency, or short timescales, *versus* low frequency, or long timescales [367]. To elaborate this point, the structures within a gel at short times (high frequency) have not had time to respond to applied force and, therefore, appear stiff and elastic. That same gel at long times (low frequency) has had time to respond and adjust, resulting in a viscous material that can flow and rearrange [381]. The crossover frequency denotes at which frequency or timescale the gel transitions from being predominately elastic ($G' > G''$) to predominately viscous ($G'' > G'$). The final gel stiffness will depend on the ratio between *G′* and *G″* at long time scales [382].

As emphasized by Yan et al., both the gelation kinetics and the final gel stiffness are essential material parameters when determining the ultimate success and utility of a hydrogel formulation for biomedical application. Specifically, these parameters will impact the ability of the hydrogel matrix to homogeneously suspend therapeutic cargo, promote cellular migration, maintain cell populations, and preserve its mechanical properties [365,367,383,366,384].

Exploration of hydrogels and polymers within the linear viscoelastic region, where the properties are independent of the magnitude of shear amplitude, clearly provides valuable insight into polymer behavior. This linearity, at a molecular level, is attributed to the presence of molecular entanglements whose destruction by flow is balanced by their formation due to Brownian motion. When the net change in the number of entanglements is zero, the material exhibits linear viscoelastic behavior. Once this balance is eliminated, the material will exit the linear region and enter into non-linearity [381,385].

These non-linearities in polymer response typically appear when the amplitude of applied shear is large or when material properties change due to deformation, such as in shear or strain-thinning and shear or strain-thickening systems, *i.e.*, in cases where the net change in molecular entanglements no longer equals zero [386]. In industrial applications, polymers are typically exposed to large deformations during processing and many hydrogels that have utility for drug delivery and tissue engineering applications shear-thin for injectable delivery [387,388]. Therefore, it is important to consider the polymer properties in the non-linear regions.

There are a number of experiments that can probe the non-linear viscoelastic response of polymer networks; two powerful techniques are the step shear rate test and large amplitude oscillatory shear (LAOS).

The step shear rate experiment measures the viscosity, η, of a polymer network as a function of shear rate, $\dot{\gamma}$, by applying a specific shear rate in a step-wise manner until the system reaches steady state. With the provided information, the polymer network can be deemed as shear-thickening, where dynamic viscosity increases with shear rate, or shear-thinning, where dynamic viscosity decreases with strain rate. Shear thinning is predominately attributed to the alignment of polymer chains or micro-structures under flow, ultimately leading to decreased drag or friction, and a reduced viscosity [382]. Shear-thickening, conversely, occurs when an ordered system, such as a colloidal solution, becomes disordered in response to applied shear. This disorder results in an increase in viscosity, hence the shear thickening behavior [389,390]. Shear-thinning or thickening behaviors affect how rapidly a polymer solution can be processed, which is essential for industrial processing techniques.

However, there are a number of limitations of this experimental technique that limit its utility. Specifically, it is unable to capture the polymer response to high deformation at short time scales because the system has yet to reach a steady state. The elastic response of the viscoelastic material is also lost because the polymer cannot be observed in its dynamic state. Finally, and most detrimentally to the investigation of the material properties of hydrogel systems, the step shear rate experiment will not work for chemically crosslinked networks or networks held together by delicate hydrogen bonds, which are responsible for a significant portions of physically crosslinked gels [8,388]. To overcome this particular limitation, a strain- or stress-controlled rheometer operated with the motor in steady mode can capture the viscosity as a function of shear rate for crosslinked materials, but the response to high deformation at short time scales is still lost [391].

LAOS is very similar to the previously described SAOS experiments used to obtain G' and G'' in the linear viscoelastic region of polymer systems. However, instead of delivering small amplitude oscillations to the system in order to exclusively probe the linear region, the amplitudes are increased and the polymer moves into the non-linear region of its behavior. Compared to the step shear rate experiment, LAOS requires no sudden or drastic change in speed and does not need the polymer system to settle to a steady-state position before obtaining the data of interest. Additionally, and most importantly, both the strain amplitude and frequency can be controlled to investigate different properties and systems of interest [382,386,388]. The imposed shear strain and the corresponding shear rate in LAOS are the sinusoidal curves $\gamma(t) = \gamma_0 \sin(\omega t)$ and $\dot{\gamma}(t) = \gamma_0 \cos(\omega t)$, respectively. Due to the periodic nature of the applied shear strain, Fourier analysis can be completed on the collected data, which allows for the filtering of noise and artifacts [385]. The Fourier decomposition of LAOS non-sinusoidal stress data provides a series containing only odd harmonics (shown in Eq. (49)):

$$\tau_{12} = \sigma(t) = \sum_{j=1}^{\infty} \sigma_j \sin(j\omega t + \delta_j) \quad (49)$$

Only odd harmonics are considered in this analysis because the even harmonics provide no valuable information to the stress output having been attributed to noise, secondary flows, slip, and transient responses [387]. The higher odd harmonics, $j = 3$ and above, contribute to the non-sinuosidal stress responsive curve in non-linear viscoelastic materials [385,387]. For the linear case, the amplitudes of these higher harmonics are all zero and the above expression will still hold true. Furthermore, σ_1 is linear for a given strain amplitude γ_0 and the parameters G', G'', and δ_1 are all independent of γ_0 [385].

In the nonlinear viscoelastic case, the stress response, $\sigma_j(\gamma_0,\omega)$, and the phase difference between the stress response and applied shear strain, $\delta_j(\gamma_o,\omega)$, are determined from discrete Fourier transforms. Notably, they both depend on the strain amplitude and frequency of the applied strain, which solidifies their non-linearity [382]. From the first harmonic of the stress response curve obtained from discrete Fourier transform, the non-linear viscoelastic properties can be adequately described [388]. The viscoelastic moduli, G' and G'', specifically, can be defined by the following expression:

$$\sigma(t) = \gamma_0 \sum_{n,\text{odd}} [G'_n(\omega, \gamma_0)\sin(n\omega t) + G''_n(\omega, \gamma_0)\cos(n\omega t)] \quad (50)$$

This expression captures the portions of the stress response that are in phase (sin) and out of phase (cos) with the applied large amplitude sinusoidal strain. While viscoelastic parameters G' and G'' are readily calculable and fully describe the material response in the linear region, this does not hold true in the non-linear case [382]. This breakdown occurs due to the dependence of G' and G'' on strain amplitude, $G'(\gamma_0)$ and $G''(\gamma_0)$, which results in a distortion of the stress response curve to a sinusoidal shear strain deformation (as shown in Fig. 23) [387,388,392]. Therefore, instead of defining the bulk material viscoelasticity, G' and G'' are specific to the particular experiment that was performed [387]. If measured

carefully at a fixed frequency, however, $G'(\gamma_0)$ and $G''(\gamma_0)$, can provide useful information about the characteristics of a gel within the non-linear region [385,388].

Four different types of non-linear strain-dependent behavior emerge upon exploration of G'(γ_0) and $G''(\gamma_0)$: (1) strain thinning, (2) strain hardening, (3) weak strain overshoot, and (4) strong strain overshoot. Strain thinning occurs when G' and G'' decrease with increasing strain amplitude. This behavior is commonly observed in polymeric systems and can be attributed to the alignment of polymeric chains in the direction of flow, much like shear thinning [381,382,388,393]. Strain hardening, or shear thickening, behaves in the exact opposite manner, with G' and G'' increasing with increasing strain amplitude. The resistance to flow alignment occurs due to the formation of microscale complexes which prevent the orientation of the polymer chains with the applied flow [382,388–390]. Weak strain overshoot describes a system whose loss modulus, G'', experiences a local maximum before decreasing along with the storage modulus, G'. This behavior is likely due to polymers with weak complexes that associate upon the initiation of strain (initial increase in G'') before being destroyed at higher strain amplitudes (subsequent decrease in G'') [382]. This behavior is extremely common in soft glassy systems, block copolymers, and xanthan gum solutions, and, therefore, of interest with hydrogel systems [382,388]. The final type, strong strain overshoot, exhibits local maxima for both G' and G''. Thus, it is an intermediate between strain-hardening, where G' and G'' both increase, and weak strain overshoot, where G'' has a maximum but G' exclusively decreases. This response is attributed to polymers with stronger associations than those seen in type (3), but weaker than those observed in type (2): most likely, hydrophobic interactions or micellar clusters [388].

Numerous mathematical and experimental methods are used to calculate these parameters and have been thoroughly reviewed by Hyun et al. [388]. However, it has been argued in literature that the first harmonics of the storage and loss moduli at a given strain amplitude, $G_1{'}(\gamma_0)$ and $G_1{''}(\gamma_0)$, are sufficient to describe the material [394]. This is because the non-linear stress response curve deviates no more than 15% from its purely sinusoidal linear counterpart due to contributions from higher harmonics [388,394]. So, while complex calculations of the non-linear viscoelastic properties, $G'(\gamma_0)$ and $G''(\gamma_0)$, can indeed be useful, it is more important to investigate the polymer network at a variety of strain amplitudes outside of the linear range to gain valuable insight into its rheology and overall behavior.

Both linear and non-linear viscoelasticity are necessary to consider when completing a rheological analysis of a hydrogel system, particularly those that exhibit any type of shear-responsive behavior. The ability and extent to which a hydrogel responds to an applied shear can affect not only the application of, but also the ultimate success of an engineered hydrogel system. The remainder of this section will be dedicated to providing several examples of shear-responsive hydrogel systems, with special focus on the mechanism by which the shear-response is conferred and the utilization of viscoelastic parameters to characterize the response.

8.2. Shear-thinning hydrogels

Shear-thinning hydrogels exhibit decreased viscosity as a function of increased applied shear force. These systems must be robust prior to the introduction of shear, flow or thin during the application of shear, and recover their mechanical properties, *i.e.*, elastic moduli, after the cessation of shear [365,367]. This behavior is predominately observed in self-assembled polymeric systems of both natural and synthetic origin. In self-assembled systems, the forces that favor assembly (hydrophobic interactions, hydrogen bonding, and electrostatic interactions) overcome the forces opposing assembly (electrostatic repulsion and solvation) to form stable, physically cross-linked networks [395]. However, these forces are inherently weak and can be disrupted during the application of a substantial shearing force, which allows the network to flow or thin. Once the external shear is removed, the hydrogel network can reassemble and recover its structure, *i.e.*, self-heal [365,395]. The kinetics of the shear-thinning and self-healing processes, as well as the mechanical properties both before and after shear, will determine the ability of the hydrogel to be utilized for biomedical applications such as injectable hydrogel systems for drug delivery and tissue engineering, wound healing, osteoarthritis treatment, and bio-film disruption on implanted biomaterials [365,383,366,384, 396–398]. The various applications and types of shear-thinning hydrogels, as well as the respective mechanisms by which they shear thin, will be discussed in detail.

8.2.1. Injectable hydrogel systems—The ability of shear-thinning hydrogels to flow under applied shear stress makes them attractive candidates for injectable systems. The requirements of injectable systems are as follows [365,384,399,400]:

1. Biocompatibility of the hydrogel network, its precursors, and any degradation products.

2. Reasonable force required to induce shear flow.

3. *Ex vivo* gelation and *in vivo* recovery after shear must occur rapidly and under physiological conditions.

4. Hydrogel network structure must be tunable for the desired biological functionality.

5. Mechanical stability for the entire duration of its use.

6. Controlled biodegradability.

The benefits of injectable hydrogels, as opposed to surgically inserted systems, are numerous and include their non-invasive implantation, ability to tightly and completely form to a cavity, and an ability to easily and homogeneously incorporate therapeutic molecules and even cells [365,366,384,400]. *In situ* forming hydrogels are injected and undergo a sol–gel transition upon entering the body cavity due to a change in pH [401–404], temperature [403,405,406], or ion concentration [407–409].

Shear-thinning hydrogels, when compared to *in situ* forming hydrogel systems, have several advantages. The shear-thinning hydrogels undergo a sol–gel transition *ex vivo*, which allows for complete and meaningful characterization of the system proper-ties prior to injection [365]. Furthermore, the gelation conditions can be tightly controlled and are not subject to

the variability experienced *in vivo* [410]. Additionally, the shear-thinning hydrogels have been shown to regain their physical properties after injection more rapidly than *in situ* forming gels and are far less likely to leach into neighboring tissues [404,411–413]. The shear-thinning hydrogels appropriate for injectable delivery for drug delivery and tissue engineering can be composed of a multitude of components ranging from naturally derived proteins to engineered peptides to synthetic polymer species and colloidal systems.

8.2.1.1. Natural protein-based hydrogels: Naturally derived protein-based hydrogels are potentially excellent candidates for biomedical applications due to their intrinsic biocompatibility, biodegradability, and desirable mechanical properties [414,415]. Fibrous proteins, such as silk, possess mechanical properties far surpassing other naturally- and synthetically-derived polymers due to repetition in their primary structure resulting in a very consistent and homogeneous secondary structure that yields incredibly strong yet flexible materials [416–418]. Silk fibroin, the main protein component in silk, will, at high enough concentrations, self-assemble into a hydrogel that is composed of β-sheet-rich fibrils [419,420]. The presence of β-sheets in the hydrogel network directly impacts the material strength and biodegradation profile resulting in a strong and tough hydrogel capable of being degraded over long time periods by enzymatic activity [419,421,422]. Additionally, silk fibroin, its resultant silk hydrogel, and degradation by-products have been shown to be cytocompatible and non-immunogenic [421,423].

Modulating temperature, pH, protein concentration, and ion concentration can control the gelation kinetics and mechanical properties of the silk fibroin hydrogels. Specifically, gels with higher compressive strength and moduli were achieved at increased temperature and initial protein concentration. Increased gelation rate is triggered by increased temperature, decreased pH, increased Ca^{2+} concentration and increased silk fibroin concentration [419,424,425]. However, the gelation kinetics achieved by modulating the previously mentioned parameters were still not rapid enough to achieve homogeneous cell encapsulation at physiological conditions. A sonication technique developed by X. Wang et al. resulted in silk fibroin hydrogels capable of gelling within 30 min to 2 h by initiating the formation of β-sheet-containing fibers *via* spinning. This acceleration of the gelation process resulted in human bone marrow derived mesenchymal stem cells (hMSCs) being successfully and homogeneously incorporated into the hydrogel matrix and capable of being sustained for 21+ days [426].

Yucel et al. expanded upon this previously developed sonication technique to form silk fibroin hydrogels capable of exhibiting shear-thinning behavior. Briefly, silk fibroin was vortexed, instead of sonicated, which initiated the formation of β-sheet-containing fibers, and enhanced the self-assembly of the hydrogel network. The gelation kinetics were controlled by varying the duration of vortexing, assembly temperature, and/or the initial protein concentration. Most importantly, these hydrogel networks exhibited shear thinning at high enough shear strain amplitudes and recovered their G' to near pre-strain values immediately after cessation of shear (Fig. 24). The shear-thinning behavior was attributed to the temporary release of intercluster dangling chain entanglements, which allows large β-sheet-rich clusters to slide past one another. This mechanism is proposed as an alternative to the rupture of permanent, intermolecular β-sheet crosslinks, which was deemed unlikely due

to the very rapid recovery of material post-shear [427]. These shear-thinning silk fibroin gels have great promise as injectable tissue engineering scaffolds for the homogeneous administration of viable cells [427,428].

8.2.1.2. Synthetic protein-based hydrogels: While naturally derived protein-based hydrogels have shown great utility for tissue engineering and drug delivery applications, there are some limitations associated with their use. Specifically, they are derived from natural sources and, therefore, suffer from a lack of batch-to-batch consistency with regards to their material properties [367]. An alternative to naturally derived proteins is the utilization of synthetic polypeptides that mimic the structure and function of the natural materials. These recombinant protein hydrogels can be engineered to not only include the necessary primary sequences to induce the desired secondary structural characteristics, such as α-helices and β-sheets, but also to contain functional epitopes to incorporate biological functionality and activity. The peptide sequence can be readily manipulated to form hydrogel networks with the properties required for the specific applications of interest [367,414,429].

Protein hydrogels composed of engineered polypeptidic sequences based on leucine zippers have shown promise as shear-thinning materials. Leucine zippers are responsible for DNA, protein, and transcription factor linking within the cell [365,430]. They contain a seven-residue heptad peptide sequence, (abcdefg) motif, which repeats over the length of the polypeptide. The 'a' and 'd' positions of the repeating sequence are hydrophobic in nature, typically leucine, while the 'e' and 'g' residues are charged species. The amino acids assemble into a helical conformation (Fig. 25) with the hydrophobic moieties relegated to one side of the helix [415,429,431]. The coiled-coil dimers are formed as a result of the hydrophobic interactions between the two (abcdefg) helices but are stabilized due to the pH-dependent interaction of the charged species [365,415,430,432]. The inclusion of responsive moieties into the a, b, e or g positions can confer environmental-responsiveness to the peptidic structures, resulting in the self-assembly of the sequences into nanostructures under desired physiological conditions [367,431]. These nanostructures can further assemble into hydrogel network materials upon the inclusion of appropriate amino acids into positions 'b', 'c', and 'f' or by forming block copolymers containing a coiled-coil motif such as the leucine zipper [413,415,432–439].

B.D. Olsen et al. formed a triblock copolymer composed of coiled-coil end blocks (P) joined by a nonapeptide linker of various length (C_x), forming $PC_{10}P$ with 10 nonapeptide repeat units or $PC_{30}P$ with 30 nonapeptide repeat units (Fig. 26). Either $PC_{10}P$ or $PC_{30}P$ protein was hydrogelated at pH 7.6 and 4 °C for 2–4 h. For gelation to occur, the coiled-coil domains formed into pentameric bundles *via* hydrophobic and ionic interactions, which function as physical crosslinks to maintain the integrity of the hydrogel network structure. Upon exposure to shear force, these systems reveal strong shear-thinning behavior and very rapid self-healing kinetics. When sheared in physiological conditions, the original modulus was recovered in less than a minute. Changing the midblock length and the endblock composition modulated the final gel properties and shear-thinning capabilities [440]. The $PC_{10}P$ hydrogel recovered to 98% of its original elastic modulus within 1 min, whereas the $PC_{30}P$ exhibited a small permanent decrease in the final modulus but did recover after shear.

This shear thinning behavior is attributed to the coiled-coil end block interactions and the yielding that occurs within the bulk of the material [413,441]. CHO K1 cells were encapsulated within the hydrogel network prior to gelation and subsequently injected through a 22-gauge needle to assess the utility of this network as an injectable system. Not only did the hydrogel shear thin while undergoing injection, but over 95% of the cells survived post-shear [413].

Another type of synthetic poly-peptide hydrogel capable of undergoing shear thinning are di-block copolymers. These copolymers are amphiphilic in nature, with a charged hydrophilic block composed of either poly(L-lysine) or poly(L-glutamic acid) salts and a hydrophobic block consisting of either poly(L-leucine) or poly(L-valine) [442]. The self-assembly was governed by the hydrophobic and electrostatic interactions between the different blocks on the copolymer. Parameters including sol–gel transition behavior and elastic modulus could be controlled by the composition of the charged block and hydrophobic to hydrophilic ratio, respectively. Upon undergoing shear deformation, the hydrogels were capable of recovering their original properties to 80–90% within a rapid period of time. The shear-thinning behavior was attributed to the transient disruption of the interconnections between gel domains, as opposed to the complete disassociation of the hydrophobic and electrostatic associations [442–444]. The high concentration of α-helices within the polymer network due to the presence of leucine also aided in the shear-thinning and self-healing behaviors, as the associations between the α-helices could be readily disrupted and reformed with rapid kinetics [445,446]. The amphiphilic diblock copolypeptide hydrogels have shown promise as tissue engineering scaffolds for tissues in the central nervous system. They readily undergo shear-thinning during injection, reform rapidly *in vivo* and, most importantly, show minimal cytotoxicity and immunogenicity while still encouraging interaction with the existing brain tissue [447].

Another class of synthetic polypeptide hydrogels are the so-called MITCH, or mixing-induced, two-component hydrogel systems [448]. The two separate components assemble *via* molecular recognition after mixing at physiological conditions. The MITCH system developed by Foo et al. consists of

1. WW domain consisting of preserved tryptophan residues linked together with an RGD-rich hydrophilic spacer [449,450].

2. Proline-rich protein domain linked together by a hydrophilic spacer.

The intracellular WW domain interacts with the proline-rich protein with micromolar binding affinities resulting in a physically crosslinked gel (Fig. 27) [451,452]. The binding strength and specificity can be modified by adjusting the frequency of the repeated domains (either tryptophan or proline) within each segment. This adjustment of binding strength at the molecular level can dramatically impact the bulk viscoelastic properties of the hydrogel. For example, the G' values can range from ~9 to 50 Pa. Furthermore, by simply increasing the binding affinities between the two components, the duration required for the polymer to self-heal decreases from ~30 min to less than 5 min [448].

Unlike many of the other protein-derived self-assembling systems, the MITCH systems undergo a sol–gel transition without the need of environmental changes in pH, temperature,

or ion concentration. For this reason, they are particularly attractive for tissue engineering applications that require cell encapsulation, due to the ability to gel under physiological conditions. Thus far, adult neural stem cells (NSC), PC-12, HUVEC, and adipose-derived stem cells have been successfully encapsulated within the MITCH gels and remain physiologically active [365,415,453].

8.2.1.3. Peptide-based hydrogels: Peptide-based hydrogels are composed of short amino-acid sequences that can self-assemble into a hydrogel network. The mode of self-assembly, material properties and biomaterial functionalities can be engineered into the peptide sequence by using both naturally- and synthetically-derived amino acids. These amino acids impart the desired behaviors through an array of non-covalent interactions such as hydrogen bonding, electrostatic interactions, and hydrophobic interactions. Certain amino acids are even capable of inducing temperature or electrochemical responsive behaviors into the peptide sequence of interest [415,454,455].

One such family of peptides, called 'MAX' peptides, self-assembles into β-hairpin structures that form hydrogel networks capable of shear thinning behavior. Developed by Pochan and Schneider, these MAX peptides have been studied for well over a decade [455–461]. The first generation peptide, dubbed MAX1, consisted of two β-strands composed of alternating hydrophilic lysine (K) and hydrophobic valine (V) residues linked by a tetra-peptide type II' β-turn spacer, *i.e.*, $(VK)_4$-Val^D-Pro-Pro-Tyr-$(VK)_4$ [455]. The lysine residues, when protonated, prevent any aggregation or self-assembly due to electrostatic repulsion [455,458]. The lysine charge can be neutralized by changing the pH of the environment [455], shielded by increasing salt concentration [458], or collapsed by increasing temperature [456]. The neutralization, collapse or shielding of the lysine charge results in a conformational change within the peptide sequence and triggers gelation. The process of gelation starts by the rearrangement of the peptide sequence into β-hairpin structures exhibiting a hydrophilic and hydrophobic face. These β-hairpins then assemble into fibrils, which interact and entangle to form rigid, fibrillar hydrogels. The presence of physical crosslinks in the form of hydrophobic interactions and hydrogen bonding stabilize the hydrogel but also allow for shear-thinning upon the introduction of a shearing force (Fig. 28) [411,458,462,463]. The manipulation of the peptide sequence, concentration, ionic strength, and temperature can result in hydrogels exhibiting vastly different porosities, moduli, and degradation kinetics [410]. For example, MAX8, a newer generation peptide in the MAX family, substitutes a lysine residue at position 15 with a glutamic acid residue. This simple modification results in a much more rapid gelation process and a stiffer gel structure [411]. Because of the easily modifiable peptide sequence, the gel properties can be tailored for a given application, such as ensuring homogeneous distribution of a therapeutic for drug delivery or cell cargo for tissue engineering [367,410,464].

MAX1 and MAX8 peptides and those self-assembled systems that rely on β-hairpin and fibril formation are highly susceptible to shearing forces [365]. Interestingly, when the MAX1 and MAX8 hydrogel networks were probed during steady shear flow, there was minimal alignment of the fibril nanostructures. Thus, the shear thinning of the gel is not due to fibril alignment and slipping under applied shear. Instead, the shear-thinning behavior is a result of the gel fracturing into microdomains (as shown in Fig. 29). These microdomains

can flow past one another under flow conditions; however, once shear stops, they immediately percolate and the gel stiffens ($G' > G'$). These domains will relax over time and interpenetrate with one another, further stiffening the gel and contributing to the self-healing properties of the system [410].

Both MAX1 and MAX8 peptide hydrogels are considered cytocompatible and noninflammatory [465]. Specifically, these hydrogels were found to exhibit minimal-to-no cytotoxicity to a variety of cell lines including NIH3T3 murine fibroblasts, C3H10T1/2 mesenchymal stem cells, hepatocytes, MG63 osteoblast progenitor cells, and primary articular chondrocytes [410,411,466,467]. The homogeneous distribution C3H10T1/2 cells in MAX8 and MAX1 hydrogels is dependent on the gelation kinetics. As shown in Fig. 29, the MAX8 gels have a much more homogeneous distribution, which can be attributed to their increased gelation speed when compared to the MAX1 system [411]. Upon cessation of shear, the MAX8 gels quickly recover their initial G' values. This rapid recovery preserves the homogeneous distribution of cells within the polymer matrix [411]. Interestingly, these hydrogel networks possess inherent anti-microbial activity against several bacterial strains including *Staphylococcus epidermidis*, *Staphylococ-cus aureus*, *Streptococcus pyogenes*, *Klebsiella pneumoniae*, and *Escherichia coli*. The hydrogels have been shown to disrupt the cellular membrane of these bacterial cells, which causes bacterial death. Intriguingly, the hydrogels appear to exhibit selective toxicity to bacterial cells but spare mammalian cells [468]. These systems may be able to act as anti-fouling surfaces for biomaterials as they would disrupt any biofilm that attempts to form around the implanted material [397].

MAX1 and MAX8 hydrogel networks have been used as injectable drug depots for the delivery of therapeutic molecules. The release kinetics of the peptide hydrogels was explored using model therapeutics of various molecular weight and charge. Specifically, dextran at 20, 70 or 150 kDa or lactoferrin protein (~77 kDa) was incorporated into the peptide hydrogel prior to gelation. The mixture was then sheared and allowed to re-solidify before being monitored for 30 days to measure bulk molecule release. It was determined that mesh size and electrostatic interactions between the macromolecule and the hydrogel had the greatest impact on release kinetics. As molecular weight increased, the interactions between the therapeutic and the hydrogel mesh hampered diffusive capability. Similarly, negatively charged species were more likely to interact with the mesh and release much slower than the positively charged molecules [469]. MAX8 peptide hydrogels were further explored as drug delivery vehicles for curcumin, a therapeutic with anti-inflammatory, anti-tumorgenic, and antioxidant abilities. Altunbas et al. determined that curcumin could be homogeneously suspended in the peptide hydrogel matrix and be released over extended periods of time (~15 days) and exert cytotoxic effect over DAOY human medulloblastoma tumor cells [470].

Alternative peptide sequences have also shown promise in the formation of shear-thinning hydrogel networks. Decapeptides composed of an alternating charged/neutral amino acid pattern, were synthesized by Yu et al. KVW10 and EVW10 consist of hydrophobic/neutral valine residues alternated with cationic lysine or anionic glutamic acid residues, respectively [471]. Either end of the decapeptide chains was capped by a functional group to remove any

additional charged moieties that could impede self-assembly. Specifically, an acetyl group capped the N-terminus, while the C-terminus was capped by an amide. The self-assembly of the decapeptides were driven by the mutually attractive but self-repulsive behavior exhibited by the KVW10 and EVW10 decapeptide sequences. Namely, when alone in solution, the species will not gel due to self-repulsion. However, when mixed together, self-assembly will occur because the mutual attraction between the charged residues of the peptides drives physical interaction. This behavior is independent of pH and ionic-strength, which is attractive for *in vivo* and *in vitro* applications, and will also occur at very low peptide concentrations [471,472]. Similar to the MITCH systems, these peptide hydrogels are capable of shear thinning because the physical interactions between the two charged peptide chains can be temporarily disrupted with applied force. The hydrogel is able to withstand repeated shear thinning and still regain up to 90% of its original pre-shear rigidity. Furthermore, adjusting the hydrophobicity of the neutral amino acid species in the peptide sequence easily controls the gel modulus [471,473].

Multi-domain peptides are peptide sequences with coded regions that either encourage or prevent assembly. They exhibit an ABA motif, where the B block is composed of hydrophilic Gln/Ser residues and hydrophobic Leu residues, and the A block consists of either positively charged Lys or negatively charged Glu. The B block residues self-assemble in such a way that the hydrophilic and hydrophobic residues reside on opposite faces, flanked by the terminal A blocks [474–479]. This self-assembly can be triggered by the protonation or deprotonation of the terminal A blocks by pH titration or charge shielding by increasing the environmental ionic strength [395]. This self-assembly stemming from each ABA block arrangement promotes fibril formation and hydrogel gelation [415]. These hydrogels shear-thin upon application of shear force and recover their properties very rapidly, within ~20 s, after cessation of shear (Fig. 30) [395,474]. These MDP gels have been shown to exhibit no cytotoxicity and can induce the migration and differentiation of MSCs from human exfoliated teeth (SHED) [478,480]. Additionally, the incorporation of degradable peptidic sequences, such as those sensitive to matrix metalloproteinases, into the MDP domains confers system biodegradability [474,478].

Another application of MDP hydrogel systems are as 'drug sponges' to provide renal protection. Wang et al. have shown that when human H9 embryonic stem cells are cultured in the presence of an MDP system, the secretome of the stem cells, *i.e.*, their particular blend of growth factors cytokines, chemokines, *etc.*, is imbied by the hydrogel network [476,481]. These hydrogels, once perfused with the stem cell secretome had renoprotective effects both *in vitro* and *in vivo* by mediated lipopolysaccharide-induced renal trauma [476]. Similar protective effects were observed in cardiac tissue when exposed to MDPs containing the secretomes of primary mouse MSCs [482].

MDPs have also been used as one component of a multi-step temporally controlled release matrix for tissue engineering applications. MDP hydrogels self-assemble around liposomes containing either a growth factor, such as placental growth factor-1 (PlGF-1), vascular endothelial growth factor (VEGF) or a chemokine such as monocyte chemoattractant protein-1 (MCP-1). A second growth factor or chemokine is passively imbibed by the already assembled MDP hydrogel containing liposomes. These multi-component systems

still exhibit shear-thinning and subsequent shear-recovery behaviors and the overall rigidity is not impacted by liposome inclusion. A bimodal drug release profile is observed and shown in Fig. 31, which emphasizes the ability of the multi-component system of MDPs and encapsulated liposomes to exert a temporally-controllable drug release [483].

8.2.1.4. Synthetic hydrogels: Synthetic hydrogels can be composed of a wide variety of polymeric materials and have the benefit of allowing the researcher to exert complete control over the composition, structure, and responsiveness of the synthesized hydrogel. One such system is a blend of hyaluronic acid (HA) and methylcellulose (MC). Methylcellulose is a thermally responsive biocompatible material that will form a gel at or above 37 °C in water. This weak gel is held together by hydrophobic interactions [484,485]. Hyaluronic acid is a non-immunogenic and biocompatible material that exhibits shear-thinning behavior due to the alignment of polymeric chains under flow [486–489]. However, unless the HA is crosslinked, it is highly soluble and will disperse after injection [396]. Therefore, blending it with a material such as methylcellulose results in a robust gel. The gelation time of the HAMC gels can be controlled by varying the HA and MC compositions with the 2% HA/7% MC formulation gelling within 2 min. The shear-thinning behavior of the HA is maintained within the HAMC hydrogel as it flows upon the application of shear force and recovers its properties after shear is removed [490]. When added to the intrathecal space of rats there was no apparent cytotoxicity or immunogenicity in reaction to the injected HAMC hydrogel [490].

Both cellular and therapeutic cargo can be incorporated into the HAMC hydrogel and homogeneously suspended during gelation. The hydrogel can be administered into the interthecal space *via* injection due to the shear thinning properties. Human umbilical tissue-derived cells were successfully incorporated into the HAMC hydrogel without any loss of mechanical rigidity. The cells were successfully maintained over the course of three days [491]. Fibroblast growth factor 2, FGF2, and poly(ethylene glycol)-modified FGF2, PEG-FGF2 were incorporated into HAMC hydrogels. The incorporation process did not adversely impact the bioactivity of the FGF2 or PEG-FGF2 as confirmed by the dose dependent proliferation of Balb/3T3 cell. The therapeutic cargo was delivered over the course of 25 h in an *in vitro* setting. However, it was shown that PEG-FGF2 entered the injured spinal tissue at much higher concentrations than the unmodified growth factor [492]. HAMC is a viable option for both tissue engineering and drug delivery applications [493,494].

In addition to being blended in with MC, hyaluronic acid and β-cyclodextrin, can be formed into shear thinning hydrogels *via* guest–host mediated self-assembly. Rodell et al. modified hyaluronic acid with either an adamantane functionality (Ad-HA) or with β-cyclodextrin (CD-HA) [495]. Adamatane and its derivatives are widely used in the pharmaceutical industry for the prophylaxis or treatment of viral diseases as well as Parkinson's [496]. Cyclodextrins are cyclic oligosaccharides of ᴅ-glucose units linked by α-1,4-linkages. The α-, β- and γ-cyclodextrins contain 5, 7, or 8 anyhydroglucose units, respectively. These components have been used in the pharmaceutical, food and cosmetic industries [497–500]. Together, adamantane-derivatives and β-cyclodextrin form a complex with a relatively high association constant, $\sim 1 \times 10^5$ M. This association is known as a guest–host assembly, which occurs when two chemical species interact *via* non-covalent associations, complexing

together and driving molecular assembly [501]. The guest–host complexation is a reversible association. Fig. 32 details the guest–host assembly, the synthesis of CD- and Ad-HA macromolecules, a visual assessment of the gelation and the reversible physical crosslinks that result in shear thinning.

Network properties are controllable by adjusting macromolecular concentration and guest–host stoichiometry. Shear-thinning behavior is observed and, once force is removed, the gel exhibits near-immediate recovery. A model therapeutic, FITC-BSA, was incorporated into the gel and its release was monitored over 60 days. The FITC-BSA exhibited a sustained release curve over the course of the experiments. The release was readily controllable by adjusting hydrogel parameters. Additionally, the hydrogel can disassemble, or biodegrade, *via* a linear erosion mechanism making it a promising candidate for injectable drug delivery and tissue engineering systems [495].

Cyclodextrins (CDs) have also shown great promise in forming shear-thinning hydrogel networks when associated with linear block copolymers, such as poly(ethylene oxide) (PEO). This association is attributed to the truncated cone configurations the CDs adapt where the hydrophilic hydroxyl groups form the outer surface and the inner cavity of the cone is hydrophobic [499,500]. The linear triblock copolymers can penetrate into the hydrophobic cavity and form complexes [502]. The complex formation is dictated by the size of the cavity, *i.e.*, α-, β- and γ-variants, and the diameter of the polymer chain [502]. When the polymer chain enters into the hydrophobic cavity of the cyclodextrins the complex is stabilized by hydrophobic interactions and hydrogen bonding. The combination of the polymer threading and stabilization results in the gelation of the hydrogel networks. Block copolymers, in particular, contain both hydro-phobic and hydrophilic moieties, which can induce polymer threading into cyclodextrin cavity and subsequent stabilization [365]. This polymer threading is a transient behavior and can be disrupted by the application of shear force and then self-heal [503].

One such triblock copolymer system is composed of a PEO-PPO-PEO, poly(ethylene oxide)-poly(propylene oxide)-poly(ethylene oxide), linear polymer and an α-cyclodextrin [503]. The same complexation behavior is observed for PEO-PCL, poly(ethylene oxide)-b-poly(ε-caprolactone) diblock copolymers [503,504]. The incorporation of biodegradable linear polymers such as poly(lactic acid) (PLA) and PEG which interact with α-cyclodextrin, can form biodegradable hydrogel systems for drug delivery applications [500]. A model protein therapeutic, FITC-BSA has been incorporated into hydrogels composed of α-CD/PEO and α-CD/PEO-PHB-PEO and exhibited release profiles that were dependent upon the erosion rate of the hydrogels [503,505]. The shear-thinning hydrogels exhibit self-healing kinetics are much slower than other injectable shear-thinning systems, ~20 min [503]. Further investigation will be necessary to optimize these systems for *in vivo* applications.

8.2.1.5. Synthetic colloidal systems: Colloidal gels are composed of suspended colloidal particles that exhibit a reversible sol–gel transition that allows the gels to shear-thin [410,506,507]. The formation of colloidal gels is driven by the mixing of two different colloidal particles that have favorable surface interactions. The interaction and self-assembly

of these particles results in the observed sol–gel transition [363]. Colloidal gel shear-thinning occurs when the surface interactions are disrupted under applied shear, while self-healing is the reinstatement of those favorable interactions [363,508–512]. A colloidal system based on charged poly(D,L-lactic-co-glycolic acid) (PLGA) nanoparticles was developed by Shi et al. One set of PLGA nanoparticles was coated with a positively charged polyvinylamine while the other set is coated with a negatively charged poly(ethylene-co-maleic acid). Their self-assembly is dictated by electrostatic attraction between the oppositely charged nanoparticle structures [511,512]. The resulting network is porous and rigid. The mechanical properties can be adjusted by the ratio of positively- to negatively-charged species. Both protein and hUCMSCs (human umbilical cord matrix stem cells) can be encapsulated within the nanoparticles. Protein will be released as a function of the PLGA degradation rate, while stem cells can encourage osteoconductive bone formation when injected into bone defects [363,508,509].

8.2.2. Other shear-thinning applications—In addition to injectable hydrogels for drug delivery and tissue engineering scaffolds, shear-thinning gels have a host of other applications including for arthritis treatment, biofilm disruption, *etc.*

Hyaluronic acid (HA) occurs naturally within the body and exists as a major component of the synovial fluid that lubricates joints during motion. The viscoelastic properties that it imparts to the synovial fluid allows joints to be lubricated by a more viscous fluid during normal motion, but upon impact, the gel becomes more elastic in nature and cushions the joint [364,382,396]. A 50% crosslinked hyaluronic acid hydrogel was developed by R. Barbucci et al. to treat osteoarthritis. Specifically, the crosslinked HA gel could be injected into a bone defect or in between the joint and persist longer than the uncrosslinked HA gels. Additionally, the mechanical properties were preserved both after shear and after ethylene oxide (EtO) and γ-ray sterilization procedures. These crosslinked gels were capable of promoting the healing of bone defects in a rabbit *in vivo* model [396].

Engineered peptide sequences exhibiting shear-thinning behaviors were developed for use to promote joint lubrication for osteoarthritis treatment. These self-assembled hydrogel materials were composed of four different peptide sequences, P_{11}-4, P_{11}-8, P_{11}-9, and P_{11}-12, which are differentiated by the number of hydroxyl groups and overall net charge. At a concentration of 20 mg/mL, all of the peptides formed fibrillar hydrogels at physiological conditions. Upon rheological examination, all of the peptide formulations exhibited shear-thinning behavior similar to that of native HA [364].

Shear-thinning hydrogels have also exhibited some inherent anti-microbial activity, as was discussed in more detail earlier [397,468]. It has been hypothesized that the bacterial-specific membrane disruption upon encountering polymeric biocides is due to the long-range interstatic reaction between the two that far surpasses that of mammalian cells [513]. Both the MAX8 and MAX1 self-assembled hydrogel systems inhibit both gram-positive and gram-negative bacterial growth by disrupting their membranes. Synthetic polymer sequences such as biodegradable poly(L-lactide)-b-poly(ethylene glycol)-b-poly(L-lactide) (PLLA-PEG-PLLA) and a polycarbonate triblock copolymer (PLDA-CPC-PLDA) can stereocomplex and form shear-thinning gels that also prevent gram-postive and gram-negative microbial growth

[397]. Another system is based on an ABA triblock copolymer composed of a hydrophilic PEG middle block and vitamin E-containing polycarbonate copolymers on either end of the copolymer. These systems exhibited desirable mechanical stiffness upon the induction of gelation but also underwent shear thinning upon application of increased shear rate. They were examined for their ability to eradicate biofilms and microbial killing efficiencies. To this end, these systems kill more than 99.9% of bacteria and fungi it contacts. Additionally, these systems eradicate biomass and also greatly disrupt established biofilms. The ability to have hydrogel materials that can disrupt bacterial membranes is a powerful tool that could ultimately be used to prevent bio-film formation on implanted biomaterials and for the prevention and treatment of skin infections [513].

The inherent viscoelastic properties of shear-thinning hydro-gels are attractive for the development of topical treatments for skin disorders such as infections and burns. They will shear thin during application and then gel for sustained contact with the wound area. One such system is a cubosome based hydrogel imbibed with silver sulfadiazine for burn treatment [398]. An emulsion between the lipid phase monoolein and Polaxamer 407, a nonionic surfactant forms the hydrogel network. Options for modification include the concentration of lipid and the inclusion of polyvinyl alcohol during emulsion. The cubosome dispersions are stable and undergo shear-thinning behavior. Furthermore, they are capable of releasing the imbibed silver sulfadiazine, which is used for burn treatment. *In vivo* studies showed that this hydrogel had great promise in the treatment of severe burns with minimal side effects [398].

8.3. Shear-thickening hydrogels

Polymers that undergo increased viscosity as a function of increased shear rate are deemed shear thickening [389,390]. Ceramic-based systems such as hydroxyapatite [514] and self-curing poly(methymethacrylate) cements [515] used for bone tissue engineering are biomaterials that exhibit strain thickening behaviors. In both ceramics and bone cement, this behavior is attributed to the colloidal nature of powder suspensions, specifically when the powder is at a high concentration and a fine enough particle diameter [516]. As described by Reynolds et al., the particles in suspension are efficiently packed with minimal fluid-filled space between them. When shear is minimal, the liquid between the particles acts as lubricant keeping the viscosity low. Once shear is increased, the distance between the particles also increases and the volume of liquid is insufficient to fill the void. This loss of fluid contact results in dramatically increased shear stress and subsequent increase in viscosity [515]. Titanium oxide (TiO_2) nanoparticles suspended in acetylacetone also shear-thicken and show promise as protective coatings on metallic and other substances for use in implanted biomaterials [517]. Hydrogels that exhibit shear-thickening behaviors tend to do so only within a certain range of shear stresses. Outside of those ranges, the hydrogel behaves as a linear viscoelastic material or can even shear-thin at high enough shear rates [427,518]. An elastin-like cysteine-containing hydrogel (Cys-ELP) undergoes gelation upon exposure to hydrogen peroxide due to disulfide linkages forming between the cysteine residues. The hydrogels post-gelation strain thicken under increasing shear rate until reaching a threshold shear rate upon which they shear-thin. This thickening is attributed to nonlinear tension along the stretched polymer chains outside of the Gaussian range. Once

the system reaches high enough shear, the network fractures and the tension is relieved resulting in the shear-thinning behavior [519]. Another such system is a telechelic polyelectrolyte consisting of a poly(-dimethyl amino ethyl methacrylate) (PDMAEMA) middle block flanked by two poly(methyl methacrylates) (PMMA). These polymers form flower-like micelles above a given concentration with a hydrophobic core and looping hydrophilic polymer chains. When a critical concentration is reached, the hydrophobic ends can transiently disassociate from the micelle core and engage with other hydrophobic ends forming a network (Fig. 33). Adjusting parameters such as pH and ionic strength controls this network formation. The shear-thickening polymer behavior has multiple theoretical causes: (1) non-linear stretching of the polymeric chains, (2) incomplete relaxation of the disassociated hydrophobic chain ends or (3) shear-induced increased density of elastic chains [518,520–522]. The dual shear-thickening and shear-thinning behavior of the hydrogel confers toughness to the material at low shear stresses but yields at higher shear stresses, which makes them compatible for injectable delivery [523]. These hydrogel systems have the ability to complex DNA by the electrostatic interactions and, therefore, have potential for biological applications [518]. Other examples of shear-thickening hydrogels include clay-polymer nanocomposites [524,525], graphene-poly(vinyl alcohol) composites [526] and crosslinked guar gum [527]. However, the biomedical applications of shear-thickening systems, particularly those that also exhibit shear-thinning at high shear rates is not as obvious and will need to be investigated in the future.

8.4. Concluding remarks

Shear-thinning hydrogel systems are versatile platforms for a number of biomedical applications. They are formed *via* intermolecular interactions that lead to self-assembled structures. They all shear-thin upon application of shear force and self-heal with varying kinetics after the cessation of shear. Varying the composition and gelation conditions controls the mechanical properties of the hydrogel networks. These systems can be used for injectable hydrogel depots for drug delivery and tissue engineering as well as for osteoarthritic treatment, biofilm disruption and skin wound healing. Shear-thickening hydrogels typically exhibit shear-thickening behaviors at low shear rates and will then shear-thin as the shear rate increases. While their biomedical applications are not as apparent as in the shear-thinning systems, their shear-thickening behavior confers hydrogel toughness at low shear rates, such as those experienced *in vivo*, but their shear-thinning capabilities at high shear means their use can be extended to injectable systems.

9. Summary

Hydrogels are an extremely diverse group of materials that have a wide variety of uses. In recent decades, a boom in research on "smart" hydrogels that exhibit responsiveness to a variety of responses has led to many novel applications of hydrogels. With an array of triggering mechanisms—including pH, temperature, external chemicals, light, electrical fields, and shear stresses—these hydrogels enable precise control over fundamental material properties, such as swelling, porosity, physical structure, and modulus. With this level of external control, numerous applications within medical and industrial fields have suddenly moved into the realm of possibility: well-controlled drug delivery; inexpensive and accurate

biosensors; artificial muscles; or effective scaffolds for tissue engineering. As research continues toward finding novel mechanisms for stimuli-responsiveness and innovative applications of the responsive hydrogels, we will indubitably see significant advances in the coming decades in both healthcare and industry that arise directly from stimuli-responsive hydrogels and tangibly improve the world.

References

1. Peppas, NA. Hydrogels in Medicine and Pharmacy. Boca Raton, FL: CRC Press; 1987.

2. Slaughter BV, Khurshid SS, Fisher OZ, Khademhosseini A, Peppas NA. Adv. Mater. 2009; 21:3307–3329. http://dx.doi.org/10.1002/adma.200802106. [PubMed: 20882499]

3. Anseth KS, Bowman CN, Brannon-Peppas L. Biomaterials. 1996; 17:1647–1657. [PubMed: 8866026]

4. Peppas NA, Merrill EW. J. Appl. Polym. Sci. 1977; 21:1763–1770.

5. Brannon-Peppas L, Peppas NA. Chem. Eng. Sci. 1991; 46:715–722.

6. Lowman, AM. Advances in Chemical Engineering. Peppas, NA., editor. Elsevier; 2004. p. 248

7. Flory PJ, Rehner J Jr. J. Chem. Phys. 1943; 11:512.

8. Peppas N, Hilt JZ, Khademhosseini A, Langer R. Adv. Mater. 2006; 18:1345–1360.

9. Billmeyer, FW. Textbook of Polymer Science. New York: John Wiley & Sons, Inc.; 1984.

10. Sperline LH, Mishra V. Polym. Adv. Technol. 1996; 7:197–208.

11. Verestiuc L, Ivanov C, Barbu E, Tsibouklis J. Int. J. Pharm. 2004; 269 (n.d.).

12. Zhang, J. Structure and morphology of poly(methacrylic acid) poly(N-isopropyl acrylamide) interpenetrating polymeric networks with pH and temperature sensitivity, (Ph.D.). Purdue University; 2000. http://search.proquest.com/docview/304654073/abstract?accountid=7118 [accessed 16.12.14]

13. Merkel TJ, Jones SW, Herlihy KP, Kersey FR, Shields AR, Napier M, Luft JC, Wu H, Zamboni WC, Wang AZ, Bear JE, DeSimone JM. Proc. Natl. Acad. Sci. 2011; 108:586–591. http://dx.doi.org/10.1073/pnas.1010013108. [PubMed: 21220299]

14. Drury JL, Mooney DJ. Biomaterials. 2003; 24:4337–4351. http://dx.doi.org/10.1016/S0142-9612(03)00340-5. [PubMed: 12922147]

15. Anseth KS, Bowman CN, Brannon-Peppas L. Biomaterials. 1996; 17:1647–1657. http://dx.doi.org/10.1016/0142-9612(96)87644-7. [PubMed: 8866026]

16. Peppas NA, Merrill EW. J. Appl. Polym. Sci. 1977; 21:1763–1770. http://dx.doi.org/10.1002/app.1977.070210704.

17. Flory, PJ. Principles of Polymer Chemistry. Cornell University Press; 1953.

18. Crank, J. The Mathematics of Diffusion. New York: Academic Press; 1975.

19. am Ende MT, Hariharan D, Peppas NA. React. Polym. 1995; 25:127–137. http://dx.doi.org/10.1016/0923-1137(94)00040-C.

20. Brannon-Peppas L, Peppas NA. J. Control. Release. 1989; 8:267–274. http://dx.doi.org/10.1016/0168-3659(89)90048-5.

21. Renkin EM. J. Gen. Physiol. 1954; 38:225–243. http://dx.doi.org/10.1085/jgp.38.2.225. [PubMed: 13211998]

22. Pappenheimer JR. J. Physiol. Rev. 1953; 1953:387–423.

23. Gudeman LF, Peppas NA. J. Membr. Sci. 1995; 107:239–248. http://dx.doi.org/10.1016/0376-7388(95)00120-7.

24. Anderson JL, Quinn JA. Biophys. J. 1974; 14:130–150. http://dx.doi.org/10.1016/S0006-3495(74)70005-4. [PubMed: 4813157]

25. Peppas NA, Reinhart CT. J. Membr. Sci. 1983; 15:275–287. http://dx.doi.org/10.1016/S0376-7388(00)82304-2.

26. Reinhart CT, Peppas NA. J. Membr. Sci. 1984; 18:227–239. http://dx.doi.org/10.1016/S0376-7388(00)85036-X.

27. Sassi AP, Blanch HW, Prausnitz JM. J. Appl. Polym. Sci. 1996; 59:1337–1346. http://dx.doi.org/10.1002/(SICI)1097-4628(19960222)59:8<1337::AID-APP18>3.0.CO;2-2.

28. am Ende MT, Peppas NA. J. Control. Release. 1997; 48:47–56. http://dx.doi.org/10.1016/S0168-3659(97)00032-1.

29. Amsden B. Mech. Models Macromol. 1998; 31:8382–8395. http://dx.doi.org/10.1021/ma980765f.

30. Muhr AH, Blanshard JMV. Polymer. 1982; 23:1012–1026. http://dx.doi.org/10.1016/0032-3861(82)90402-5.

31. Peppas NA, Meadows DL. J. Membr. Sci. 1983; 16:361–377. http://dx.doi.org/10.1016/S0376-7388(00)81321-6.

32. Gupta P, Vermani K, Garg S. Drug Discov. Today. 2002; 7:569–579. [PubMed: 12047857]

33. Fallingborg J. Dan. Med. Bull. 1999; 46:183–196. [PubMed: 10421978]

34. Guyton, AC.; Hall, JE. Textbook of Medical Physiology. 11th. Philadelphia: Elsevier; 2006.

35. Lang WR. Obstet. Gynecol. Surv. 1955; 10:546–560. [PubMed: 13244967]

36. Wike-Hooley JL. Eur. J. Cancer Clin. Oncol. 1985; 21:785–787. [PubMed: 4043168]

37. Steichen SD, Caldorera-Moore M, Peppas NA. Eur. J. Pharm. Biopharm. 2013; 48:416–427.

38. Vaupel P, Kallinowski F, Okunieff P. Cancer Res. 1989; 49:6449–6465. [PubMed: 2684393]

39. Dissemond J, Witthoff M, Brauns TC, Haberer D, Goos M. Hautarzt Z. Dermatol. Venerol. Verwandte Geb. 2003; 54:959–965.

40. Grabe M, Oster G. J. Gen. Physiol. 2011; 117:329–344. [PubMed: 11279253]

41. Asokan A, Cho MJ. J. Pharm. Sci. 2002; 91:903–913. [PubMed: 11948528]

42. Sharpe LA, Daily AM, Horava SD, Peppas NA. Expert Opin. Drug Deliv. 2014; 11:901–915. [PubMed: 24848309]

43. Peppas NA, Bures P, Leobandung W, Ichikawa H. Eur. J. Pharm. Biopharm. 2000; 50:27–46. [PubMed: 10840191]

44. Lowman, AM.; Peppas, NA. Encyclopedia of Controlled Drug Delivery. John Wiley & Sons; 1999. p. 397-418.

45. Park HY, Song IH, Kim JH, Kim WS. Int. J. Pharm. 1998; 175:231–236.

46. Welz MM, Ofner CM III. J. Pharm. Sci. 1992; 81:85–90. [PubMed: 1619576]

47. Chan AW, Whitney RA, Neufield RJ. Biomacromolecules. 2008; 9:2536–2545. [PubMed: 18666793]

48. Chan AW, Neufield RJ. Biomaterials. 2009; 30:6119–6129. [PubMed: 19660810]

49. Kim SY, Cho SM, Lee YM, Kim SJ. J. Appl. Polym. Sci. 2000; 78:1381–1391.

50. Qu X, Wirsen A, Albertsson A-C. Polymer. 2000; 41:4589–4598.

51. Schmaljohann D. Adv. Drug Deliv. Rev. 2006; 58:1655–1670. [PubMed: 17125884]

52. Kwan IC, Bae YH, Okano T, Kim SW, Berner B. Macromol. Symp. 1990; 33

53. Khare AR, Peppas NA, Massimo G, Colombo P. J. Control. Release. 1992; 22:239–244.

54. Peppas NA, Hilt JZ, Khademhosseini A, Langer R. Adv. Mater. 2006; 18:1345–1360.

55. Khare AR, Peppas NA. Biomaterials. 2009; 16:559–567. [PubMed: 7492721]

56. Peppas, NA.; Barr-Howell, BD. Hydrogels in Medicine and Pharmacy: Fundamentals. CRC Press; 1986. p. 27-54.

57. Brannon-Peppas L, Peppas NA. J. Controll. Release. 1991; 16:319–330.

58. Firestone BA, Siegel RA. J. Appl. Polym. Sci. 1991; 43:901–914.

59. Bettini R, Colombo P, Peppas NA. J. Control. Release. 1995; 37:105–111.

60. Canal T, Peppas NA. J. Biomed. Mater. Res. A. 1989; 23:1183–1193.

61. Elliot JE, Macdonald M, Nie J, Bowman CN. Polymer. 2004; 45:1503–1510.

62. Koetting MC, Peppas NA. Int. J. Pharm. 2014; 471:83–91. [PubMed: 24853463]

63. Peppas NA, Wood KM, Blanchette JO. Expert Opin. Biol. Ther. 2004; 4:881–887. [PubMed: 15174970]

64. Bronich TK, Vinogradov SV, Kabanov AV. Nano Lett. 2001; 1:535–540.

65. Schoener CA, Hutson HN, Peppas NA. J. Biomed. Mater. Res. A. 2013; 101A:2229–2236. [PubMed: 23281185]

66. Forbes DC, Peppas NA. Macromol. Biosci. 2014; 14:1096–1105. [PubMed: 24753265]

67. Lowman AM, Morishita M, Kajita M, Nagai T. J. Pharm. Sci. 1999; 88:933–937. [PubMed: 10479357]

68. Hu Y, Atukorale PU, Lu JJ, Moon JJ, Um SH, Cho EC. Biomacromolecules. 2009; 10:756–765. [PubMed: 19239276]

69. Peppas NA, Langer R. AIChE J. 2004; 50:536–546.

70. Bell CL, Peppas NA. J. Control. Release. 1996; 39:201–207.

71. Lowman AM, Peppas NA. Macromolecules. 1997; 30:4959–4965.

72. Klier J, Scranton AB, Peppas NA. Macromolecules. 1990; 23:4944–4949.

73. Peppas NA, Klier J. J. Control. Release. 1991; 16:203–214.

74. Davis SS. Drug Discov. Today. 2005; 10:249–257. [PubMed: 15708743]

75. Peppas NA, Huang Y. Adv. Drug Deliv. Rev. 2004; 56:1675–1687. [PubMed: 15350296]

76. Park H, Robinson JR. Pharm. Res. 1987; 4:457–464. [PubMed: 3508557]

77. Peppas NA, Keys KB, Torres-Lugo M, Lowman AM. J. Control. Release. 1999; 62:81–87. [PubMed: 10518639]

78. Wood KM, Stone GM, Peppas NA. Biomacromolecules. 2008; 9:1293–1298. [PubMed: 18330990]

79. Lopez JE, Peppas NA. Drug Dev. Ind. Pharm. 2004; 30:497–504. [PubMed: 15244085]

80. Nakamura K, Murray RJ, Joseph JI, Peppas NA, Morishita M, Lowman AM. J. Control. Release. 2004; 95:589–599. [PubMed: 15023469]

81. Kim B, Peppas NA. Int. J. Pharm. 2003; 266:29–37. [PubMed: 14559391]

82. Morishita M, Goto T, Nakamura K, Lowman AM, Takayama K, Peppas NA. J. Control. Release. 2006; 110:587–594. [PubMed: 16325951]

83. Kamei N, Morishita M, Chiba H, Kavimandan NJ, Peppas NA, Takayama K. J. Control. Release. 2009; 134:98–102. [PubMed: 19095021]

84. Torres-Lugo M, Peppas NA. Biomaterials. 2000; 21:1191–1196. [PubMed: 10811300]

85. Carr DA, Peppas NA. Macromol. Biosci. 2009; 9:497–505. [PubMed: 19016502]

86. Carr DA, Peppas NA. J. Biomed. Mater. Res. A. 2010; 92A:504–512. [PubMed: 19213059]

87. Carr DA, Gomez-Burgaz M, Boudes MC, Peppas NA. Ind. Eng. Chem. Res. 2010; 49:11991–11995. [PubMed: 21344059]

88. Gambotz WR, Wee SF. Adv. Drug Deliv. Rev. 2012; 64:194–205.

89. Yotsuyanagi T, Ohkubo T, Ohhashi T, Ikeda K. Chem. Pharm. Bull. (Tokyo). 1987; 35:1555–1563.

90. Chen S-C, Wu Y-C, Mi F-L, Lin Y-H, Yu L-C, Sung H-W. J. Control. Release. 2004; 96:285–300. [PubMed: 15081219]

91. Romalde JL, Luzardo-Alvarez A, Ravelo C, Toranzo AE, Blanco-Mendez J. Aquaculture. 2004; 236:119–129.

92. Lee B-J, Min G-H. Int. J. Pharm. 1996; 144:37–46.

93. Sugawara S, Imai T, Otagiri M. Pharm. Res. 1994; 11 (n.d.).

94. Zhang T, Sturgis TF, Youan B-BC. Eur. J. Pharm. Biopharm. 2011; 79:526–536. [PubMed: 21736940]

95. Woolfson AD, Umrethia ML, Kett VL, Malcolm RK. Int. J. Pharm. 2010; 388:136–143. [PubMed: 20045043]

96. Morrow RJ, Woolfson AD, Donnelly L, Curran R, Andrews G, Katinger D, Malcolm RK. Eur. J. Pharm. Biopharm. 2011; 77:3–10. [PubMed: 21055465]

97. Garg S, Vermani K, Garg A, Anderson RA, Rencher WB, Zaneveld LJD. Pharm. Res. 2005; 22:584–595. [PubMed: 15846466]

98. Parikh UM, Dobard C, Sharma S, Cong M, Jia H, Martin A, Pau C-P, Hanson DL, Guenthner P, Smith J, Kersh E, Garcia-Lerma JG, Novembre FJ, Otten R, Folks T, Heneine W. J. Virol. 2009; 83:10358–10365. [PubMed: 19656878]

99. Zhang T, Zhang C, Agrahari V, Murowchick JB, Oyler NA, Youan B-BC. Antivir. Res. 2013; 97:334–346. [PubMed: 23274788]

100. Agnihotri SA, Mallikarjuna NN, Aminabhavi TM. J. Control. Release. 2004; 100:5–28. [PubMed: 15491807]

101. Bernkop-Schnürch A, Dünnhaupt S. Eur. J. Pharm. Biopharm. 2012; 81:463–469. [PubMed: 22561955]

102. Hejazi R, Amiji MM. J. Control. Release. 2003; 89:151–165. [PubMed: 12711440]

103. Patel VR, Amiji MM. Pharm. Res. 1996; 13:588–593. [PubMed: 8710751]

104. Dai Y-N, Li P, Zhang J-P, Wang A-Q, Wei Q. Biopharm. Drug Dispos. 2008; 29:173–184. [PubMed: 18215011]

105. Liechty WB, Kryscio DR, Slaughter BV, Peppas NA. Annu. Rev. Chem. Biomol. Eng. 2010; 1:149–173. [PubMed: 22432577]

106. Fisher OZ, Peppas NA. Macromolecules. 2009; 42:3391–3398. [PubMed: 20526378]

107. Fisher OZ, Kim T, Dietz SR, Peppas NA. Pharm. Res. 2009; 26:51–60. [PubMed: 18751960]

108. Liechty WB, Scheuerle RL, Peppas NA. Polymer. 2013; 54:3784–3795.

109. Forbes DC, Creixell M, Frizzell H, Peppas NA. Eur. J. Pharm. Biopharm. 2013; 84:472–478. [PubMed: 23396094]

110. Forbes DC, Peppas NA. ACS Nano. 2014; 8:2908–2917. [PubMed: 24548237]

111. Liechty WB. Eur. J. Pharm. Biopharm. 2012; 80:241–246. [PubMed: 21888972]

112. Raemdonck K, Demeester J, Smedt SD. Soft Matter. 2009; 5:707–715.

113. Zhang H, Mardyani S, Chan WCW, Kumacheva E. Biomacromolecules. 2006; 7:1568–1572. [PubMed: 16677040]

114. Oishi M, Hayashi H, Iijima M, Nagasaki Y. J. Mater. Chem. 2007; 17:3720–3725.

115. Klouda L, Mikos AG. Eur. J. Pharm. Biopharm. 2008; 68:34–45. http://dx.doi.org/10.1016/j.ejpb. 2007.02.025. [PubMed: 17881200]

116. Purushotham S, Ramanujan RV. Acta Biomater. 2010; 6:502–510. http://dx.doi.org/10.1016/j.actbio.2009.07.004. [PubMed: 19596094]

117. Bae YH, Okano T, Kim SW. J. Polym. Sci. B: Polym. Phys. 1990; 28:923–936. http://dx.doi.org/10.1002/polb.1990.090280609.

118. Katono H, Maruyama A, Sanui K, Ogata N, Okano T, Sakurai Y. J. Control. Release. 1991; 16:215–227. http://dx.doi.org/10.1016/0168-3659(91)90045-F.

119. Owens DE, Jian Y, Fang JE, Slaughter BV, Chen Y-H, Peppas NA. Macro-molecules. 2007; 40:7306–7310. http://dx.doi.org/10.1021/ma071089x.

120. Owens, DE. Thermally-Responsive Interpenetrating Polymer Network Nano-particles as Intelligent Therapeutic Systems. The University of Texas at Austin; 2006. http://gradworks.umi.com/32/66/3266943.html [accessed 14.12.14]

121. Liu R, Fraylich M, Saunders BR. Colloid Polym. Sci. 2009; 287:627–643. http://dx.doi.org/10.1007/s00396-009-2028-x.

122. Platé NA, Lebedeva TL, Valuev LI. Polym. J. 1999; 31:21–27. http://dx.doi.org/10.1295/polymj.31.21.

123. Meenach SA, Anderson KW, Hilt JZ. J. Polym. Sci. A: Polym. Chem. 2010; 48:3229–3235. http://dx.doi.org/10.1002/pola.24087.

124. Escobar-Chávez JJ, López-Cervantes M, Naik A, Kalia Y, Quintanar-Guerrero D, Ganem-Quintanar A. J. Pharm. Pharm. Sci. 2006; 9:339–358. [PubMed: 17207417]

125. Bhattacharjee RR, Chakraborty M, Mandal TK. J. Phys. Chem. B. 2006; 110:6768–6775. http://dx.doi.org/10.1021/jp056675b. [PubMed: 16570984]

126. Verestiuc L, Nastasescu O, Barbu E, Sarvaiya I, Green KL, Tsibouklis J. J. Biomed. Mater. Res. A. 2006; 77A:726–735. http://dx.doi.org/10.1002/jbm.-a.30668. [PubMed: 16555266]

127. Arndt K-F, Schmidt T, Reichelt R. Polymer. 2001; 42:6785–6791. http://dx.doi.org/10.1016/S0032-3861(01)00164-1.

128. Beija M, Marty J-D, Destarac M. Chem. Commun. 2011; 47:2826. http://dx.doi.org/10.1039/c0cc05184e.

129. Echeverria C, López D, Mijangos C. Macromolecules. 2009; 42:9118–9123. http://dx.doi.org/10.1021/ma901316k.

130. Xiao X-C, Chu L-Y, Chen W-M, Wang S, Li Y. Adv. Funct. Mater. 2003; 13:847–852. http://dx.doi.org/10.1002/adfm.200304513.

131. Francis R, Baby DK, Kumar DS. J. Appl. Polym. Sci. 2012; 124:5079–5088. http://dx.doi.org/10.1002/app.35644.

132. Nolan CM, Serpe MJ, Lyon LA. Biomacromolecules. 2004; 5:1940–1946. http://dx.doi.org/10.1021/bm049750h. [PubMed: 15360309]

133. Gan D, Lyon LA. Macromolecules. 2002; 35:9634–9639. http://dx.doi.org/10.1021/ma021186k.

134. Phillips MA, Gran ML, Peppas NA. Nano Today. 2010; 5:143–159. http://dx.doi.org/10.1016/j.nantod.2010.03.003. [PubMed: 20543895]

135. Gabizon A, Shmeeda H, Barenholz Y. Clin. Pharmacokinet. 2003; 42:419–436. http://dx.doi.org/10.2165/00003088-200342050-00002. [PubMed: 12739982]

136. Galperin A, Long TJ, Ratner BD. Biomacromolecules. 2010; 11:2583–2592. http://dx.doi.org/10.1021/bm100521x. [PubMed: 20836521]

137. Hacker MC, Klouda L, Ma BB, Kretlow JD, Mikos AG. Biomacromolecules. 2008; 9:1558–1570. http://dx.doi.org/10.1021/bm8000414. [PubMed: 18481893]

138. Turturro SB, Guthrie MJ, Appel AA, Drapala PW, Brey EM, Pérez-Luna VH, Mieler WF, Kang-Mieler JJ. Biomaterials. 2011; 32:3620–3626. http://dx.doi.org/10.1016/j.biomaterials.2011.01.058. [PubMed: 21320724]

139. Canavan HE, Cheng X, Graham DJ, Ratner BD, Castner DG. J. Biomed. Mater. Res. A. 2005; 75A:1–13. http://dx.doi.org/10.1002/jbm.a.30297. [PubMed: 16086418]

140. Recum HV, Kikuchi A, Yamato M, Sakurai Y, Okano T, Kim SW. Tissue Eng. 1999; 5:251–265. http://dx.doi.org/10.1089/ten.1999.5.251. [PubMed: 10434072]

141. Hoare T, Santamaria J, Goya GF, Irusta S, Lin D, Lau S, Padera R, Langer R, Kohane DS. Nano Lett. 2009; 9:3651–3657. http://dx.doi.org/10.1021/nl9018935. [PubMed: 19736912]

142. Gant RM, Hou Y, Grunlan MA, Coté GL. J. Biomed. Mater. Res. A. 2009; 90A:695–701. http://dx.doi.org/10.1002/jbm.a.32135. [PubMed: 18563815]

143. Abu-Lail NI, Kaholek M, LaMattina B, Clark RL, Zauscher S. Sens. Actuators B: Chem. 2006; 114:371–378. http://dx.doi.org/10.1016/j.snb.2005.06.003.

144. WHO. WHO; 2014. Country and Regional Data on Diabetes. (n.d.). http://www.who.int/diabetes/facts/world_figures/en/ [accessed 13.12.14]

145. Wu Q, Wang L, Yu H, Wang J, Chen Z. Chem. Rev. 2011; 111:7855–7875. http://dx.doi.org/10.1021/cr200027j. [PubMed: 21902252]

146. Bernfeld P, Wan J. Science. 1963; 142:678–679. http://dx.doi.org/10.1126/science.142.3593.678. [PubMed: 14068215]

147. Horbett, TA.; Kost, J.; Ratner, BD. Polymers as Biomaterials. Shalaby, SW.; Hoffman, AS.; Ratner, BD.; Horbett, TA., editors. US: Springer; 1984. p. 193-207.http://link.springer.com/chapter/10.1007/978-1-4613-2433-1_14 [accessed 13.12.14]

148. Horbett, TA.; Ratner, BD.; Kost, J.; Singh, M. Recent Advances in Drug Delivery Systems. Anderson, JM.; Kim, SW., editors. US: Springer; 1984. p. 209-220.http://link.springer.com/chapter/10.1007/978-1-4613-2745-5_14 [accessed 30.11.14]

149. Albin G, Horbett TA, Ratner BD. J. Control. Release. 1985; 2:153–164. http://dx.doi.org/10.1016/0168-3659(85)90041-0.

150. Klumb LA, Horbett TA. J. Control. Release. 1992; 18:59–80. http://dx.doi.org/10.1016/0168-3659(92)90212-A.

151. Podual K, Doyle FJ III, Peppas NA. Polymer. 2000; 41:3975–3983. http://dx.doi.org/10.1016/S0032-3861(99)00620-5.

152. Zhang K, Wu XY. J. Control. Release. 2002; 80:169–178. http://dx.doi.org/10.1016/S0168-3659(02)00024-X. [PubMed: 11943396]

153. Gordijo CR, Shuhendler AJ, Wu XY. Adv. Funct. Mater. 2010; 20:1404–1412. http://dx.doi.org/10.1002/adfm.200901581.

154. Malitesta C, Palmisano F, Torsi L, Zambonin PG. Anal. Chem. 1990; 62:2735–2740. http://dx.doi.org/10.1021/ac00223a016. [PubMed: 2096737]

155. Podual K, Doyle FJ III, Peppas NA. J. Control. Release. 2000; 67:9–17. http://dx.doi.org/10.1016/S0168-3659(00)00195-4. [PubMed: 10773324]

156. Hassan CM, Doyle FJ, Peppas NA. Macromolecules. 1997; 30:6166–6173. http://dx.doi.org/10.1021/ma970117g.

157. Kang SI, Bae YH. J. Control. Release. 2003; 86:115–121. http://dx.doi.org/10.1016/S0168-3659(02)00409-1. [PubMed: 12490377]

158. Jung D-Y, Magda JJ, Han IS. Macromolecules. 2000; 33:3332–3336. http://dx.doi.org/10.1021/ma992098b.

159. Miyata T, Jikihara A, Nakamae K, Hoffman AS. Macromol. Chem. Phys. 1996; 197:1135–1146. http://dx.doi.org/10.1002/macp.1996.021970330.

160. Ballerstadt R, Schultz JS. Sens. Actuators B: Chem. 1998; 46:50–55. http://dx.doi.org/10.1016/S0925-4005(97)00327-4.

161. Adams GG, Cui Y, Mitchell JH, Taylor MJ. Rheol. Acta. 2006; 45:611–620. http://dx.doi.org/10.1007/s00397-005-0013-y.

162. Kim JJ, Park K. J. Control. Release. 2001; 77:39–47. http://dx.doi.org/10.1016/S0168-3659(01)00447-3. [PubMed: 11689258]

163. Kim JJ, Park K. Pharm. Res. 2001; 18:794–799. http://dx.doi.org/10.1023/A:1011084312134. [PubMed: 11474783]

164. Tanna S, Sahota T, Clark J, Taylor MJ. J. Pharm. Pharmacol. 2002; 54:1461–1469. http://dx.doi.org/10.1211/00223570290. [PubMed: 12495548]

165. Miyata T, Jikihara A, Nakamae K, Hoffman AS. J. Biomater. Sci. Polym. Ed. 2004; 15:1085–1098. http://dx.doi.org/10.1163/1568562041753061. [PubMed: 15503627]

166. Taylor MJ, Tanna S, Sahota TS, Voermans B. Eur. J. Pharm. Biopharm. 2006; 62:94–100. http://dx.doi.org/10.1016/j.ejpb.2005.07.005. [PubMed: 16183269]

167. Makino K, Mack EJ, Okano T, Kim SW. J. Control. Release. 1990; 12:235–239. http://dx.doi.org/10.1016/0168-3659(90)90104-2.

168. Kim SW, Paii CM, Kimiko M, Seminoff LA, Holmberg DL, Gleeson JM, Wilson DE, Mack EJ. J. Control. Release. 1990; 11:193–201. http://dx.doi.org/10.1016/0168-3659(90)90132-D.

169. Liu F, Song SC, Mix D, Baudyš M, Kim SW. Bioconjug. Chem. 1997; 8:664–672. http://dx.doi.org/10.1021/bc970128e. [PubMed: 9327129]

170. Kuivila HG, Keough AH, Soboczenski EJ. J. Org. Chem. 1954; 19:780–783. http://dx.doi.org/10.1021/jo01370a013.

171. Lorand JP, Edwards JO. J. Org. Chem. 1959; 24:769–774. http://dx.doi.org/10.1021/jo01088a011.

172. Barker SA, Chopra AK, Hatt BW, Somers PJ. Carbohydr. Res. 1973; 26:33–40. http://dx.doi.org/10.1016/S0008-6215(00)85019-3.

173. Yang T, Ji R, Deng X-X, Du F-S, Li Z-C. Soft Matter. 2014; 10:2671. http://dx.doi.org/10.1039/c3sm53059k. [PubMed: 24647364]

174. Hoare T, Pelton R. Biomacromolecules. 2008; 9:733–740. http://dx.doi.org/10.1021/bm701203r. [PubMed: 18198833]

175. Kataoka K, Miyazaki H, Bunya M, Okano T, Sakurai Y. J. Am. Chem. Soc. 1998; 120:12694–12695. http://dx.doi.org/10.1021/ja982975d.

176. Kitano S, Koyama Y, Kataoka K, Okano T, Sakurai Y. J. Control. Release. 1992; 19:161–170. http://dx.doi.org/10.1016/0168-3659(92)90073-Z.

177. James TD, Sandanayake KRAS, Iguchi R, Shinkai S. J. Am. Chem. Soc. 1995; 117:8982–8987. http://dx.doi.org/10.1021/ja00140a013.

178. Horgan AM, Marshall AJ, Kew SJ, Dean KES, Creasey CD, Kabilan S. Biosens. Bioelectron. 2006; 21:1838–1845. http://dx.doi.org/10.1016/j.bios.2005.11.028. [PubMed: 16414255]

179. Wang D, Liu T, Yin J, Liu S. Macromolecules. 2011; 44:2282–2290. http://dx.doi.org/10.1021/ma200053a.

180. De Geest BG, Jonas AM, Demeester J, De Smedt SC. Langmuir. 2006; 22:5070–5074. http://dx.doi.org/10.1021/la053368o. [PubMed: 16700596]

181. Shiino D, Murata Y, Kubo A, Kim YJ, Kataoka K, Koyama Y, Kikuchi A, Yokoyama M, Sakurai Y, Okano T. J. Control. Release. 1995; 37:269–276. http://dx.doi.org/10.1016/0168-3659(95)00084-4.

182. Drobník J, Kope ek J, Labský J, Rejmanová P, Exner J, Saudek V, Kálal J. Makromol. Chem. 1976; 177:2833–2848. http://dx.doi.org/10.1002/macp.1976.021771003.

183. Kope ek J, Cífková I, Rejmanová P, Strohalm J, Obereigner B, Ulbrich K. Makromol. Chem. 1981; 182:2941–2949. http://dx.doi.org/10.1002/macp.1981.021821102.

184. Kope ek J, Kope ková P, Minko T, Lu Z-R. Eur. J. Pharm. Biopharm. 2000; 50:61–81. http://dx.doi.org/10.1016/S0939-6411(00)00075-8. [PubMed: 10840193]

185. Minko T, Kope ková P, Kope ek J. Int. J. Cancer. 2000; 86:108–117. http://dx.doi.org/10.1002/(SICI)1097-0215(20000401)86:1<108::AID-IJC17>3.0.CO;2-8. [PubMed: 10728603]

186. Omelyanenko V, Kope ková P, Gentry C, Shiah J-G, Kope ek J. J. Drug Target. 1996; 3:357–373. http://dx.doi.org/10.3109/10611869608996827. [PubMed: 8866655]

187. Rejmanová P, Kope ek J, Duncan R, Lloyd JB. Biomaterials. 1985; 6:45–48. http://dx.doi.org/10.1016/0142-9612(85)90037-7. [PubMed: 3971018]

188. Rejmanová P, Kope ek J, Pohl J, Baudyš M, Kostka V. Makromol. Chem. 1983; 184:2009–2020. http://dx.doi.org/10.1002/macp.1983.021841006.

189. Rejmanová P, Labský J, Kope ek J. Makromol. Chem. 1977; 178:2159–2168. http://dx.doi.org/10.1002/macp.1977.021780803.

190. Solovsky MV, Ulbrich K, Kopecek J. Biomaterials. 1983; 4:44–48. http://dx.doi.org/10.1016/0142-9612(83)90069-8. [PubMed: 6301566]

191. Šubr V, Kope ek J, Pohl J, Baudyš M, Kostka V. J. Control. Release. 1988; 8:133–140. http://dx.doi.org/10.1016/0168-3659(88)90039-9.

192. Št'astný M, íhová B, Strohalm J, Ulbrich K. J. Control. Release. 1996; 42:229–236. http://dx.doi.org/10.1016/0168-3659(96)01463-0.

193. Chytrý V, Vrána A, Kope ek J. Makromol. Chem. 1978; 179:329–336. http://dx.doi.org/10.1002/macp.1978.021790207.

194. Kim S, Healy KE. Biomacromolecules. 2003; 4:1214–1223. http://dx.doi.org/10.1021/bm0340467. [PubMed: 12959586]

195. Glangchai LC, Caldorera-Moore M, Shi L, Roy K. J. Control. Release. 2008; 125:263–272. http://dx.doi.org/10.1016/j.jconrel.2007.10.021. [PubMed: 18053607]

196. West JL, Hubbell JA. Macromolecules. 1998; 32:241–244. http://dx.doi.org/10.1021/ma981296k.

197. Hermanson, GT. Bioconjugate Techniques. 2nd. Hermanson, GT., editor. New York: Academic Press; 2008. p. 213-233.http://www.sciencedirect.com/science/article/pii/B9780123705013000035 [accessed 14.12.14]

198. Ansell RJ. J. Chromatogr. B. 2004; 804:151–165. http://dx.doi.org/10.1016/j.jchromb.2004.02.022.

199. Hock B, Rahman M, Rauchalles S, Dankwardt A, Seifert M, Haindl S, Kramer K. J. Mol. Catal. B: Enzym. 1999; 7:115–124. http://dx.doi.org/10.1016/S1381- 1177(99)00036-3.

200. Butler JE. Methods. 2000; 22:4–23. http://dx.doi.org/10.1006/meth.2000.1031. [PubMed: 11020313]

201. Esen C, Andac M, Bereli N, Say R, Henden E, Denizli A. Mater. Sci. Eng. C. 2009; 29:2464–2470. http://dx.doi.org/10.1016/j.msec.2009.07.012.

202. Tang Y, Huang Z, Yang T, Hu X, Jiang X. Anal. Lett. 2005; 38:219–226. http://dx.doi.org/10.1081/AL-200045122.

203. Zeng Z, Hoshino Y, Rodriguez A, Yoo H, Shea KJ. ACS Nano. 2009; 4:199–204. http://dx.doi.org/10.1021/nn901256s. [PubMed: 20014822]

204. Whitcombe MJ, Vulfson EN. Adv. Mater. 2001; 13:467–478. http://dx.doi.org/10.1002/1521-4095(200104)13:7<467::AID-ADMA467>3.0.CO;2-T.

205. Mosbach K. Trends Biochem. Sci. 1994; 19:9–14. http://dx.doi.org/10.1016/0968-0004(94)90166-X. [PubMed: 8140624]

206. Haupt K, Mosbach K. Trends Biotechnol. 1998; 16:468–475. http://dx.doi.org/10.1016/S0167-7799(98)01222-0. [PubMed: 9830155]

207. Cormack PAG, Mosbach K. React. Funct. Polym. 1999; 41:115–124. http://dx.doi.org/10.1016/S1381-5148(99)00024-3.

208. Wulff G, Schönfeld R. Adv. Mater. 1998; 10:957–959. http://dx.doi.org/10.1002/(SICI)1521-4095(199808)10:12<957::AID-ADMA957>3.0.CO;2-4.

209. Wulff, G.; Gross, T.; Schönfeld, R.; Schrader, T.; Kirsten, C. Molecular and Ionic Recognition with Imprinted Polymers. American Chemical Society; 1998. p. 10-28.http://dx.doi.org/10.1021/bk-1998-0703.ch002 [accessed 09.12.14]

210. Spivak D, Shea KJ. J. Org. Chem. 1999; 64:4627–4634. http://dx.doi.org/10.1021/jo982118s. [PubMed: 11674532]

211. Lübke C, Lübke M, Whitcombe MJ, Vulfson EN. Macromolecules. 2000; 33:5098–5105. http://dx.doi.org/10.1021/ma000467u.

212. Poma A, Turner APF, Piletsky SA. Trends Biotechnol. 2010; 28:629–637. http://dx.doi.org/10.1016/j.tibtech.2010.08.006. [PubMed: 20880600]

213. Lv Y, Tan T, Svec F. Biotechnol. Adv. 2013; 31:1172–1186. http://dx.doi.org/10.1016/j.biotechadv.2013.02.005. [PubMed: 23466364]

214. Verheyen E, Schillemans JP, van Wijk M, Demeniex M-A, Hennink WE, van Nostrum CF. Biomaterials. 2011; 32:3008–3020. http://dx.doi.org/10.1016/j.biomaterials.2011.01.007. [PubMed: 21288565]

215. Byrne ME, Salian V. Int. J. Pharm. 2008; 364:188–212. http://dx.doi.org/10.1016/j.ijpharm.2008.09.002. [PubMed: 18824226]

216. Steinke, J.; Sherrington, DC.; Dunkin, IR. Synthesis and Photosynthesis. Heidelberg: Springer, Berlin; 1995. p. 81-125.http://link.springer.com/chapter/10.1007/3-540-58908-2_3 [accessed 09.12.14]

217. Mayes AG, Mosbach K. TrAC Trends Anal. Chem. 1997; 16:321–332. http://dx.doi.org/10.1016/S0165-9936(97)00037-X.

218. Takeuchi T, Haginaka J. J. Chromatogr. B: Biomed. Sci. App. 1999; 728:1–20. http://dx.doi.org/10.1016/S0378-4347(99)00057-2.

219. Whitcombe MJ, Chianella I, Larcombe L, Piletsky SA, Noble J, Porter R, Horgan A. Chem. Soc. Rev. 2011; 40:1547. http://dx.doi.org/10.1039/c0cs00049c. [PubMed: 21132204]

220. RNCOS. Global In Vitro Diagnostic Market Analysis. 2014 http://www.rncos.com/Market-Analysis-Reports/Global-In-Vitro-Diagnostic-Market-Analysis-IM103.htm.

221. Lavignac N, Allender CJ, Brain KR. Anal. Chim. Acta. 2004; 510:139–145. http://dx.doi.org/10.1016/j.aca.2003.12.066.

222. Reddy SM, Phan QT, El-Sharif H, Govada L, Stevenson D, Chayen NE. Biomacromolecules. 2012; 13:3959–3965. http://dx.doi.org/10.1021/bm301189f. [PubMed: 23106501]

223. Aghaei A, Milani Hosseini MR, Najafi M. Electrochim. Acta. 2010; 55:1503–1508. http://dx.doi.org/10.1016/j.electacta.2009.09.033.

224. Chen P-Y, Vittal R, Nien P-C, Liou G-S, Ho K-C. Talanta. 2010; 80:1145–1151. http://dx.doi.org/10.1016/j.talanta.2009.08.041. [PubMed: 20006066]

225. Chen P-Y, Nien P-C, Hu C-W, Ho K-C. Sens. Actuators B: Chem. 2010; 146:466–471. http://dx.doi.org/10.1016/j.snb.2009.11.035.

226. Sontimuang C, Suedee R, Dickert F. Anal. Biochem. 2011; 410:224–233. http://dx.doi.org/10.1016/j.ab.2010.11.043. [PubMed: 21130066]

227. Alizadeh T, Zare M, Ganjali MR, Norouzi P, Tavana B. Biosens. Bioelectron. 2010; 25:1166–1172. http://dx.doi.org/10.1016/j.bios.2009.10.003. [PubMed: 19892541]

228. Tran TT, Li J, Feng H, Cai J, Yuan L, Wang N, Cai Q. Sens. Actuators B: Chem. 2014; 190:745–751. http://dx.doi.org/10.1016/j.snb.2013.09.048.

229. Vlatakis G, Andersson LI, Müller R, Mosbach K. Nature. 1993; 361:645–647. http://dx.doi.org/10.1038/361645a0. [PubMed: 8437624]

230. Muldoon MT, Stanker LH. J. Agric. Food Chem. 1995; 43:1424–1427. http://dx.doi.org/10.1021/jf00054a002.

231. Siemann M, Andersson LI, Mosbach K. J. Agric. Food Chem. 1996; 44:141–145. http://dx.doi.org/10.1021/jf950233n.

232. Andersson LI, Müller R, Vlatakis G, Mosbach K. Proc. Natl. Acad. Sci. 1995; 92:4788–4792. [PubMed: 7761401]

233. Ramström O, Ye L, Mosbach K. Chem. Biol. 1996; 3:471–477. http://dx.doi.org/10.1016/S1074-5521(96)90095-2. [PubMed: 8807877]

234. Berglund J, Nicholls IA, Lindbladh C, Mosbach K. Bioorg. Med. Chem. Lett. 1996; 6:2237–2242. http://dx.doi.org/10.1016/0960-894X(96)00406-4.

235. Mayes AG, Andersson LI, Mosbach K. Anal. Biochem. 1994; 222:483–488. http://dx.doi.org/10.1006/abio.1994.1521. [PubMed: 7864377]

236. Andersson LI. Anal. Chem. 1996; 68:111–117. http://dx.doi.org/10.1021/ac950668+ [PubMed: 21619226]

237. Bengtsson H, Roos U, Andersson LI. Anal. Commun. 1997; 34:233–235. http://dx.doi.org/10.1039/A703977H.

238. Merkoçi A, Alegret S. TrAC Trends Anal. Chem. 2002; 21:717–725. http://dx.doi.org/10.1016/S0165-9936(02)01119-6.

239. Blanco-López MC, Lobo-Castañón MJ, Miranda-Ordieres AJ, Tuñón-Blanco P. TrAC Trends Anal. Chem. 2004; 23:36–48. http://dx.doi.org/10.1016/S0165-9936(04)00102-5.

240. Okuno J, Maehashi K, Kerman K, Takamura Y, Matsumoto K, Tamiya E. Biosens. Bioelectron. 2007; 22:2377–2381. http://dx.doi.org/10.1016/j.bi-os.2006.09.038. [PubMed: 17110096]

241. Panasyuk TL, Mirsky VM, Piletsky SA, Wolfbeis OS. Anal. Chem. 1999; 71:4609–4613. http://dx.doi.org/10.1021/ac9903196.

242. Delaney TL, Zimin D, Rahm M, Weiss D, Wolfbeis OS, Mirsky VM. Anal. Chem. 2007; 79:3220–3225. http://dx.doi.org/10.1021/ac062143v. [PubMed: 17358046]

243. Suwansa-ard S, Kanatharana P, Asawatreratanakul P, Wongkittisuksa B, Limsakul C, Thavarungkul P. Biosens. Bioelectron. 2009; 24:3436–3441. http://dx.doi.org/10.1016/j.bios.2009.04.008. [PubMed: 19553100]

244. Birnbaumer GM, Lieberzeit PA, Richter L, Schirhagl R, Milnera M, Dickert FL, Bailey A, Ertl P. Lab. Chip. 2009; 9:3549–3556. http://dx.doi.org/10.1039/B914738A. [PubMed: 20024035]

245. Li J, Kendig CE, Nesterov EE. J. Am. Chem. Soc. 2007; 129:15911–15918. http://dx.doi.org/10.1021/ja0748027. [PubMed: 18044891]

246. Jakusch M, Janotta M, Mizaikoff B, Mosbach K, Haupt K. Anal. Chem. 1999; 71:4786–4791. http://dx.doi.org/10.1021/ac990050q.

247. Tai D-F, Jhang M-H, Chen G-Y, Wang S-C, Lu K-H, Lee Y-D, Liu H-T. Anal. Chem. 2010; 82:2290–2293. http://dx.doi.org/10.1021/ac9024158. [PubMed: 20184289]

248. Hayden O, Haderspöck C, Krassnig S, Chen X, Dickert FL. Analyst. 2006; 131:1044–1050. http://dx.doi.org/10.1039/B608354B. [PubMed: 17047805]

249. Lin T-Y, Hu C-H, Chou T-C. Biosens. Bioelectron. 2004; 20:75–81. http://dx.doi.org/10.1016/j.bios.2004.01.028. [PubMed: 15142579]

250. Piliarik, M.; Vaisocherová, H.; Homola, J. Biosensors and Bioelectronics. Rasooly, A.; Herold, KE., editors. Humana Press; 2009. p. 65-88.http://link.springer.com/protocol/10.1007/978-1-60327-567-5_5 [accessed 11.12.14]

251. Choong C-L, Bendall JS, Milne WI. Biosens. Bioelectron. 2009; 25:652–656. http://dx.doi.org/10.1016/j.bios.2008.11.025. [PubMed: 19162461]

252. Lee H-Y, Kim BS. Biosens. Bioelectron. 2009; 25:587–591. http://dx.doi.org/10.1016/j.bios.2009.03.040. [PubMed: 19394212]

253. Zhang Z, Hu Y, Zhang H, Luo L, Yao S. J. Electroanal. Chem. 2010; 644:7–12. http://dx.doi.org/10.1016/j.jelechem.2010.03.015.

254. Riskin M, Tel-Vered R, Lioubashevski O, Willner I. J. Am. Chem. Soc. 2009; 131:7368–7378. http://dx.doi.org/10.1021/ja9001212. [PubMed: 19425579]

255. Du D, Chen S, Cai J, Tao Y, Tu H, Zhang A. Electrochim. Acta. 2008; 53:6589–6595. http://dx.doi.org/10.1016/j.electacta.2008.04.027.

256. Wang H-F, He Y, Ji T-R, Yan X-P. Anal. Chem. 2009; 81:1615–1621. http://dx.doi.org/10.1021/ac802375a. [PubMed: 19170523]

257. Lin H-Y, Ho M-S, Lee M-H. Biosens. Bioelectron. 2009; 25:579–586. http://dx.doi.org/10.1016/j.bios.2009.03.039. [PubMed: 19409771]

258. Lee M-H, Chen Y-C, Ho M-H, Lin H-Y. Anal. Bioanal. Chem. 2010; 397:1457–1466. http://dx.doi.org/10.1007/s00216-010-3631-x. [PubMed: 20349227]

259. Lin CI, Joseph AK, Chang CK, Lee YD. J. Chromatogr. A. 2004; 1027:259–262. http://dx.doi.org/10.1016/j.chroma.2003.10.037. [PubMed: 14971510]

260. Lin CI, Joseph AK, Chang CK, Lee YD. Biosens. Bioelectron. 2004; 20:127–131. http://dx.doi.org/10.1016/j.bios.2003.10.017. [PubMed: 15142585]

261. Diltemiz SE, Say R, Büyüktiryaki S, Hür D, Denizli A, Ersöz A. Talanta. 2008; 75:890–896. http://dx.doi.org/10.1016/j.talanta.2007.12.036. [PubMed: 18585161]

262. Alvarez-Lorenzo C, Concheiro A. J. Chromatogr. B. 2004; 804:231–245. http://dx.doi.org/10.1016/j.jchromb.2003.12.032.

263. Zaidi SA. Drug Deliv. 2014:1–10. http://dx.doi.org/10.3109/10717544.2014.970297.

264. Norell MC, Andersson HS, Nicholls IA. J. Mol. Recognit. 1998; 11:98–102. http://dx.doi.org/10.1002/(SICI)1099-1352(199812)11:1/6<98::AID-JMR399>3.0.CO;2-Y. [PubMed: 10076816]

265. Ciardelli G, Cioni B, Cristallini C, Barbani N, Silvestri D, Giusti P. Biosens. Bioelectron. 2004; 20:1083–1090. http://dx.doi.org/10.1016/j.bios.2004.06.028. [PubMed: 15556352]

266. Suedee R. Pharm. Anal. Acta. 2013; 04 http://dx.doi.org/10.4172/2153-2435.1000264.

267. Suedee R, Srichana T, Martin GP. J. Control. Release. 2000; 66:135–147. http://dx.doi.org/10.1016/S0168-3659(99)00261-8. [PubMed: 10742575]

268. Berrueta LA, Gallo B, Vicente F. Chromatographia. 1995; 40:474–483. http://dx.doi.org/10.1007/BF02269916.

269. Lv Y, Lin Z, Feng W, Zhou X, Tan T. Biochem. Eng. J. 2007; 36:221–229. http://dx.doi.org/10.1016/j.bej.2007.02.023.

270. Lv Y, Lin Z, Tan T, Feng W, Qin P, Li C. Sens. Actuators B. Chem. 2008; 133:15–23. http://dx.doi.org/10.1016/j.snb.2008.01.067.

271. Matsui J, Okada M, Tsuruoka M, Takeuchi T. Anal. Commun. 1997; 34:85–87. http://dx.doi.org/10.1039/A700103G.

272. Sellergren B. Anal. Chem. 1994; 66:1578–1582. http://dx.doi.org/10.1021/ac00081a036.

273. González-Mariño I, Quintana JB, Rodríguez I, Rodil R, González-Peñas J, Cela R. J. Chromatogr. A. 2009; 1216:8435–8441. http://dx.doi.org/10.1016/j.chro-ma.2009.09.069. [PubMed: 19846101]

274. Beltran A, Borrull F, Marcé RM, Cormack PAG. TrAC Trends Anal. Chem. 2010; 29:1363–1375. http://dx.doi.org/10.1016/j.trac.2010.07.020.

275. Qu G, Wu A, Shi X, Niu Z, Xie W, Zhang D. Anal. Lett. 2008; 41:1443–1458. http://dx.doi.org/10.1080/00032710802119566.

276. Yan H, Tian M, Row KH. J. Sep. Sci. 2008; 31:3015–3020. http://dx.doi.org/10.1002/jssc.200800315. [PubMed: 18693325]

277. Xiong Y, Zhou H, Zhang Z, He D, He C. Analyst. 2006; 131:829–834. http://dx.doi.org/10.1039/B606779B. [PubMed: 16802029]

278. Shi X-L, Feng M-Q, Shi J, Shi Z-H, Zhong J, Zhou P. Protein Expr. Purif. 2007; 54:24–29. http://dx.doi.org/10.1016/j.pep.2007.02.008. [PubMed: 17408968]

279. Urraca JL, Marazuela MD, Moreno-Bondi MC. Anal. Bioanal. Chem. 2006; 385:1155–1161. http://dx.doi.org/10.1007/s00216-006-0343-3. [PubMed: 16628404]

280. Cacho C, Turiel E, Martín-Esteban A, Ayala D, Pérez-Conde C. J. Chromatogr. A. 2006; 1114:255–262. http://dx.doi.org/10.1016/j.chroma.2006.02.051. [PubMed: 16529760]

281. Tamayo FG, Martin-Esteban A. J. Chromatogr. A. 2005; 1098:116–122. http://dx.doi.org/10.1016/j.chroma.2005.08.068. [PubMed: 16314167]

282. Hu M, Jiang M, Wang P, Mei S, Lin Y, Hu X, Shi Y, Lu B, Dai K. Anal. Bioanal. Chem. 2007; 387:1007–1016. http://dx.doi.org/10.1007/s00216-006-1004-2. [PubMed: 17186227]

283. Chapuis F, Mullot J-U, Pichon V, Tuffal G, Hennion M-C. J. Chromatogr. A. 2006; 1135:127–134. http://dx.doi.org/10.1016/j.chroma.2006.09.076. [PubMed: 17055520]

284. Hugon-Chapuis F, Mullot JU, Tuffal G, Hennion M-C, Pichon V. J. Chromatogr. A. 2008; 1196–1197:73–80. http://dx.doi.org/10.1016/j.chroma.2008.04.038.

285. Caro E, Marcé RM, Cormack PAG, Sherrington DC, Borrull F. Anal. Chim. Acta. 2006; 562:145–151. http://dx.doi.org/10.1016/j.aca.2006.01.080.

286. Claude B, Morin P, Bayoudh S, de Ceaurriz J. J. Chromatogr. A. 2008; 1196–1197:81–88. http://dx.doi.org/10.1016/j.chroma.2008.05.022.

287. Beltran A, Marcé RM, Cormack PAG, Sherrington DC, Borrull F. J. Sep. Sci. 2008; 31:2868–2874. http://dx.doi.org/10.1002/jssc.200800085. [PubMed: 18666169]

288. Beltran A, Fontanals N, Marcé RM, Cormack PAG, Borrull F. J. Sep. Sci. 2009; 32:3319–3326. http://dx.doi.org/10.1002/jssc.200900268. [PubMed: 19722176]

289. Suedee R, Seechamnanturakit V, Canyuk B, Ovatlarnporn C, Martin GP. J. Chromatogr. A. 2006; 1114:239–249. http://dx.doi.org/10.1016/j.chroma.2006.02.033. [PubMed: 16530207]

290. Le Noir M, Plieva F, Hey T, Guieysse B, Mattiasson B. J. Chromatogr. A. 2007; 1154:158–164. http://dx.doi.org/10.1016/j.chroma.2007.03.064. [PubMed: 17449053]

291. Carabias-Martínez R, Rodríguez-Gonzalo E, Herrero-Hernández E. J. Chromatogr. A. 2005; 1085:199–206. http://dx.doi.org/10.1016/j.chroma.2005.05.084. [PubMed: 16106699]

292. Hoshina K, Horiyama S, Matsunaga H, Haginaka J. J. Chromatogr. A. 2009; 1216:4957–4962. http://dx.doi.org/10.1016/j.chroma.2009.04.071. [PubMed: 19439306]

293. Sun Z, Schüssler W, Sengl M, Niessner R, Knopp D. Anal. Chim. Acta. 2008; 620:73–81. http://dx.doi.org/10.1016/j.aca.2008.05.020. [PubMed: 18558126]

294. Alexiadou DK, Maragou NC, Thomaidis NS, Theodoridis GA, Koupparis MA. J. Sep. Sci. 2008; 31:2272–2282. http://dx.doi.org/10.1002/jssc.200700643. [PubMed: 18615828]

295. DeForest CA, Anseth KS. Nat. Chem. 2011; 3:925–931. http://dx.doi.org/10.1038/nchem.1174. [PubMed: 22109271]

296. Wayne, RP. Photochemistry. 1st. The Butterworth Group; 1970.

297. Tibbitt MW, Kloxin AM, Anseth KS. J. Polym. Sci. A: Polym. Chem. 2013; 51:1899–1911. http://dx.doi.org/10.1002/pola.26574. [PubMed: 24496479]

298. Adzima BJ, Tao Y, Kloxin CJ, DeForest CA, Anseth KS, Bowman CN. Nat. Chem. 2011; 3:256–259. http://dx.doi.org/10.1038/nchem.980. [PubMed: 21336334]

299. Barrett CJ, Mamiya J, Yager KG, Ikeda T. Soft Matter. 2007; 3:1249. http://dx.doi.org/10.1039/b705619b.

300. Kageyama Y, Tanigake N, Kurokome Y, Iwaki S, Takeda S, Suzuki K, Sugawara T. Chem. Commun. 2013; 49:9386. http://dx.doi.org/10.1039/c3cc43488e.

301. Matsumoto S, Yamaguchi S, Ueno S, Komatsu H, Ikeda M, Ishizuka K, Iko Y, Tabata KV, Aoki H, Ito S, Noji H, Hamachi I. Chem. Eur. J. 2008; 14:3977–3986. http://dx.doi.org/10.1002/chem.200701904. [PubMed: 18335444]

302. Sugiura S, Szilágyi A, Sumaru K, Hattori K, Takagi T, Filipcsei G, Zrinyi M, Kanamori T. Lab. Chip. 2009; 9:196. http://dx.doi.org/10.1039/b810717c. [PubMed: 19107273]

303. Wang S, Choi M-S, Kim S-H. J. Photochem. Photobiol. Chem. 2008; 198:150–155. http://dx.doi.org/10.1016/j.jphotochem.2008.03.002.

304. Griffin DR, Kasko AM. J. Am. Chem. Soc. 2012; 134:13103–13107. http://dx.doi.org/10.1021/ja305280w. [PubMed: 22765384]

305. Fomina N, McFearin C, Sermsakdi M, Edigin O, Almutairi A. J. Am. Chem. Soc. 2010; 132:9540–9542. http://dx.doi.org/10.1021/ja102595j. [PubMed: 20568765]

306. Kodzwa MG, Staben ME, Rethwisch DG. J. Membr. Sci. 1999; 158:85–92. http://dx.doi.org/10.1016/S0376-7388(99)00008-3.

307. Chujo Y, Sada K, Saegusa T. Macromolecules. 1990; 23:2693–2697. http://dx.doi.org/10.1021/ma00212a017.

308. He J, Tremblay L, Lacelle S, Zhao Y. Soft Matter. 2011; 7:2380. http://dx.doi.org/10.1039/c0sm01383h.

309. Andreopoulos FM, Deible CR, Stauffer MT, Weber SG, Wagner WR, Beckman EJ, Russell AJ. J. Am. Chem. Soc. 1996; 118:6235–6240. http://dx.doi.org/10.1021/ja954117c.

310. Zheng Y, Micic M, Mello SV, Mabrouki M, Andreopoulos FM, Konka V, Pham SM, Leblanc RM. Macromolecules. 2002; 35:5228–5234. http://dx.doi.org/10.1021/ma012263z.

311. Ramanan VV, Katz JS, Guvendiren M, Cohen ER, Marklein RA, Burdick JA. J. Mater. Chem. 2010; 20:8920. http://dx.doi.org/10.1039/c0jm00734j.

312. Azagarsamy MA, Alge DL, Radhakrishnan SJ, Tibbitt MW, Anseth KS. Biomacromolecules. 2012; 13:2219–2224. http://dx.doi.org/10.1021/bm300646q. [PubMed: 22746981]

313. Griffin DR, Kasko AM. ACS Macro Lett. 2012; 1:1330–1334. http://dx.doi.org/10.1021/mz300366s. [PubMed: 25285242]

314. Gong JP, Nitta T, Osada Y. J. Phys. Chem. 1994; 98:9583–9587. http://dx.doi.org/10.1021/j100089a036.

315. Osada Y, Okuzaki H, Hori H. Nature. 1992; 355:242–244. http://dx.doi.org/10.1038/355242a0.

316. Liu Z, Calvert P. Adv. Mater. 2000; 12:288–291. http://dx.doi.org/10.1002/(SICI)1521-4095(200002)12:4<288::AID-ADMA288>3.0.CO;2-1.

317. Liu F, Urban MW. Prog. Polym. Sci. 2010; 35:3–23. http://dx.doi.org/10.1016/j.progpolymsci.2009.10.002.

318. Kim SJ, Kim HI, Shin SR, Kim SI. J. Appl. Polym. Sci. 2004; 92:915–919. http://dx.doi.org/10.1002/app.20059.

319. Zrínyi M, Fehér J, Filipcsei G. Macromolecules. 2000; 33:5751–5753. http://dx.doi.org/10.1021/ma000253c.

320. He C, Kim SW, Lee DS. J. Control. Release. 2008; 127:189–207. http://dx.doi.org/10.1016/j.jconrel.2008.01.005. [PubMed: 18321604]

321. Li, H. Smart Hydrogel Modelling. Springer Science & Business Media; 2010.

322. Helfferich, FG. Ion Exchange. Courier Corporation; 1962.

323. Khare AR, Peppas NA. Biomaterials. 1995; 16:559–567. http://dx.doi.org/10.1016/0142-9612(95)91130-Q. [PubMed: 7492721]

324. Yew YK, Ng TY, Li H, Lam KY. Biomed. Microdevices. 2007; 9:487–499. http://dx.doi.org/10.1007/s10544-007-9056-4. [PubMed: 17520372]

325. Li H, Ng TY, Yew YK, Lam KY. Biomacromolecules. 2005; 6:109–120. http://dx.doi.org/10.1021/bm0496458. [PubMed: 15638511]

326. Kim SJ, Kim MS, Kim SI, Spinks GM, Kim BC, Wallace GG. Chem. Mater. 2006; 18:5805–5809. http://dx.doi.org/10.1021/cm060988h.

327. Otero, Tf; Cortés, Mt. Adv. Mater. 2003; 15:279–282. http://dx.doi.org/10.1002/adma.200390066.

328. Baughman, RH.; Shacklette, LW.; Elsenbaumer, RL.; Plichta, E.; Becht, C. Conjugated Polymeric Materials: Opportunities in Electronics, Optoelectronics, and Molecular Electronics. Brédas, JL.; Chance, RR., editors. Netherlands: Springer; 1990. p. 559-582.http://link.springer.com/chapter/10.1007/978-94-009-2041-5_44 [accessed 14.12.14]

329. Baughman RH. Synth. Met. 1996; 78:339–353. http://dx.doi.org/10.1016/0379-6779(96)80158-5.

330. Wallace, GG.; Teasdale, PR.; Spinks, GM.; Kane-Maguire, LAP. Conductive Electroactive Polymers: Intelligent Materials Systems. 2nd. CRC Press; 2002.

331. Lewis TW, Spinks GM, Wallace GG, Mazzoldi A, De Rossi D. Synth. Met. 2001; 122:379–385. http://dx.doi.org/10.1016/S0379-6779(00)00397-0.

332. Mazzoldi, A.; De Rossi, D. Conductive-Polymer-Based Structures for a Steerable Catheter. Bar-Cohen, Y., editor. 2000. p. 273-280.http://dx.doi.org/10.1117/12.387786

333. Madden JD, Madden PG, Hunter IW. Conducting Polymer Actuators as Engineering Materials. 2002:176–190. http://dx.doi.org/10.1117/12.475163.

334. Takashima W, Kaneko M, Kaneto K, MacDiarmid AG. Synth. Met. 1995; 71:2265–2266. http://dx.doi.org/10.1016/0379-6779(94)03252-2.

335. Ha SM, Yuan W, Pei Q, Pelrine R, Stanford S. Adv. Mater. 2006; 18:887–891. http://dx.doi.org/10.1002/adma.200502437.

336. Liang S, Xu J, Weng L, Zhang L, Guo X, Zhang X. J. Phys. Chem. B. 2007; 111:941–945. http://dx.doi.org/10.1021/jp0673821. [PubMed: 17266246]

337. Hirai T, Nemoto H, Suzuki T, Hayashi S, Hirai M. J. Intell. Mater. Syst. Struct. 1993; 4:277–279. http://dx.doi.org/10.1177/1045389X9300400219.

338. Hirai T, Nemoto H, Hirai M, Hayashi S. J. Appl. Polym. Sci. 1994; 53:79–84. http://dx.doi.org/10.1002/app.1994.070530109.

339. Hirai, T.; Hirai, M. Polymer Sensors and Actuators. Osada, PY.; Rossi, PDED., editors. Berlin, Heidelberg: Springer; 2000. p. 245-258.http://link.springer.com/chapter/10.1007/978--3-662-04068-3_8 [accessed 14.12.14]

340. Murdan S. J. Control. Release. 2003; 92:1–17. http://dx.doi.org/10.1016/S0168-3659(03)00303-1. [PubMed: 14499181]

341. Delgado-Charro MB, Guy RH. STP Pharma Sci. 2001; 11:404–414.

342. Vanbever R, Préat V. Adv. Drug Deliv. Rev. 1999; 35:77–88. http://dx.doi.org/10.1016/S0169-409X(98)00064-7. [PubMed: 10837690]

343. Riviere JE, Heit MC. Pharm. Res. 1997; 14:687–697. http://dx.doi.org/10.1023/A:1012129801406. [PubMed: 9210183]

344. Santini JT, Cima MJ, Langer R. Nature. 1999; 397:335–338. http://dx.doi.org/10.1038/16898. [PubMed: 9988626]

345. Grimshaw PE, Grodzinsky AJ, Yarmush ML, Yarmush DM. Chem. Eng. Sci. 1989; 44:827–840. http://dx.doi.org/10.1016/0009-2509(89)85256-X.

346. Pasechnik, VA.; Cherkasov, AN.; Zhemkov, VP.; Chechina, VV.; Alimardanov, RS. Effect of Direct-Current on the Permeability of Ultrafiltration Membranes. New York, NY: Plenum Publ. Corp. Consultants Bureau; 1979.

347. Burgmayer P, Murray RW. J. Am. Chem. Soc. 1982; 104:6139–6140. http://dx.doi.org/10.1021/ja00386a061.

348. Bhaskar RK, Sparer RV, Himmelstein KJ. J. Membr. Sci. 1985; 24:83–96. http://dx.doi.org/10.1016/S0376-7388(00)83210-X.

349. Kim SY, Lee YM. J. Appl. Polym. Sci. 1999; 74:1752–1761. http://dx.doi.org/10.1002/(SICI)1097-4628(19991114)74:7<1752::AID-APP18>3.0.CO;2-H.

350. Ramanathan S, Block LH. J. Control. Release. 2001; 70:109–123. http://dx.doi.org/10.1016/S0168-3659(00)00333-3. [PubMed: 11166412]

351. Sawahata K, Hara M, Yasunaga H, Osada Y. J. Control. Release. 1990; 14:253–262. http://dx.doi.org/10.1016/0168-3659(90)90165-P.

352. Sutani K, Kaetsu I, Uchida K. Radiat. Phys. Chem. 2001; 61:49–54. http://dx.doi.org/10.1016/S0969-806X(00)00381-9.

353. Yuk SH, Cho SH, Lee HB. Pharm. Res. 1992; 9:955–957. http://dx.doi.org/10.1023/A:1015821504229. [PubMed: 1438013]

354. Kwon IC, Bae YH, Okano T, Kim SW. J. Control. Release. 1991; 17:149–156. http://dx.doi.org/10.1016/0168-3659(91)90054-H.

355. Hsu C-S, Block LH. Pharm. Res. 1996; 13:1865–1870. http://dx.doi.org/10.1023/A:1016045427545. [PubMed: 8987086]

356. Jensen M, Birch Hansen P, Murdan S, Frokjaer S, Florence AT. Eur. J. Pharm. Sci. 2002; 15:139–148. http://dx.doi.org/10.1016/S0928-0987(01)00193-2. [PubMed: 11849910]

357. Kwon IC, Bae YH, Kim SW. Nature. 1991; 354:291–293. http://dx.doi.org/10.1038/354291a0. [PubMed: 1956379]

358. Kwon IC, Bae YH, Kim SW. J. Control. Release. 1994; 30:155–159. http://dx.doi.org/10.1016/0168-3659(94)90262-3.

359. Hopfenberg, HB. Control. Release Polym. Formul. American Chemical Society; 1976. p. 26-32.http://dx.doi.org/10.1021/bk-1976-0033.ch003 [accessed 27.11.14]

360. Kagatani S, Shinoda T, Konno Y, Fukui M, Ohmura T, Osada Y. J. Pharm. Sci. 1997; 86:1273–1277. http://dx.doi.org/10.1021/js9700762. [PubMed: 9383739]

361. Hoffman AS. Adv. Mater. 2013; 65:10–16.

362. Qiu Y, Park K. Adv. Drug Deliv. Rev. 2001; 53:321–339. [PubMed: 11744175]

363. Wang Q, Wang L, Detamore MS, Berkland C. Adv. Mater. 2008; 20:236–239.

364. Bell CJ, Carrick LM, Katta J, Jin Z, Ingham E, Aggeli A, Boden N, Waigh TA, Fisher J. J. Biomed. Mater. Res. A. 2006; 78A:236–246. [PubMed: 16628707]

365. Guvendiren M, Lu HD, Burdick JA. Soft Matter. 2012; 8:260–272.

366. Gutowska A, Jeong B, Jasionowski M. Anat. Rec. 2001; 263:342–349. [PubMed: 11500810]

367. Yan C, Pochan DJ. Chem. Soc. Rev. 2010; 39:3528–3540. [PubMed: 20422104]

368. Ferry, JD. Viscoelastic Properties of Polymers. 3rd. John Wiley & Sons; 1980.

369. McCrum, NG.; Buckley, CP.; Bucknall, CB. Princples of Polymer Engineering. 2nd. Oxford Science Publications; 1977.

370. Hiemenz, PC.; Lodge, TP. Polymer Chemistry. 2nd. Taylor & Francis; 2007.

371. Mezger, TG. Rheology Handbook. 2nd. Hannover: Vincentz Network; 2006.

372. Meyers, MA.; Chawla, KK. Mechanical Behavior of Materials. 2nd. Cambridge University Press; 2008.

373. Sundaram H, Voigts B, Beer K, Meland M. Dermatol. Surg. 2010; 36:1859–1865. [PubMed: 20969663]

374. Findley, WN.; Lai, JS.; Onaran, K. Creep and Relaxation of Nonlinear Viscoelastic Materials. Dover Publications; 1976.

375. Roylance D. Engineering Viscoelasticity. 2001 http://web.mit.edu/course/3/3.11/www/modules/visco.pdf.

376. Ross-Murphy SB. Polym. Gels Netw. 1994; 2:229–237.

377. Kavanagh GM, Ross-Murphy SB. Prog. Polym. Sci. 1998; 23:533–562.

378. Macosko, CW. Rheology: Principles, Measurements, and Applications. Wiley-VCM; 1994.

379. Fang Y, Nishinari K. Biopolymers. 2004; 73:44–60. [PubMed: 14691938]

380. Pal K, Banthia AK, Majumdar DK. Des. Monomers Polym. 2009; 12:197–220.

381. Barnes HA. J. Non-Newton. Fluid Mech. 1997; 70:1–33.

382. Hyun K, Kim SH, Ahn KH, Lee SJ. J. Non-Newton. Fluid Mech. 2002; 107:51–65.

383. Engler AJ, Sen S, Sweeney HL, Discher DE. Cell. 2006; 126:677–689. [PubMed: 16923388]

384. Kretlow JD, Klouda L, Mikos AG. Adv. Drug Deliv. Rev. 2007; 59:263–273. [PubMed: 17507111]

385. Jeyaseelan RS, Giacomin J. J. Non-Newton. Fluid Mech. 2008; 148:24–32.

386. Ewoldt RH, Hosoi AE, McKinley GH. Integr. Comp. Biol. 2009; 49:40–50. [PubMed: 21669845]

387. Tan K, Cheng S, Juge L, Bilston LE. J. Biomech. 2013; 46:1060–1066. [PubMed: 23481421]

388. Hyun K, Wilhelm M, Klein CO, Cho KS, Nam JG, Ahn KH, Lee SJ, Ewoldt RH, McKinley GH. Prog. Polym. Sci. 2011; 36:1697–1753.

389. Boersma WH, Laven J, Stein HN. AIChE J. 1990; 36:321–332.

390. Morrison, ID.; Ross, S. Colloidal Dispersions: Suspensions, Emulsions, and Foams. New York: Wiley-Interscience; 2002.

391. Patel PN, Smith CK, Patrick CW Jr. Biomed. Mater. Res. A. 2005; 73A:313–319.

392. Brinson, HF.; Brinson, LC. Polymer Engineering Science and Viscoelasticity: An Introduction. Springer; 2007.

393. Harrison G, Franks GV, Tirtaatmadja V, Boger DV. Korea–Aust. Rheol. J. 1999; 11:197–218.

394. Heymann L, Peukert S, Aksel N. J. Rheo. 2002; 46:93–112.

395. Aulisa L, Dong H, Hartgerink JD. Biomacromolecules. 2009; 10:2694–2698. [PubMed: 19705838]

396. Barbucci R, Lamponi S, Borzacchiello A, Ambrosio L, Fini M, Torricelli P, Giardino R. Biomaterials. 2002; 23:4503–4513. [PubMed: 12322970]

397. Li Y, Fukushima K, Coady DJ, Engler AC, Liu S, Huang Y, Cho JS, Guo Y, Miller LS, Tan JPK, Ee PLR, Fan W, Yang YY, Hedrick JL. Angew. Chem. 2013; 52:674–678. [PubMed: 23161823]

398. Morsi NM, Abdelbary GA, Ahmed MA. Eur. J. Pharm. Biopharm. 2014; 86:178–189. [PubMed: 23688805]

399. Yu L, Ding J. Chem. Soc. Rev. 2008; 37:1473–1481. [PubMed: 18648673]

400. Temenoff JS, Mikos AG. Biomaterials. 2000; 21:2405–2412. [PubMed: 11055288]

401. Shim WS, Kim J, Park HK, Kim KM, Kwan IC, Lee DS. Biomaterials. 2006; 27:5178–5185. [PubMed: 16797693]

402. Garbern JC, Minami E, Stayton PS, Murry CE. Biomaterials. 2011; 32:2407–2416. [PubMed: 21186056]

403. Shim WS, Yoo JS, Bae YH, Lee DS. Biomacromolecules. 2005; 6:2930–2934. [PubMed: 16283710]

404. Chiu Y-L, Chen S-C, Su C-J, Hsiao C-W, Chen Y-M, Chen H-L, Sung H-W. Biomaterials. 2009; 30:4877–4888. [PubMed: 19527916]

405. Ruel-Garièpy E, Leroux J-C. Eur. J. Pharm. Biopharm. 2004; 58:409–426. [PubMed: 15296964]

406. Jeong B, Kim SW, Bae YH. Adv. Drug Deliv. Rev. 2002; 54:37–51. [PubMed: 11755705]

407. Rozier A, Mazuel C, Grove J, Plazonnet B. Int. J. Pharm. 1989; 57:163–168.

408. Westerhaus E, Messersmith PB. Biomaterials. 2001; 22:453–462. [PubMed: 11214756]

409. Suri S, Banerjee R. J. Biomed. Mater. Res. A. 2006; 79A:650–664. [PubMed: 16826595]

410. Yan C, Altunbas A, Yucel T, Nagarkar RP, Schneider JP, Pochan DJ. Soft Matter. 2010; 6:5143–5156. [PubMed: 21566690]

411. Haines-Butterick L, Rajagopal K, Branco M, Salick D, Rughani R, Pilarz M, Lamm MS, Pochan DJ, Schneider JP. Proc. Natl. Acad. Sci. 2007; 104:7791–7796. [PubMed: 17470802]

412. Niece KL, Czeisler C, Sahni V, Tysseling-Mattiace V, Pashuck ET, Kessler JA, Stupp SI. Biomaterials. 2008; 29:4501–4509. [PubMed: 18774605]

413. Olsen BD, Kornfield JA, Tirrell DA. Macromolecules. 2010; 43:9094–9099. [PubMed: 21221427]

414. Sui Z, King WJ, Murphy WL. Adv. Funct. Mater. 2008; 18:1824–1831.

415. Jonker AM, Löwik DWPM, van Hest JCM. Chem. Mater. 2012; 24:759–773.

416. Altman GH, Diaz F, Jakuba C, Calabro T, Horan RL, Chen J, Lu H, Richmond J, Kaplan DL. Biomaterials. 2003; 24:401–416. [PubMed: 12423595]

417. Perez-Riguerio J, Viney C, Llorca J, Elices M, Appl J. Polym. Sci. 1998; 70:2439–2447.

418. Kaplan DL. Polym. Degrad. Stab. 1998; 59:25–32.

419. Matsumoto A, Chen J, Collette AL, Kim U-J, Altman GH, Cebe P, Kaplan DL. J. Phys. Chem. B. 2006; 110:21630–21638. [PubMed: 17064118]

420. Inoue S, Tanaka K, Arisaka F, Kimura S, Ohtomo K, Mizuno S. J. Biol. Chem. 2000; 275:40517–40528. [PubMed: 10986287]

421. Cao Y, Wang B. Int. J. Mol. Sci. 2009; 10:1514–1524. [PubMed: 19468322]

422. Horan RL, Antle K, Collette AL, Wang Y, Huang J, Moreau JE, Volloch V, Kaplan DL, Altman GH. Biomaterials. 2005; 26:3385–3393. [PubMed: 15621227]

423. Wang Y, Kim H-J, Vunjak-Novakovic G, Kaplan DL. Biomaterials. 2006; 27:6064–6082. [PubMed: 16890988]

424. Zuglul AH, Mitsuo A, Kiyoshi H. Biosci. Biotechnol. Biochem. 1993; 57:1910–1912.

425. Vepari C, Kaplan DL. Prog. Polym. Sci. 2007; 32:991–1007. [PubMed: 19543442]

426. Wang X, Kluge JA, Leisk GG, Kaplan DL. Biomaterials. 2008; 29:1054–1064. [PubMed: 18031805]

427. Yucel T, Cebe P, Kaplan DL. Biophys. J. 2009; 97:2044–2050. [PubMed: 19804736]

428. Sah MK, Pramanik K. Afr. J. Biotechnol. 2013; 10:7878–7892.

429. Banta S, Wheeldon IR, Blenner M. Annu. Rev. Biomed. Eng. 2010; 12:167–186. [PubMed: 20420519]

430. Landschulz WH, Johnson PF, McKnight SL. Science. 1988; 240:1759–1764. [PubMed: 3289117]

431. Ciani B, Hutchinson EG, Sessions RB, Woolfson DN. J. Biol. Chem. 2002; 227:10150–10155. [PubMed: 11751929]

432. Kennedy SB, deAzevedo ER, Petka WA, Russell TP, Tirrell DA, Hong M. Macromolecules. 2001; 34:8675–8685.

433. Mi L, Fischer S, Chung B, Sundelacruz S, Harden JL. Biomacromolecules. 2006; 7:38–47. [PubMed: 16398496]

434. Kennedy SB, Littrell K, Thiyagarajan P, Tirrell DA, Russell TP. Macromolecules. 2005; 38:7470–7475.

435. Klok H-A. Macromol. Perspect. 2009; 42:7990–8000.

436. Wang C, Kope ek J, Stewart RJ. Biomacromolecules. 2001; 2:912–920. [PubMed: 11710049]

437. Wang C, Stewart RJ, Kope ek J. Nature. 1999; 397:417–420. [PubMed: 9989405]

438. Tang A, Wang C, Stewart RJ, Kope ek J. J. Control. Release. 2001; 72:57–70. [PubMed: 11389985]

439. Fischer S, Liu X, Mao H-Q, Harden JL. Biomaterials. 2007; 28:3325–3337. [PubMed: 17459470]

440. Shen W, Kornfield JA, Tirrell DA. Soft Matter. 2007; 3:99–107.

441. Skrzeszewska PJ, Sprakel J, de Wolf FA, Fokkink R, Stuart MAC, van der Gucht J. Macromolecules. 2010; 43:3542–3548.

442. Nowak AP, Breedveld V, Pakstis L, Ozbas B, Pine DJ, Pochan D, Deming TJ. Nature. 2002; 417:424–428. [PubMed: 12024209]

443. Pakstis L, Ozbas B, Hales KD, Nowak AP, Deming TJ, Pochan DJ. Biomacromolecules. 2004; 5:312–318. [PubMed: 15002989]

444. Breedveld V, Nowak AP, Sato J, Deming TJ, Pine DJ. Macromolecules. 2004; 37:3943–3953.

445. Li Z, Deming TJ. Soft Matter. 2010; 6:2546–2551.

446. Deming TJ. Soft Matter. 2005; 1:28–35.

447. Yang C-Y, Song B, Ao Y, Nowak AP, Abelowitz RB, Korsak RA, Havton LA, Deming TJ, Sofroniew MV. Biomaterials. 2009; 30:2881–2898. [PubMed: 19251318]

448. Foo CTSWP, Lee JS, Mulyasasmita W, Parisi-Amon A, Heilshorn SC. Proc. Natl. Acad. Sci. 2009; 106:22067–22072. [PubMed: 20007785]

449. Chen HI, Einbond A, Kwak S-J, Linn H, Koepf E, Peterson S, Kelly JW, Sudol M. J. Biol. Chem. 1997; 272:17070–17077. [PubMed: 9202023]

450. Sudol M, Chen HI, Bougeret C, Einbond A, Bork P. FEBS Lett. 1995; 369:67–71. [PubMed: 7641887]

451. Pires JR, Taha-Nejad F, Toepert F, Ast T, Hoffmüller U, Schneider-Mergener J, Kühne R, Macias MJ, Oschkinat H. J. Mol. Biol. 2001; 314:1147–1156. [PubMed: 11743730]

452. Kanelis V, Rotin D, Forman-Kay JD. Nat. Struct. Mol. Biol. 2001; 8:407–412.

453. Parisi-Amon A, Mulyasasmita W, Chung C, Heilshorn SC. Adv. Healthc. Mater. 2013; 2:428–432. [PubMed: 23184882]

454. Mart RJ, Osborne RD, Stevens MM, Ulijn RV. Soft Matter. 2006; 2:822–835.

455. Schneider JP, Pochan DJ, Ozbas B, Rajagopal K, Pakstis L, Kretsinger J. J. Am. Chem. Soc. 2002; 124:15030–15037. [PubMed: 12475347]

456. Pochan DJ, Schneider JP, Kretsinger J, Ozbas B, Rajagopal K, Haines L. J. Am. Chem. Soc. 2003; 125:11802–11803. [PubMed: 14505386]

457. Haines L, Rajagopal K, Ozbas B, Salick D, Pochan DJ, Schneider JP. J. Am. Chem. Soc. 2005; 127:17025–17029. [PubMed: 16316249]

458. Ozbas B, Rajagopal K, Schneider JP, Pochan DJ. Phys. Rev. Lett. 2004; 93:268106. [PubMed: 15698028]

459. Salick D, Pochan DJ, Schneider JP. Adv. Mater. 2009; 21:4120–4123.

460. Rajagopal K, Lamm MS, Haines-Butterick L, Pochan DJ, Schneider JP. Biomacromolecules. 2009; 10:2619–2625. [PubMed: 19663418]

461. Rughani R, Salick D, Lamm MS, Yucel T, Pochan DJ, Schneider JP. Biomacromolecules. 2009; 10:1295–1304. [PubMed: 19344123]

462. Ozbas B, Kretsinger J, Rajagopal K, Schneider JP, Pochan DJ. Macromolecules. 2004; 37:7331–7337.

463. Yucel T, Micklitsch CM, Schneider JP, Pochan DJ. Macromolecules. 2008; 41:5763–5772. [PubMed: 19169385]

464. Yan C, Mackay ME, Czymmek K, Nagarkar RP, Schneider JP, Pochan DJ. Langmuir. 2012; 28:6076–6087. [PubMed: 22390812]

465. Haines-Butterick L, Salick D, Pochan DJ, Schneider JP. Biomaterials. 2008; 29:4164–4169. [PubMed: 18687464]

466. Rughani R, Schneider JP. MRS Bull. 2008; 33:530–535. [PubMed: 19662109]

467. Kretsinger J, Haines L, Ozbas B, Pochan DJ, Schneider JP. Biomaterials. 2005; 26:5177–5186. [PubMed: 15792545]

468. Salick D, Kretsinger J, Pochan DJ, Schneider JP. J. Am. Chem. Soc. 2007; 129:14793–14799. [PubMed: 17985907]

469. Branco M, Pochan DJ, Wagner N, Schneider JP. Biomaterials. 2009; 30:1339–1347. [PubMed: 19100615]

470. Altunbas A, Lee SJ, Rajasekaran SA, Schneider JP, Pochan DJ. Biomaterials. 2011; 32:5906–5914. [PubMed: 21601921]

471. Ramachandran S, Tseng Y, Yu YB. Biomacromolecules. 2005; 6:1316–1321. [PubMed: 15877347]

472. Ramachandran S, Flynn P, Tseng Y, Yu YB. Chem. Mater. 2005; 17:6583–6588.

473. Ramachandran S, Trewhella J, Yiider Tseng Y, Yu Bruce. Chem. Mater. 2006; 18:6157–6162.

474. Bakota EL, Wang Y, Danesh FR, Hartgerink JD. Biomacromolecules. 2011; 12:1651–1657. [PubMed: 21417437]

475. Lamm MS, Rajagopal K, Schneider JP, Pochan DJ. J. Am. Chem. Soc. 2005; 127:16692–16700. [PubMed: 16305260]

476. Wang Y, Bakota EL, Chang BHJ, Entman M, Hartgerink JD, Danesh FR. J. Am. Soc. Nephrol. 2011; 22:704–717. [PubMed: 21415151]

477. Pagel K, Wagner SC, Samedov K, von Berlepsch H, Böttcher C, Koksch B. J. Am. Chem. Soc. 2006; 128:2196–2197. [PubMed: 16478157]

478. Galler KM, Aulisa L, Regan KR, D'Souza RN, Hartgerink JD. J. Am. Chem. Soc. 2010; 132:3217–3223. [PubMed: 20158218]

479. Bakota EL, Sensoy O, Ozgur B, Sayar M, Hartgerink JD. Biomacromolecules. 2013; 14:1370–1378. [PubMed: 23480446]

480. Kang MK, Colombo JS, D'Souza RN, Hartgerink JD. Biomacromolecules. 2014; 15:2004–2011. [PubMed: 24813237]

481. Drago D, Cossetti C, Iraci N, Gaude E, Musco G, Bachi A, Pluchino S. Biochimie. 2013; 95:2271–2285. [PubMed: 23827856]

482. Webber M, Han X, Murthy SNP, Rajangam K, Stupp SI, Lomasney JW. J. Tissue Eng. Regen. Med. 2010; 4:600–610. [PubMed: 20222010]

483. Wickremasinghe NC, Kumar VA, Hartgerink JD. Biomacromolecules. 2014; 15:3587–3595. [PubMed: 25308335]

484. Li L, Hangamathesvaran PMT, Yue CY, Tam KC, Hu X, Lam YC. Langmuir. 2001; 17:8062–8068.

485. Tate MC, Shear DA, Hoffman SW, Stein DG, LaPlaca MC. Biomaterials. 2001; 22:1113–1123. [PubMed: 11352091]

486. Vercruysse KP, Prestwich GD. Crit. Rev. Ther. Carr. Syst. 1998; 15:513–555.

487. Balazs, EA. Medical Applications of Hyaluronan and Its Derivatives. New York: Plenum Press; 1991.

488. Moriyama K, Ooya T, Yui N. J. Control. Release. 1999; 59:77–86. [PubMed: 10210724]

489. Weiss, C. New Frontiers in Medical Sciences: Redefining Hyaluronan. Weigel GAaPH; 2000. p. 89

490. Gupta D, Tator CH, Shoichet MS. Biomaterials. 2006; 27:2370–2379. [PubMed: 16325904]

491. Caicco MJ, Zahir T, Mothe AJ, Ballios BG, Kihm AJ, Tator CH, Shoichet MS. J. Biomed. Mater. Res. A. 2012; 101A:1472–1477. [PubMed: 23129254]

492. Kang C, Tator CH, Shoichet MS. J. Control. Release. 2010; 144:25–31. [PubMed: 20114065]

493. Shoichet MS, Tator CH, Poon P, Kang C, Baumann MD. Prog. Brain Res. 2007; 161:385–392. [PubMed: 17618992]

494. Wang Y, Lapitsky Y, Kang C, Shoichet MS. J. Control. Release. 2009; 140:218–223. [PubMed: 19470396]

495. Rodell CB, Kaminski AL, Burdick JA. Biomacromolecules. 2013; 14:4125–4134. [PubMed: 24070551]

496. Spasov AA, Khamidova TV, Bugaeva LI, Morozov IS. Pharm. Chem. J. 2000; 34:1–7.

497. Szejtli J. Chem. Rev. 1998; 98:1743–1753. [PubMed: 11848947]

498. Hashidzume A, Harada A. Polym. Chem. 2011; 2:2146–2154.

499. Li J, Loh XJ. Adv. Drug Deliv. Rev. 2008; 60:1000–1017. [PubMed: 18413280]

500. Araki J, Ito K. Soft Matter. 2007; 3:1456–1473.

501. Chen G, Jiang M. Chem. Soc. Rev. 2011; 40:2254–2266. [PubMed: 21344115]

502. Harada A, Li J, Kamachi M. Nature. 1992; 356:325–327.

503. Li J, Ni X, Zhou Z, Leong KW. J. Am. Chem. Soc. 2003; 125:1788–1795. [PubMed: 12580604]

504. Harada A, Kataoka K. Prog. Polym. Sci. 2006; 31:949–982.

505. Li J, Li X, Ni X, Wang X, Li H, Leong KW. Biomaterials. 2006; 27:4132–4140. [PubMed: 16584769]

506. Solomon MJ, Spicer PT. Soft Matter. 2010; 6:1391–1400.

507. Zaccarelli E. J. Phys. Condens. Matter. 2007; 19:323101.

508. Wang Q, Wang J, Lu Q, Detamore MS, Berkland C. Biomaterials. 2010; 31:4980–4986. [PubMed: 20303585]

509. Wang Q, Jamal S, Detamore MS, Berkland C. J. Biomed. Mater. Res. A. 2011; 96A:520–527. [PubMed: 21254383]

510. Keegan ME, Falcone JL, Leung TC, Saltzman WM. Macromolecules. 2004; 37:9779–9784.

511. Shi L, Berkland C. Adv. Mater. 2006; 18:2315–2319.

512. Shi L, Berkland C. Macromolecules. 2007; 40:4635–4643. [PubMed: 18797513]

513. Lee ALZ, Ng VWL, Wang W, Hedrick JL, Yang YY. Biomaterials. 2013; 34:10278–10286. [PubMed: 24090835]

514. Cyster LA, Grant DM, Howdle SM, Rose FRAJ, Irvine DJ, Freeman D, Scotchford CA, Shakesheff KM. Biomaterials. 2005; 26:697–702. [PubMed: 15350773]

515. Nzihou A, Attias L, Sharrock P, Ricard A. Powder Technol. 1998; 99:60–69.

516. Lewis JA. J. Am. Ceram. Soc. 2000; 83:2341–2359.

517. Santillan MJ, Membrives F, Quaranta N, Boccaccini AR. J. Nanopart. Res. 2008; 10:787–793.

518. Bossard F, Aubry T, Gotzamanis G, Tsitsilianis C. Soft Matter. 2006; 2:510–516.

519. Xu D, Asai D, Chilkoti A, Craig SL. Biomacromolecules. 2012; 13:2315–2321. [PubMed: 22789001]

520. Milner ST, Witten TA. Macromolecules. 1992; 25:5495–5503.

521. Tam KC, Jenkins RD, Winnik MA. Macromolecules. 1998; 31:4149–4159.

522. Marrucci G, Bhargava S, Cooper SL. Macromolecules. 1993; 26:6483–6488.

523. Tominaga T, Tirumala VR, Lin EK, Gong JP, Furukawa H, Osada Y, Wu W. Polymer. 2007; 48:7449–7454.

524. Shibayama, M. Encyclopedia of Polymer Nanocomposites. Berlin, Heidelberg: Springer-Verlag; 2013. p. 1-12.

525. Martin JE, Patil AJ, Butler MF, Mann S. Adv. Funct. Mater. 2011; 21:674–681.

526. Kim JE, Lee HS. Polymer. 2014; 55:287–294.

527. Hu YT. J. Rheol. 2014; 58:1789–1807.
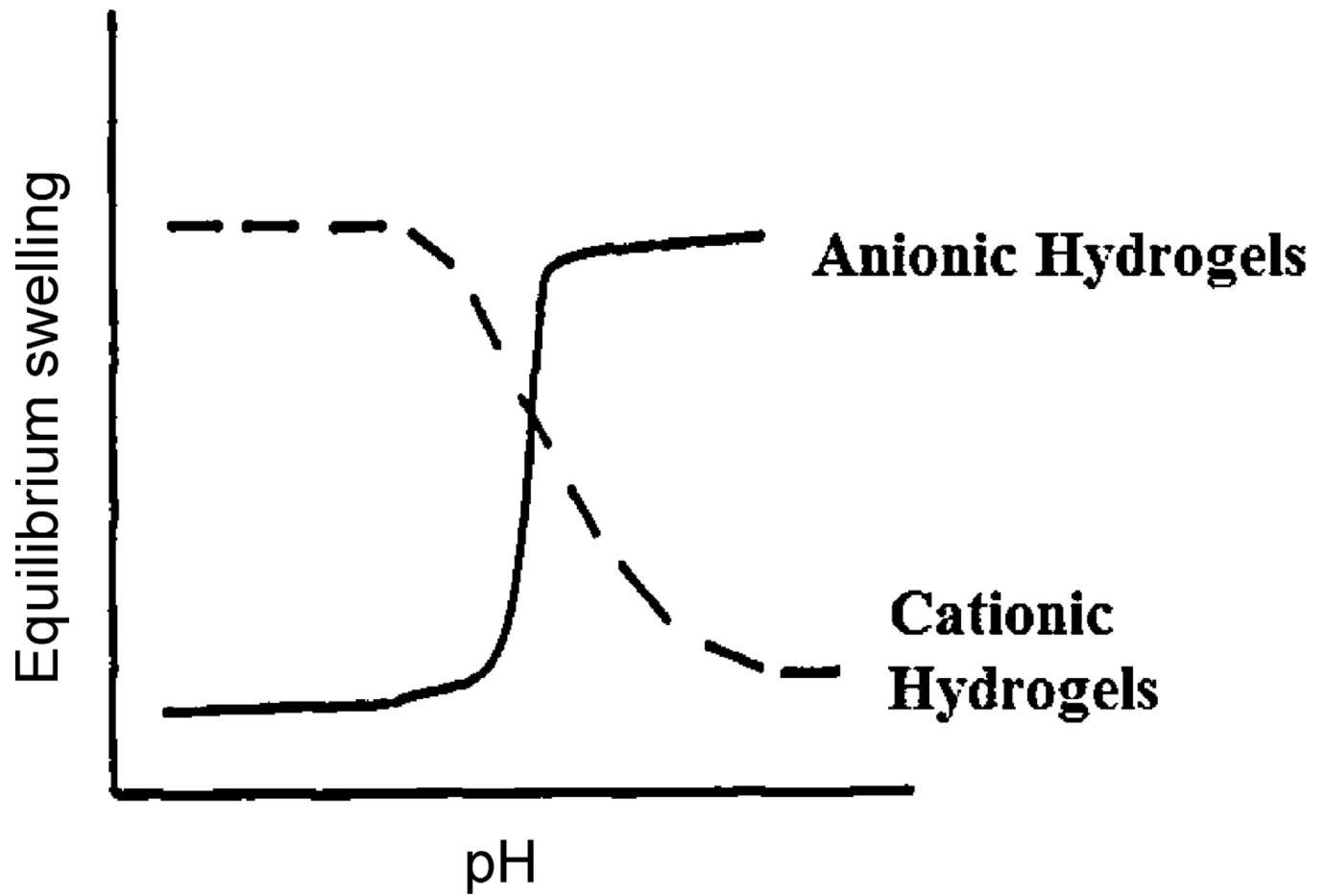
Fig. 1.
Equilibrium swelling behaviors of anionic and cationic hydrogels. Behavior is dependent on the ionic pendant groups.
Reprinted with permission from Khare et al. [53].
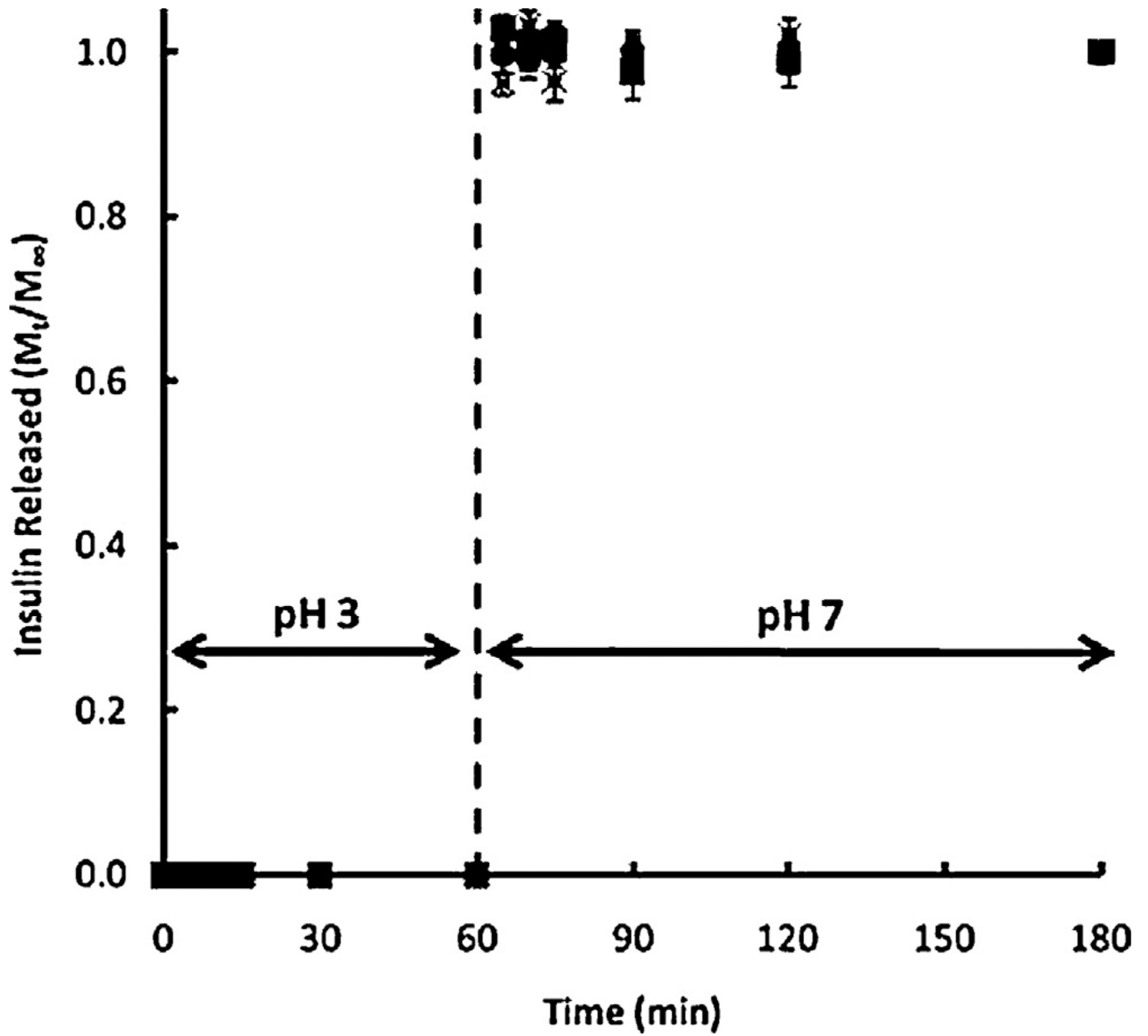
Fig. 2.
Insulin release from P(MAA-co-NVP) at both low pH (~3) and neutral pH (~7) conditions.
Reprinted with permission from Carr and Peppas [86].
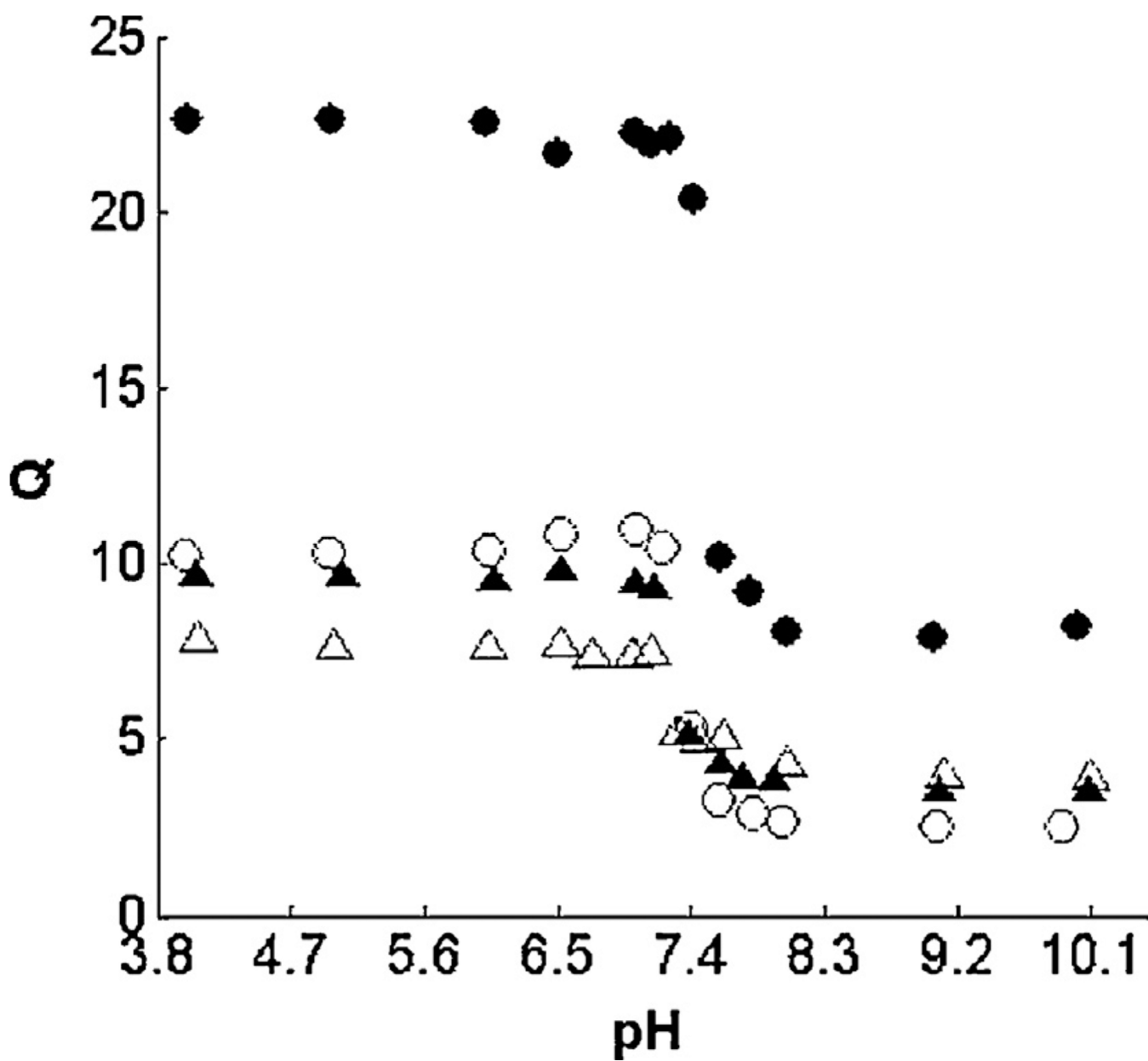
Fig. 3.
Volume swelling ratio, Q, as a function of pH for Cationic PDBP nanogels of various crosslinking ratios: ●, 0.01; ○, 0.025; ▲, 0.05; △, 0.1.
Reprinted with permission from Fisher and Peppas [106].
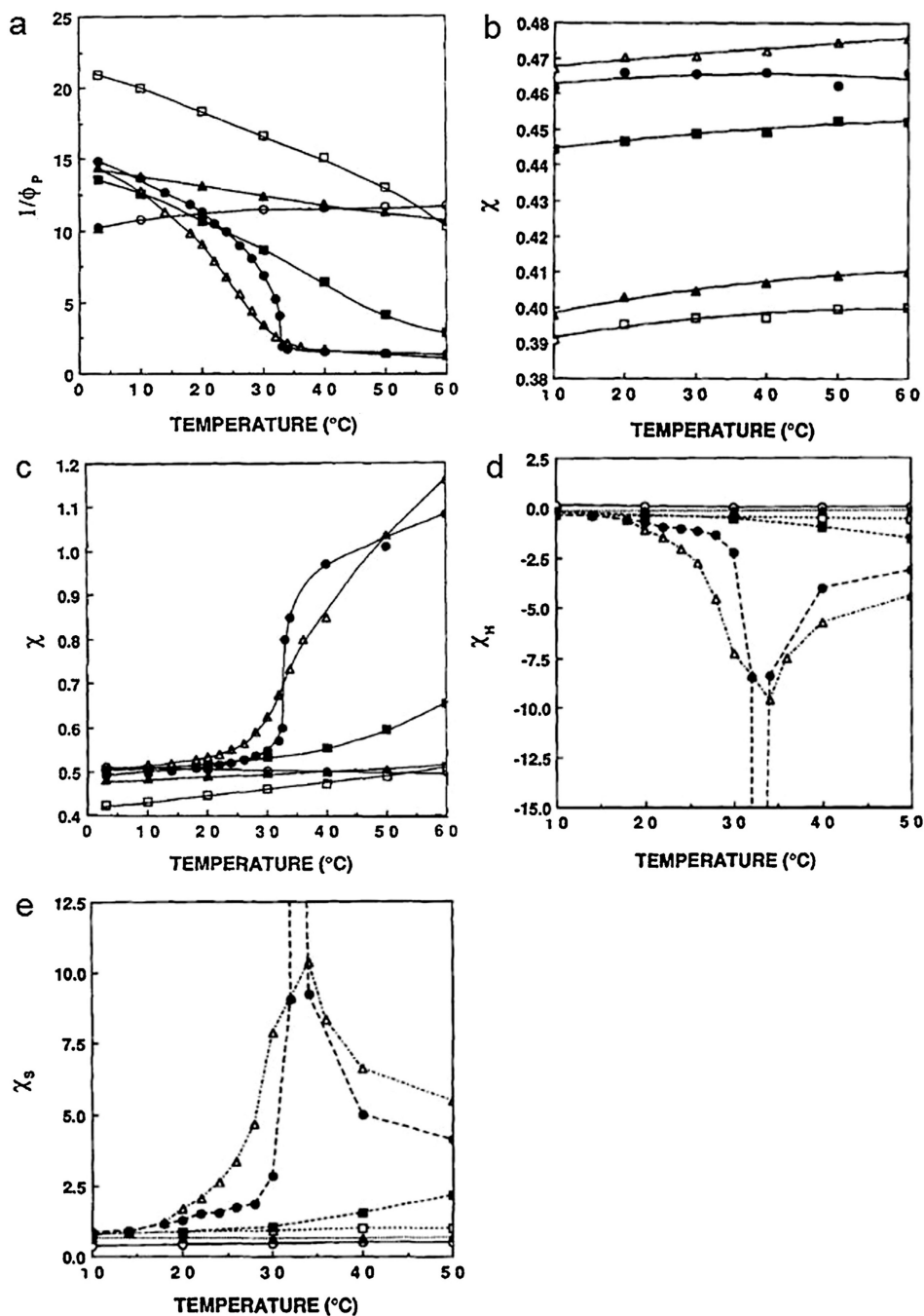
Fig. 4.
(a) Inverse polymer volume fraction as a function of time. (b) Polymer interaction parameter in ethanol. (c) polymer interaction parameter in water. (d) Enthalpic contribution to the polymer interaction parameter in water. (e) Entropic contribution to the polymer interaction parameter in water. ○ poly(acrylamide), ▲ poly(dimethyl acrylamide), □ poly(ethyl acrylamide), ■ poly(acrylroylpyrolidine), △ poly(diethylacrylamide), ● poly(*N*-isoproylacrylamide).
Reprinted with permission from Bae et al. [117].
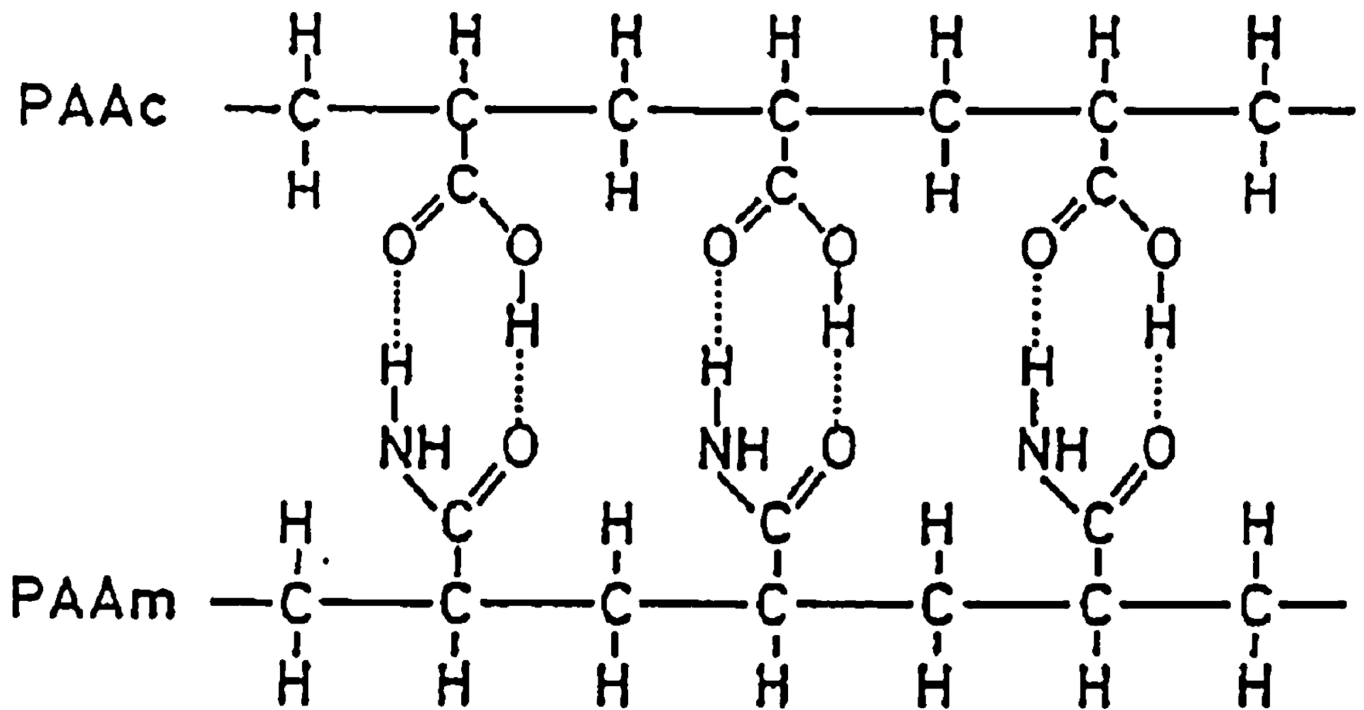
Fig. 5.
Zipper-like hydrogen bonding of PAA-PAAm IPN. Reprinted with permission from Katono et al. [118]. Copyright 1991 Elsevier.
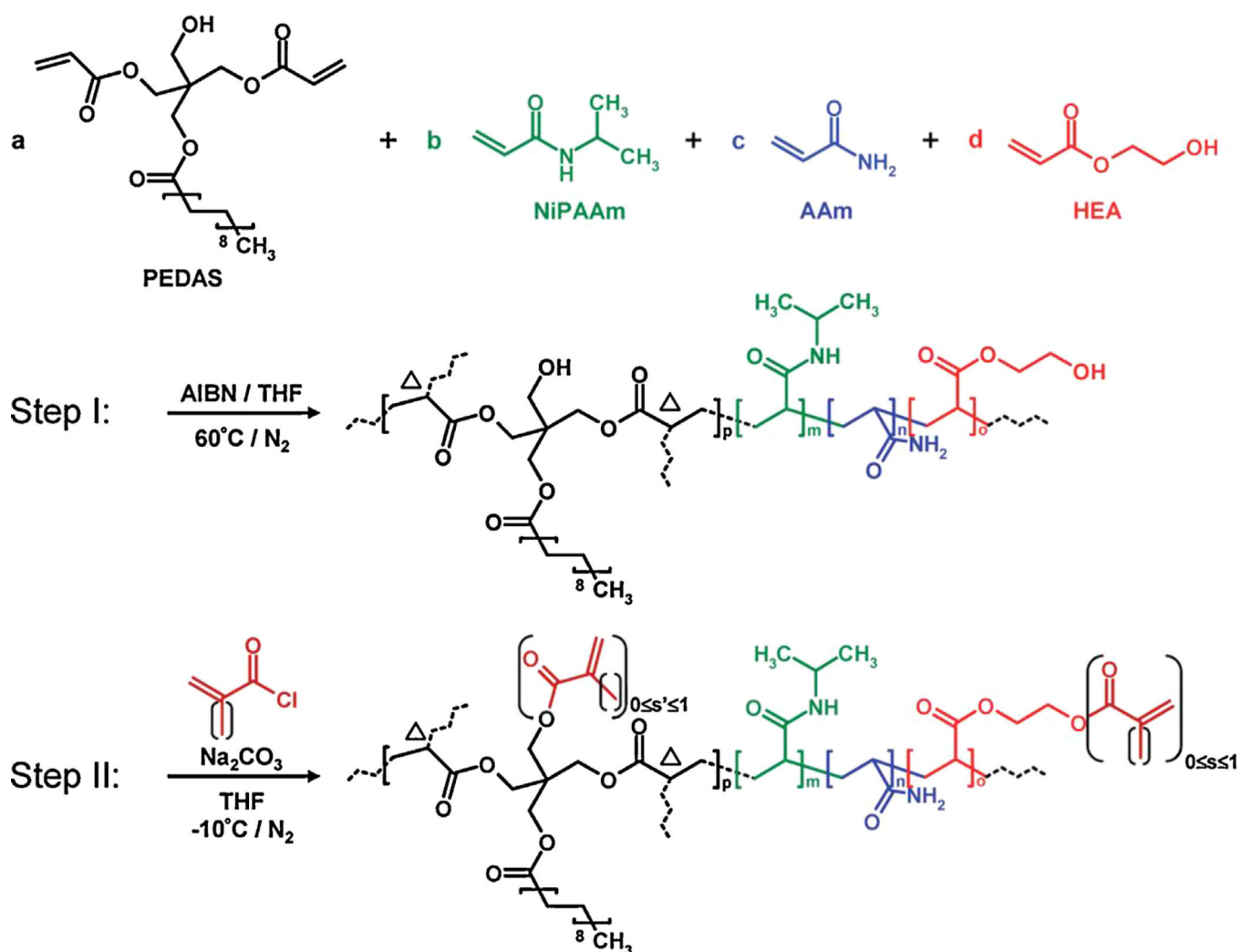
Fig. 6.
Thermo-gelling schematic for injectable PNIPAAm based hydrogels. Reprinted with permission from Hacker et al. [137]. Copyright 2008 American Chemical Society.
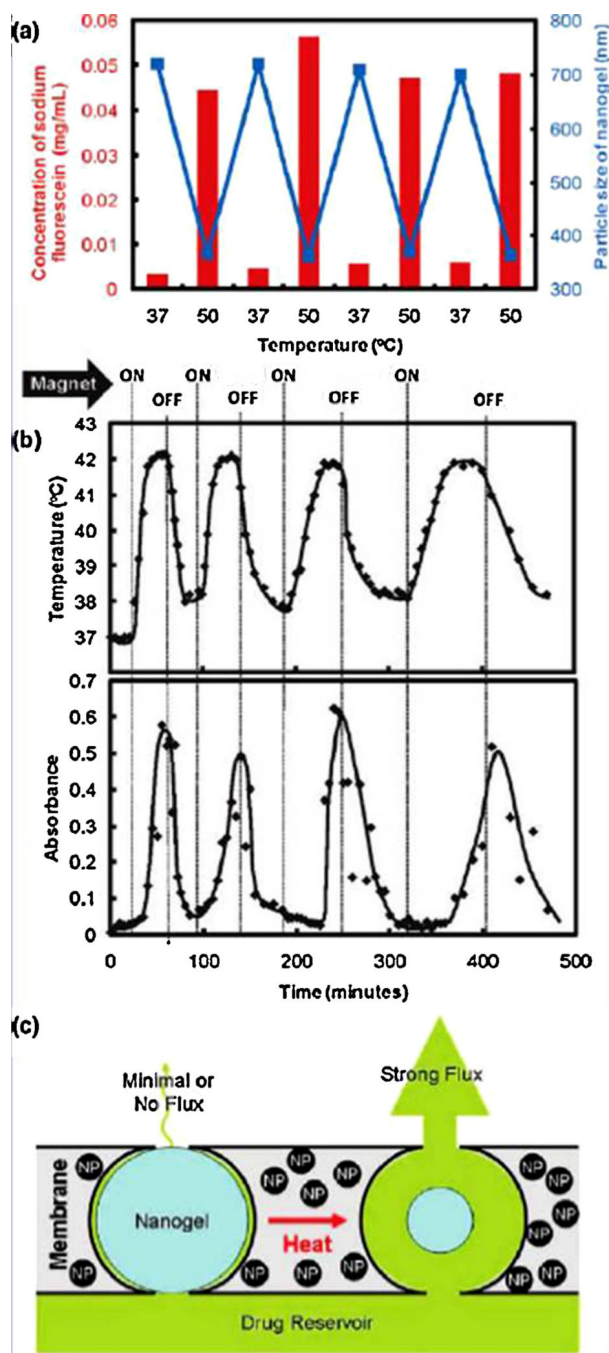
Fig. 7.
Stimulus-responsive membrane: (a) temperature-triggering, comparison of nanogel particle size in suspension (blue data, right *y*-axis) and differential flux of sodium fluorescein through the nanogel-loaded membranes (red data, left *y*-axis) as a function of temperature; (b) magnetic triggering, temperature profile in the sample chamber and differential flux of sodium fluorescein out of membrane-capped devices as a function of time over four successive on/off cycles of the external magnetic field; (c) schema of the proposed mechanism of membrane function. Reprinted with permission from Hoare et al. [141].

Copyright 2009 American Chemical Society. (For interpretation of the references to color in this figure legend, the reader is referred to the web version of the article.)
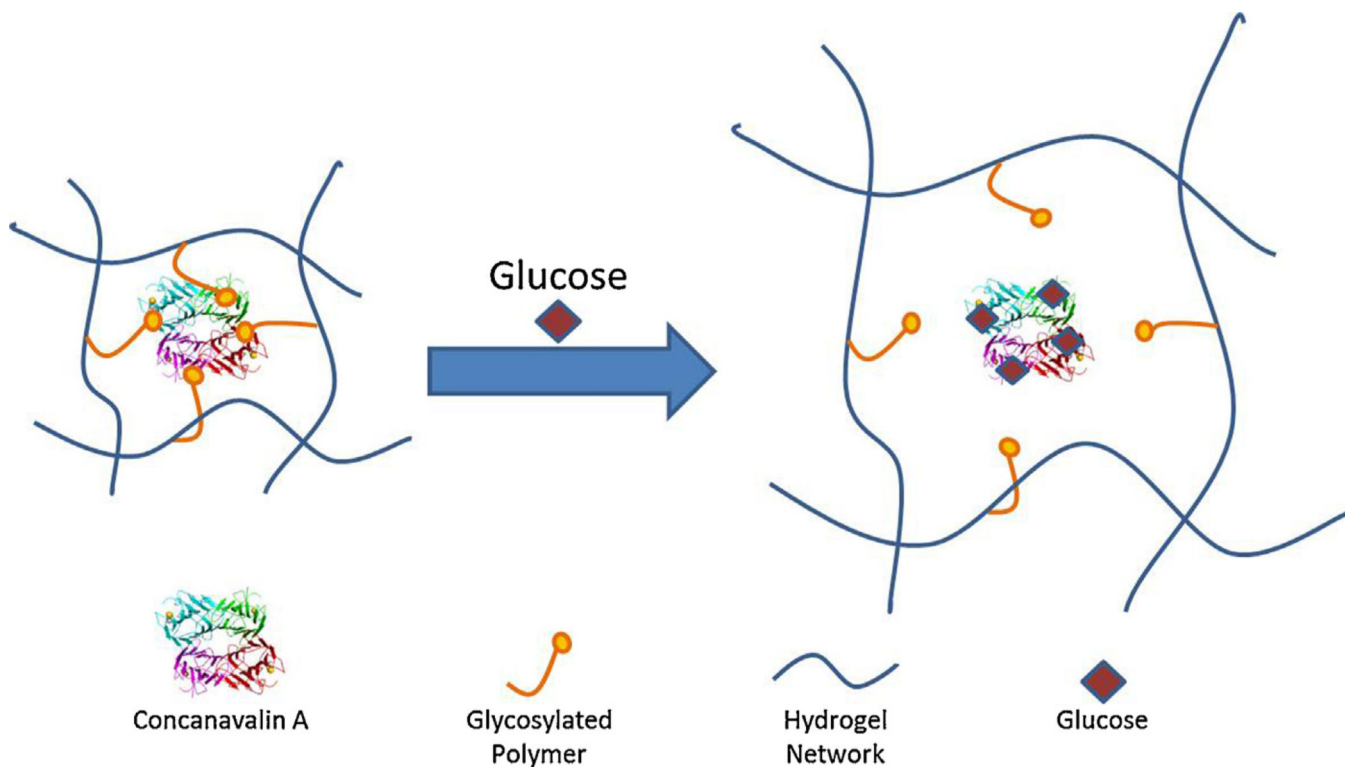
Fig. 8.
Concanavalin A-based glucose-responsive hydrogel swelling mechanism.
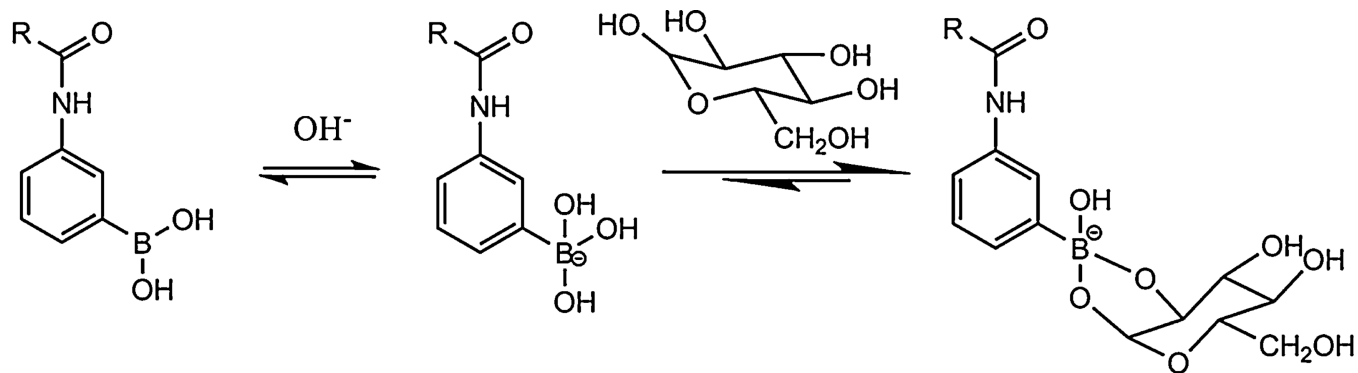
Fig. 9.
Reaction of glucose with phenylboronic acid (PBA). Binding of glucose to PBA yields more negatively charged and thus hydrophilic hydrogel, leading to the observed swelling response.
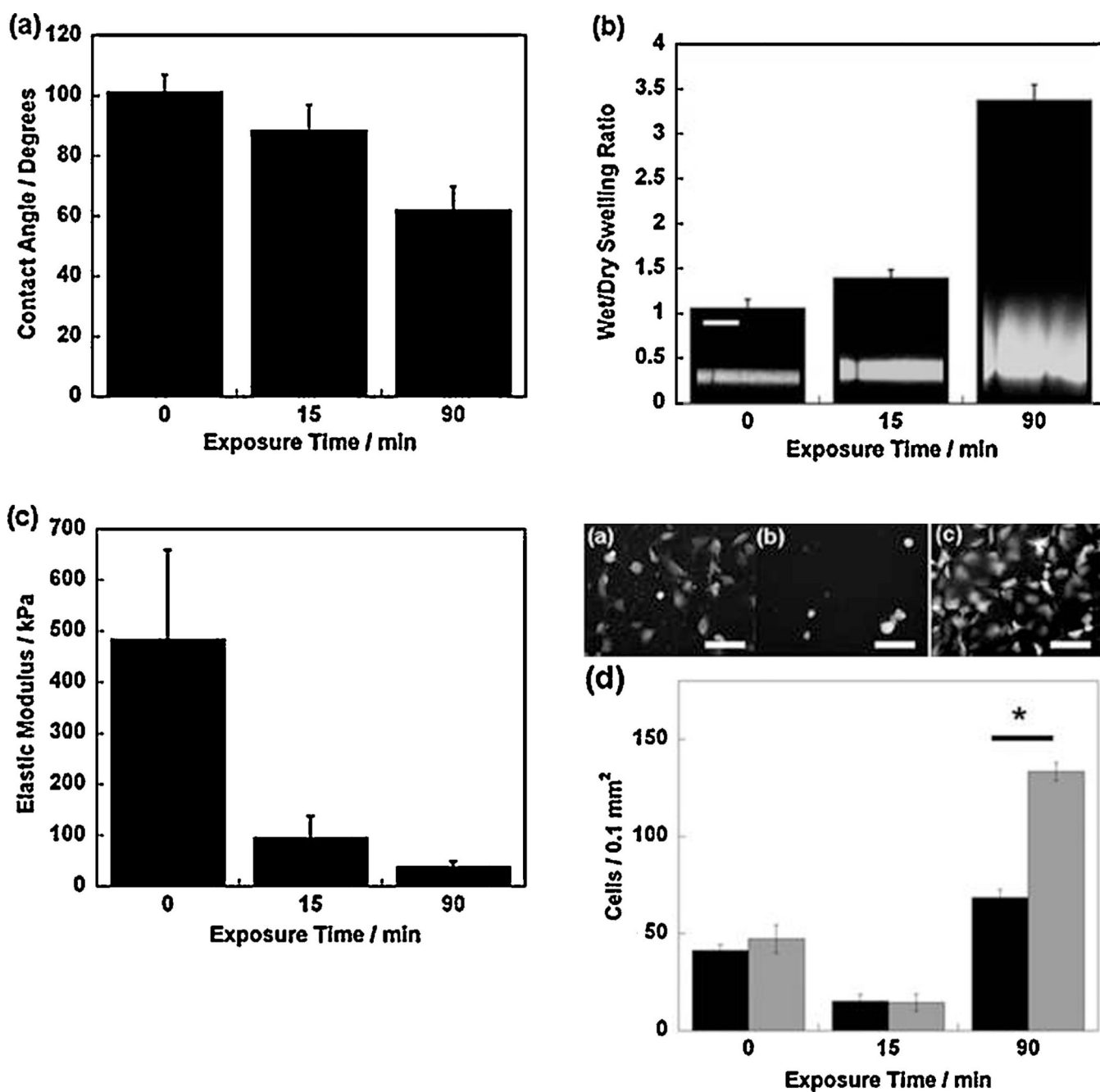
Fig. 10.
Effect of exposure time and degradation on (a) Wettability of poly(Hydroxyethylacrylate-co-2-nitrobenzyl acrylate (p(HEA-co-2-NBA)). (b) Swelling ratio of P(HEA-co-2-NBA). (c) Elastic modulus of P(HEA-co-2-NBA). (d) Cell concentration in P(HEA-co-2-NBA) with fluorescent imagages of (a) 0, (b) 15, and (c) 90 min exposure times. Reprinted with permission from Ramanan et al. [311]. Copyright 2010 The Royal Chemical Society.
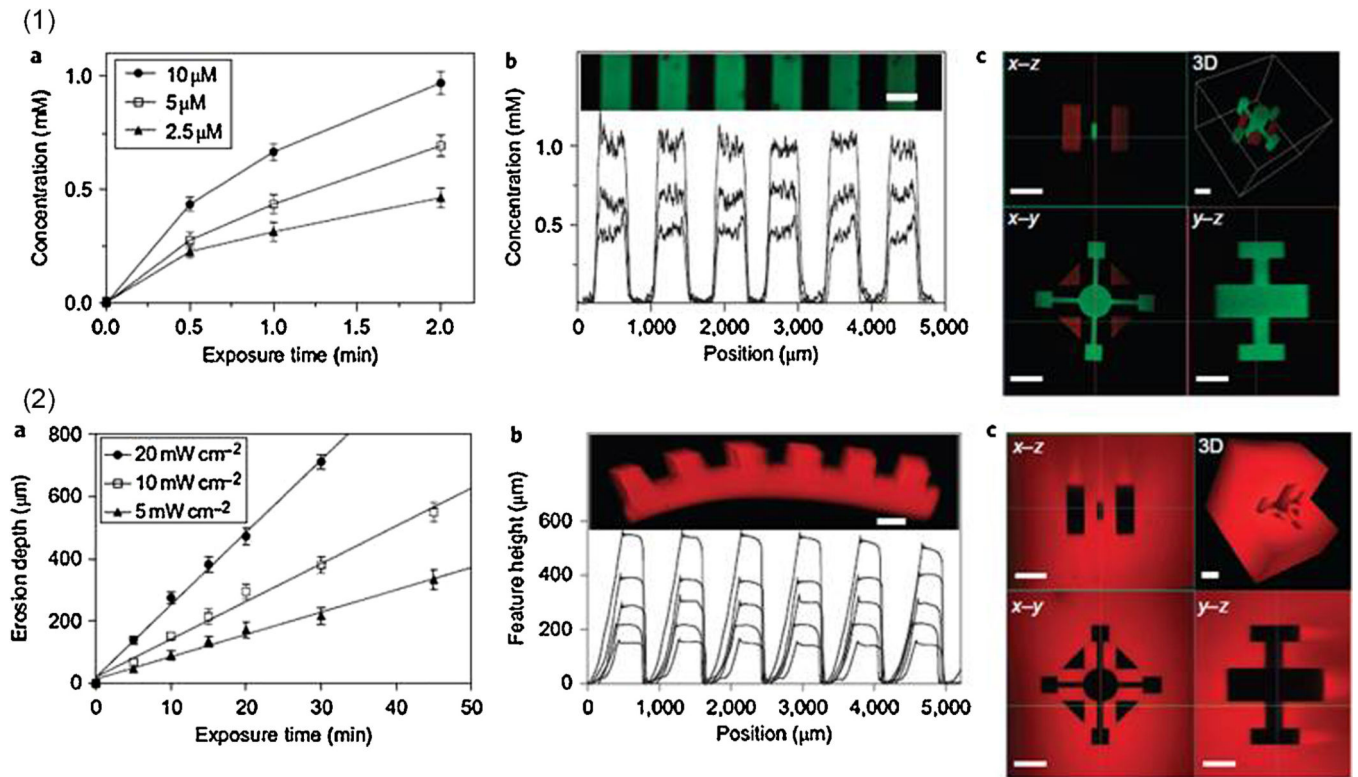
Fig. 11.

(a) exposure sensitivity, (b) 2 D patterning, and (c) 3 D patterning of (1) photo-modified and (2) photodegradeable hydrogels. Reprinted with permission from DeForest and Anseth [295]. Copyright 2011 Macmillan Publishers Limited.
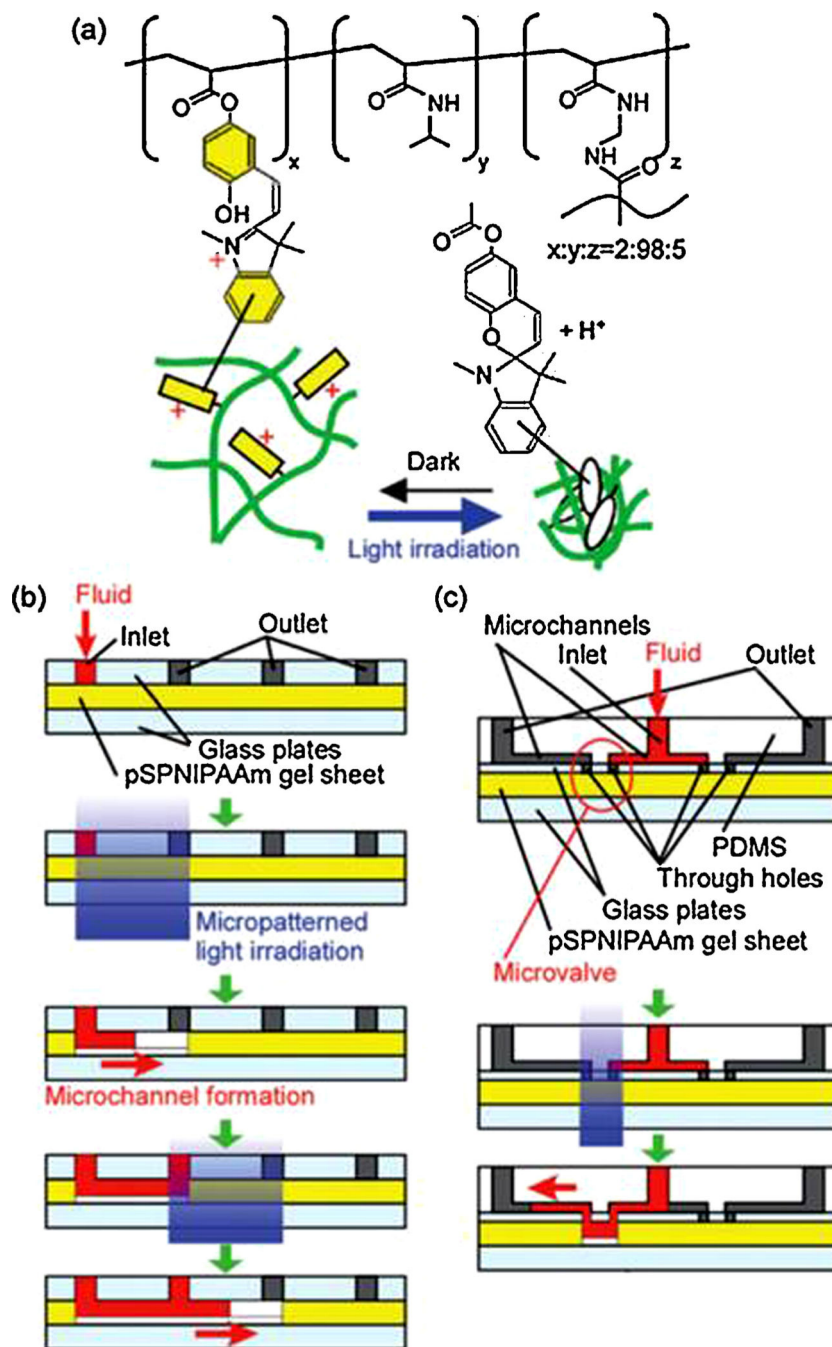
Fig. 12.
(a) Chemical schematic for swellable photoresponsive micro-well patterning. (b) Photoresponsive microchannel formation schematic. (c) Microvalve photo-actuation schematic. Reprinted with permission from Sugiura et al. [302]. Copyright 2009 The Royal Chemical Sociery.
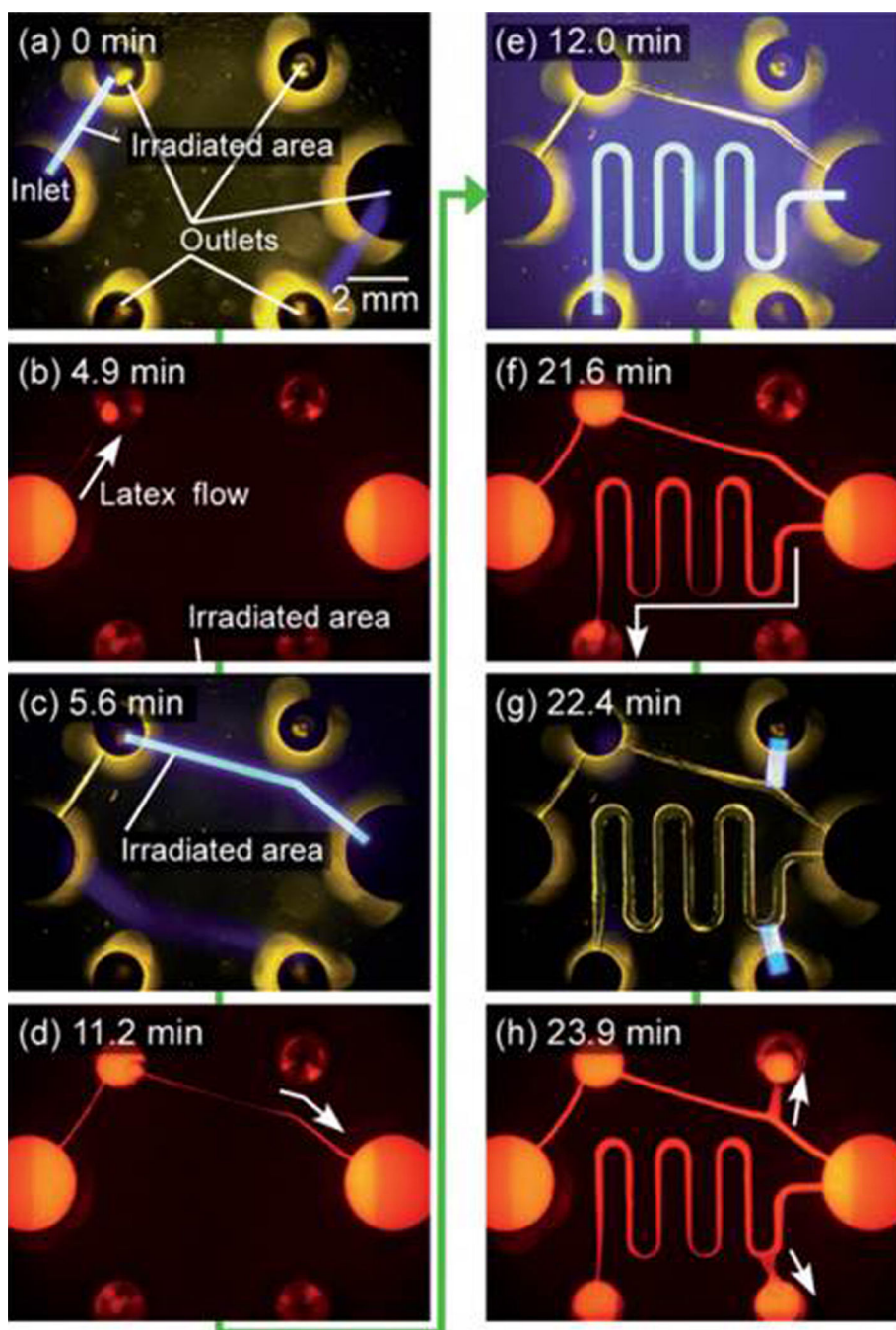
Fig. 13.
Time lapse of micrographs of photo-actuated microchannels. (a), (c), (e), and (g) are irradiation steps. (b), (d), (f), and (h) are subsequent visualizations of latex flow through the formed microchannels. Reprinted with permission from Sugiura et al. [302]. Copyright 2009 The Royal Chemical Sociery.
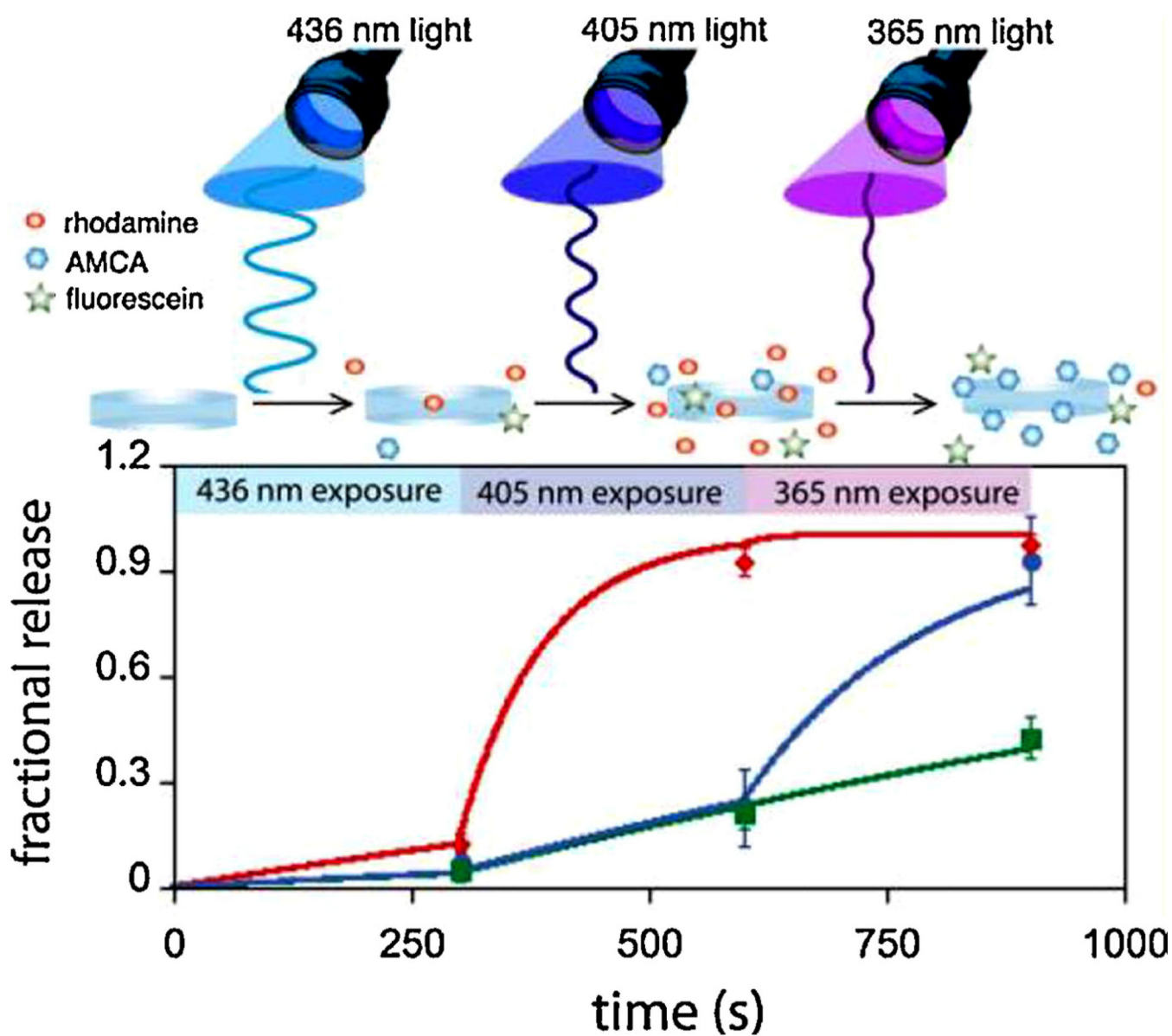
Fig. 14.
Fractional release of rhodamine, AMCA, and fluorescein from a hydrogel as a function of light exposure (λ = 436 nm, I_0 = 44.6 ± 1.0 mW/cm^2, t = 5 min; λ = 405 nm, I_0 = 21.4 ± 1.1 mW/cm^2, t = 5 min; and then λ = 365 nm, I_0 = 5.53 ± 0.14 mW/cm^2, t = 5 min); solid lines depict predicted release, actual release shown as data points. Reprinted with permission from Griffin and Kasko [313]. Copyright 2012 American Chemical Society.
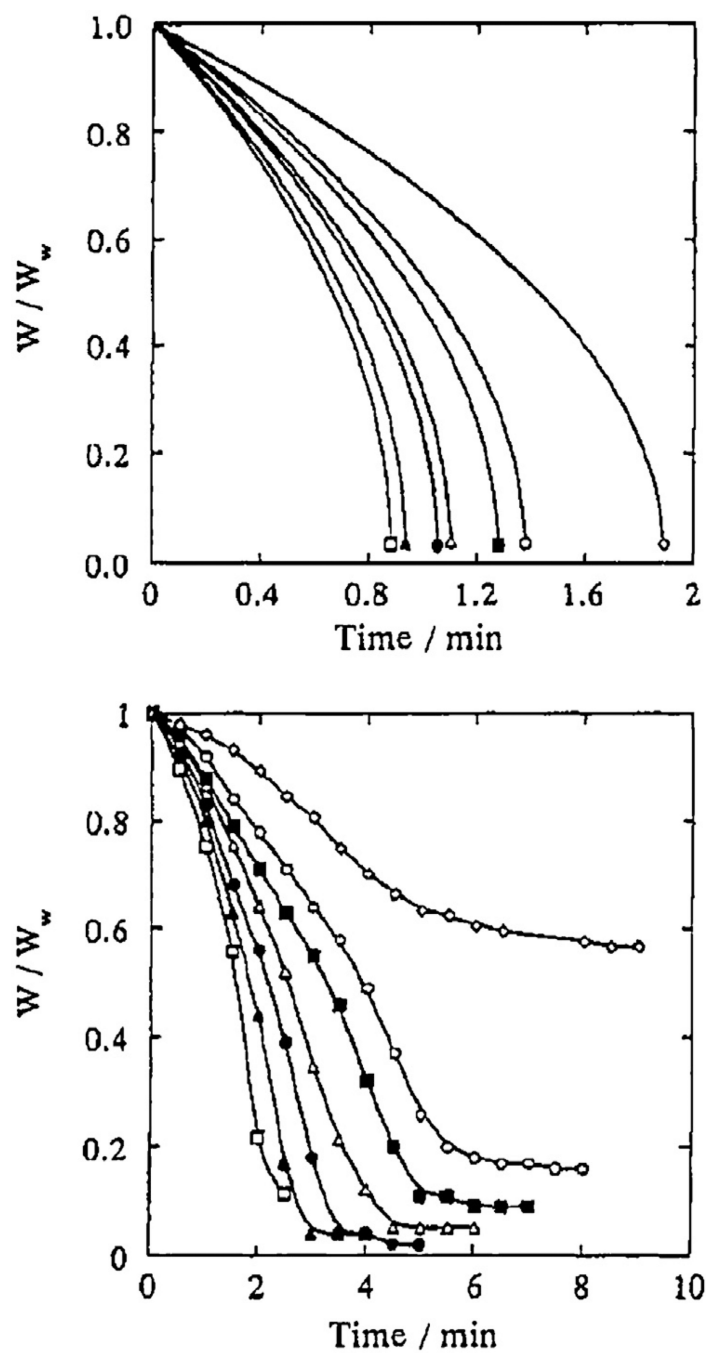
Fig. 15.
Relative hydrogel weight change for various degrees of swelling, *q*. Top: simulated results; Bottom: experimental results with PAMPS hydrogel. , $q = 25$; $\bigcirc$, $q = 70$; $\blacksquare$, $q = 100$; $\triangle$, $q = 200$; $\bullet$, $q = 256$; $\blacktriangle$, $q = 512$; $\square$, $q = 750$. Reprinted with permission from Gong et al. [314]. Copyright 1994 American Chemical Society.
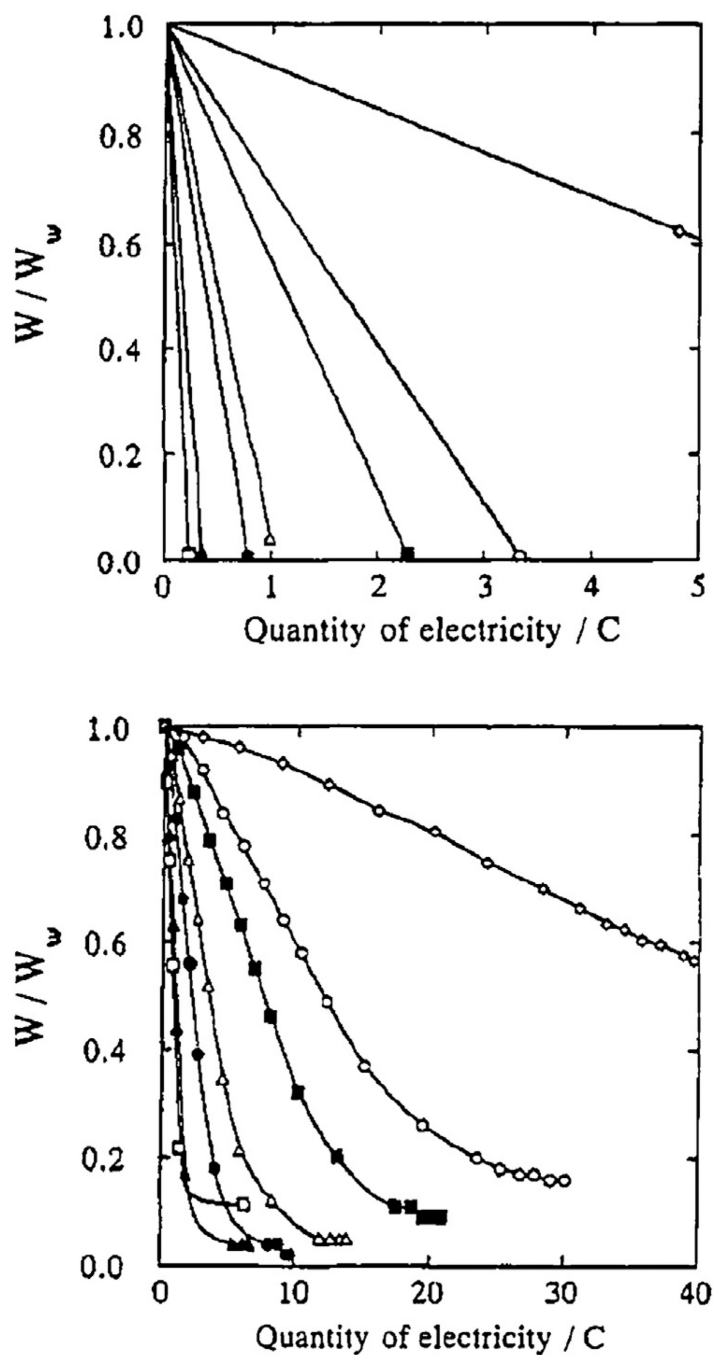
Fig. 16.
Relative hydrogel weight change as a function of quantity of electric flow. Top: simulated results; Bottom: experimental results with PAMPS hydrogel. Symbols are the same as in Figure MK3. Reprinted with permission from Gong et al. [314]. Copyright 1994 American Chemical Society.
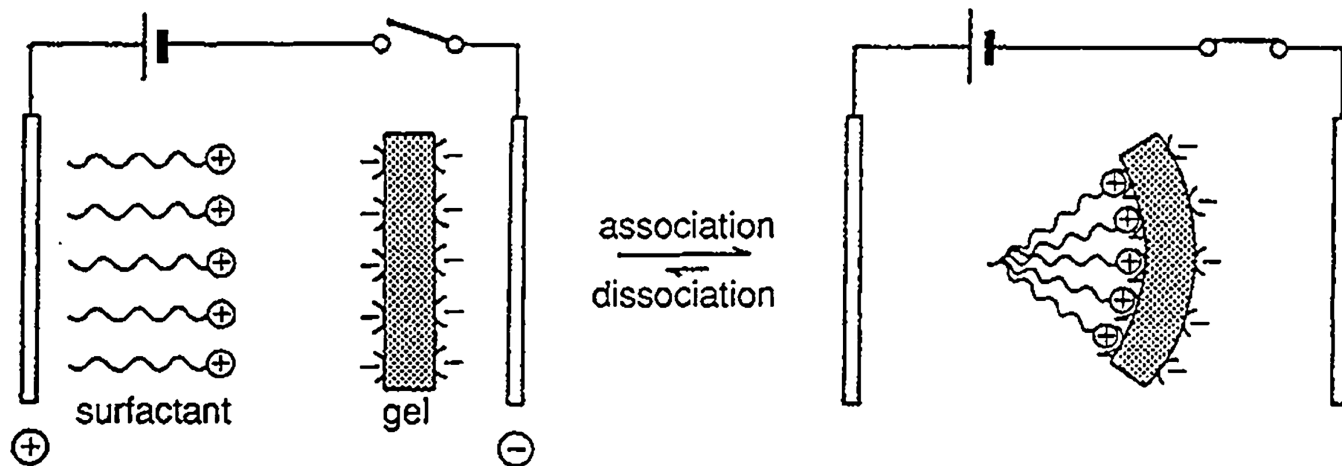
Fig. 17.
Schematic of hydrogel bending mechanism by association of surfactant molecules in electric field. Reprinted with permission from Osada et al. [315]. Copyright 1992 Nature Publishing Group.
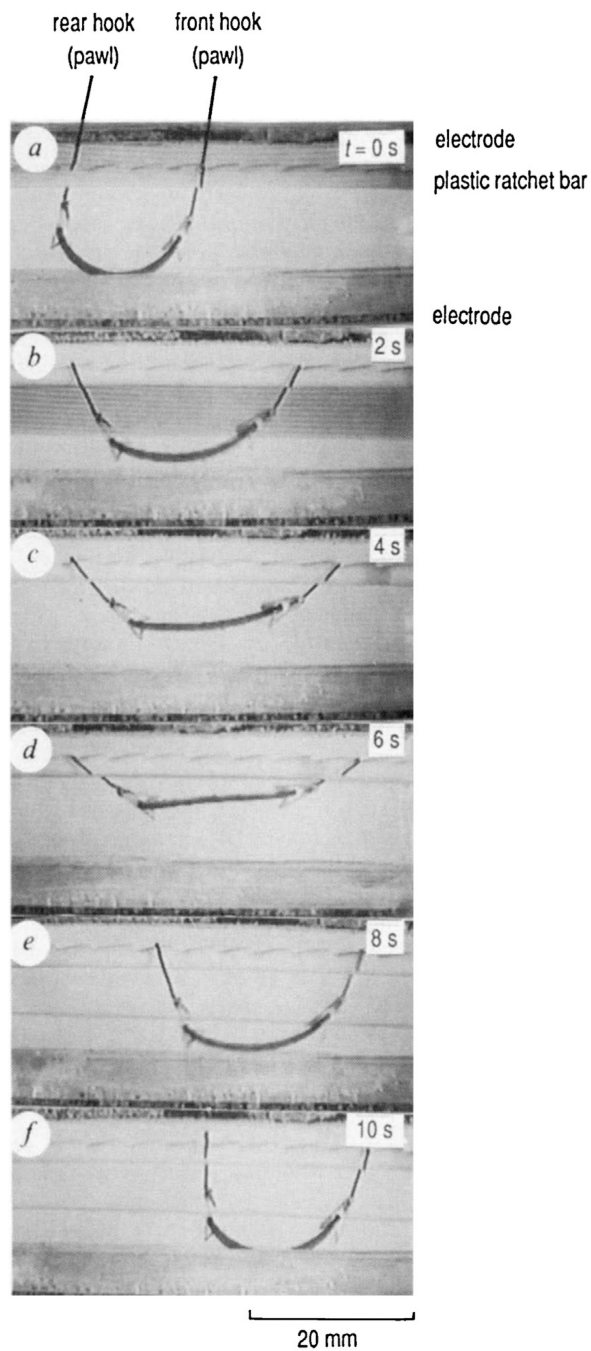
Fig. 18.
PAMPS hydrogel bending and movement from application of electric field. The front hook and rear hooks can only slide forward along the rail, as prevented by ratchet teeth. Thus, with repeated on/off application of a 20 V electric field and the bending mechanism shown in Figure MK5, the hydrogel slides unidirectionally forward. Reprinted with permission from Osada et al. [315]. Copyright 1992 Nature Publishing Group.
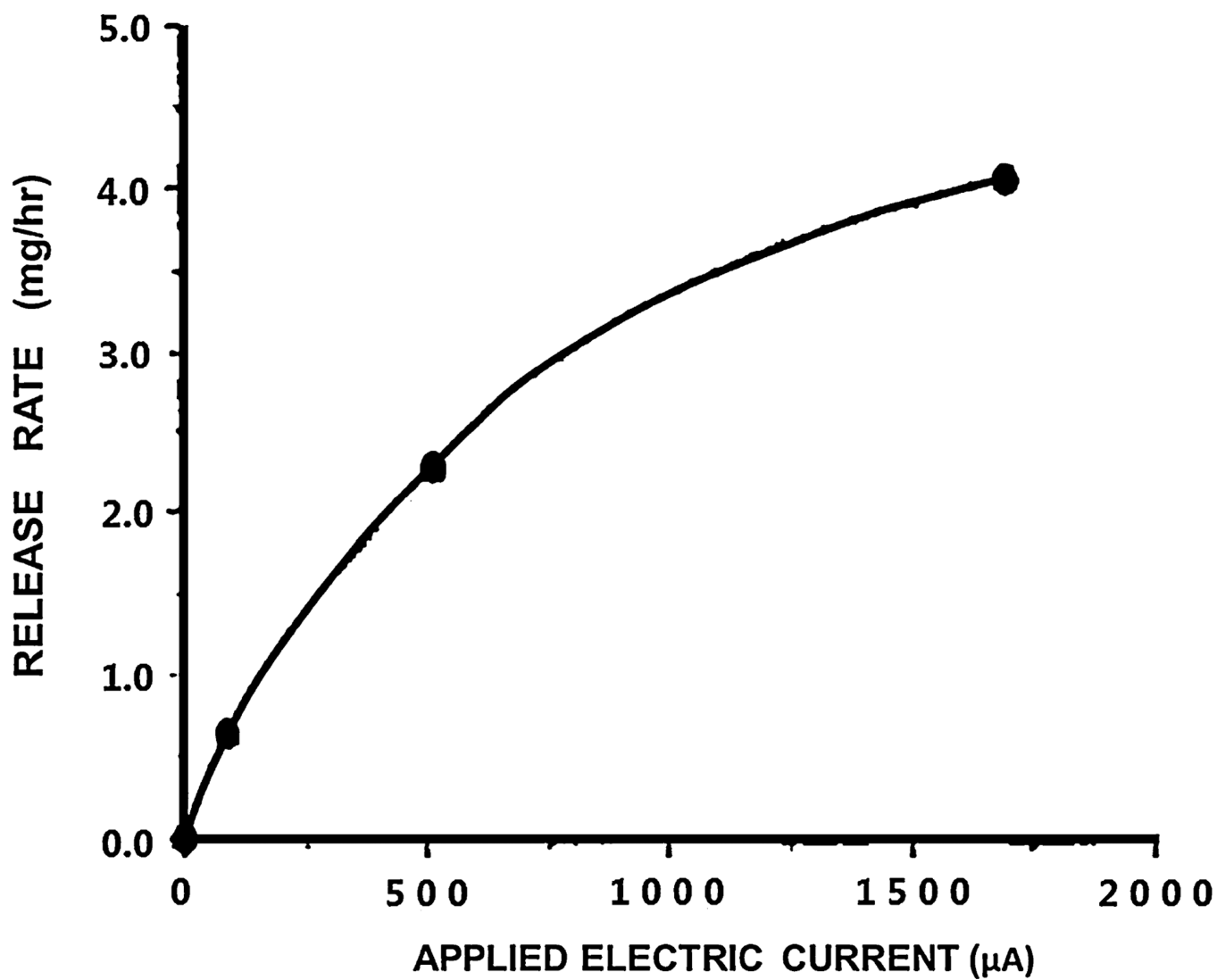
Fig. 19.
Release rate of model drug (edrophonium chloride) as a Function of Electric Current.
Edrophonium chloride was released from a 14 mm P(AMPS/BMA) hydrogel disk with
various electric currents applied. Reprinted with permission from Kwon et al. [354].
Copyright 1991 Elsevier
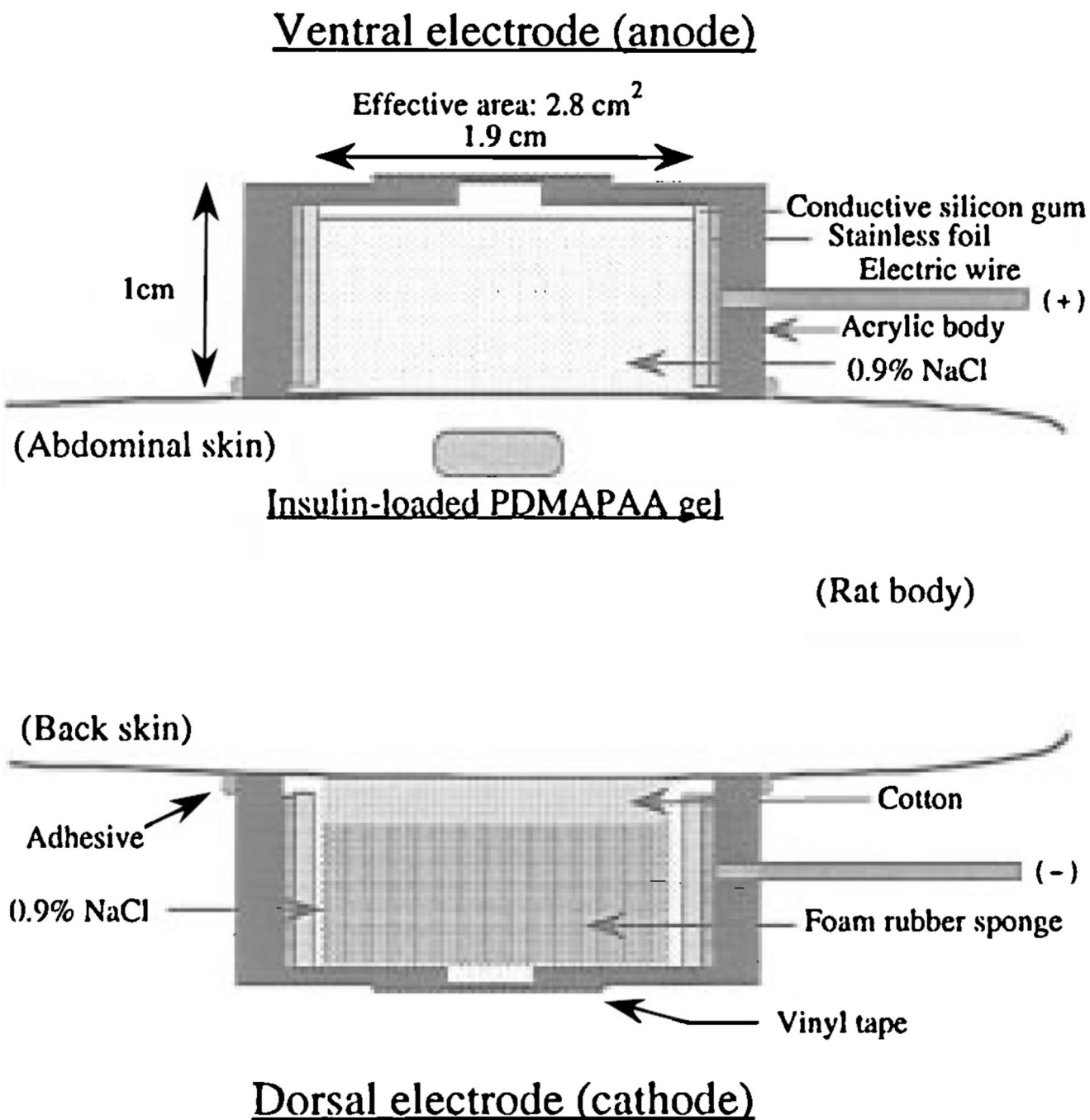
Fig. 20.
Schematic of electrode system used for *In Vivo* test of electrically-responsive PDMAPAA hydrogel insulin delivery system in rats. Reprinted with permission from Kagatani et al. [360]. Copyright 1997 Wiley-Liss, Inc. and the American Pharmaceutical Association.
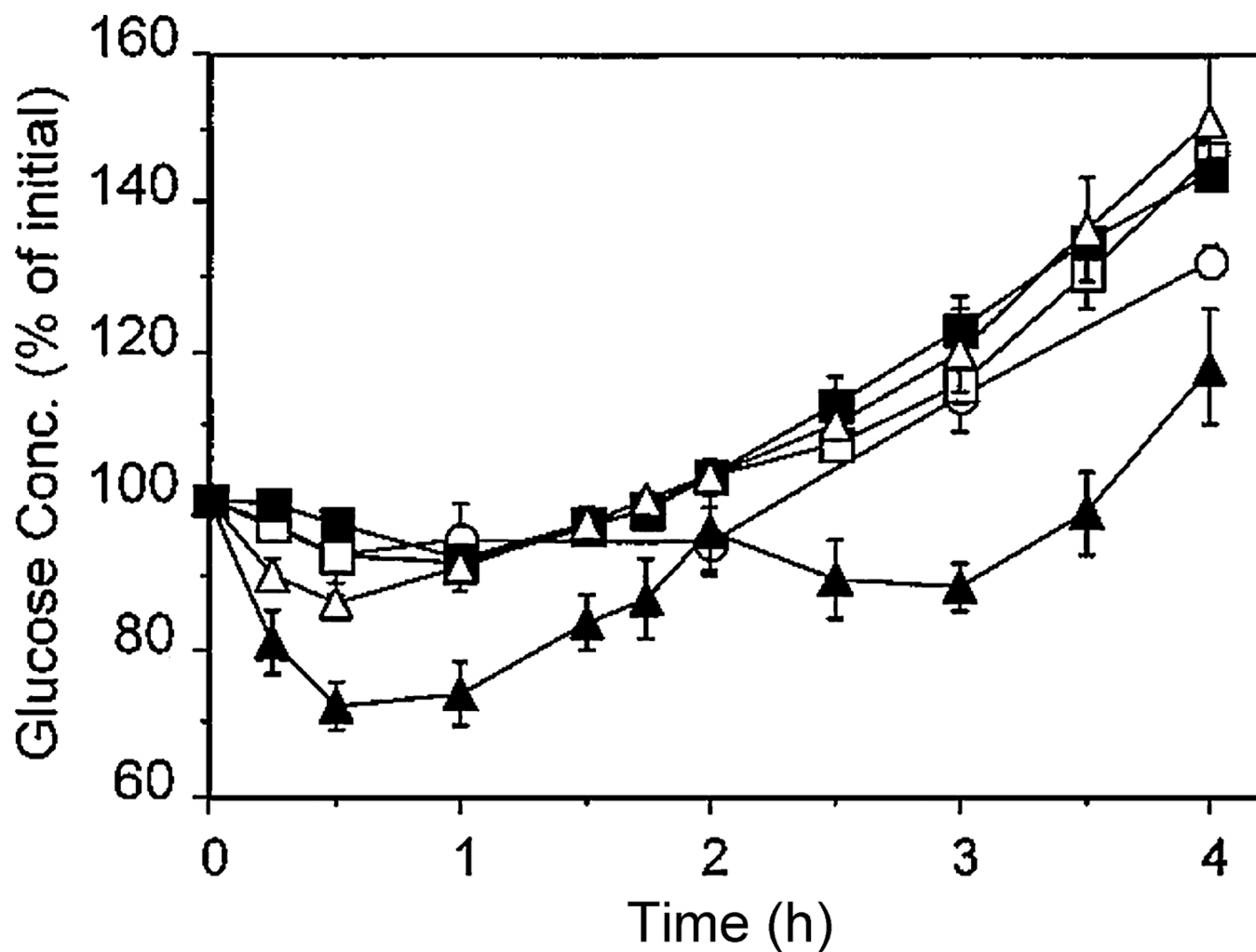
Fig. 21.
Plasma Glucose Concentration Profile with Insulin Administration by PDMAPAA
Electrically-Responsive Hydrogel. Current of 1.0 mA was applied for 1 min at $t = 0$ h and
for 10 min at $t = 2$ h. A noticeable decrease in glucose levels is observed at each time,
indicating pulsatile release. ○, PBS; □, PDMAPAA gel only; ■, PDMAPAA gel with
current; △, insulin-loaded PDMAPAA gel; ▲, insulin-loaded PDMAPAA gel with current.
Reprinted with permission from Kagatani et al. [360]. Copyright 1997 Wiley-Liss, Inc. and
the American Pharmaceutical Association.
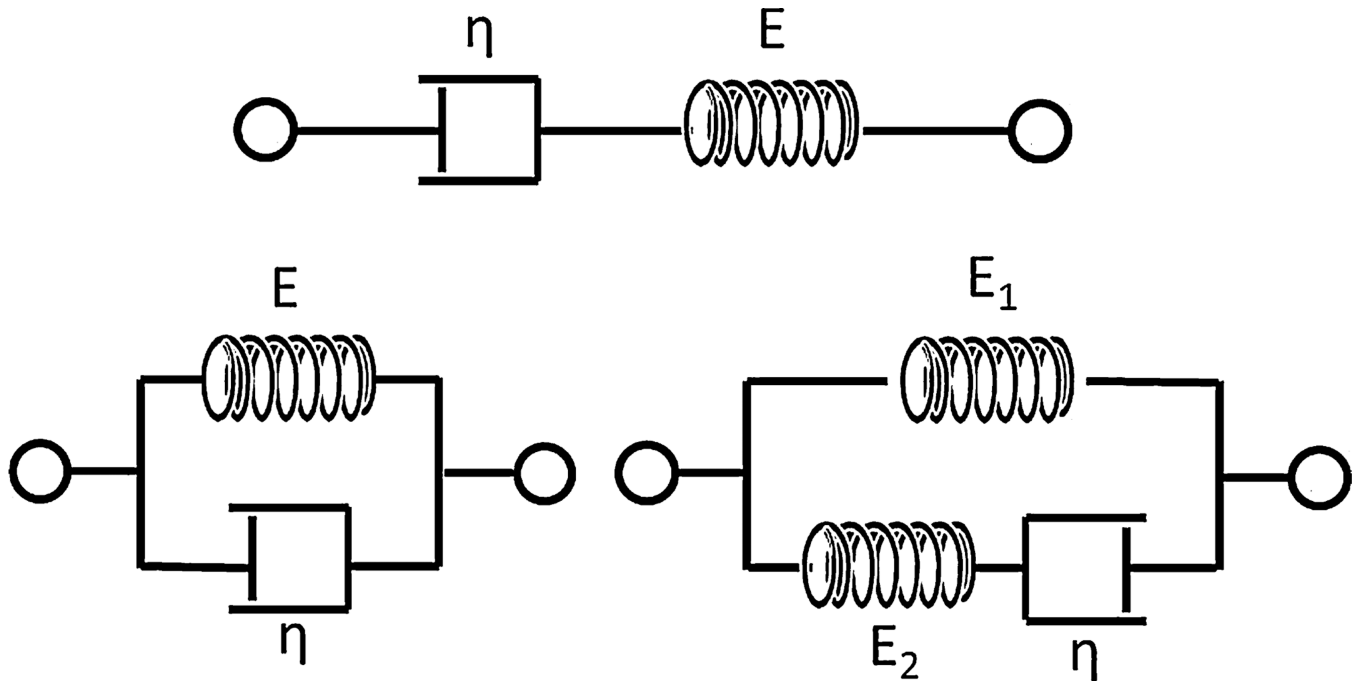
Fig. 22.
Models for linear viscoelastic polymer systems (top) Maxwell (bottom left) Kelvin–Voigt and (bottom right) Standard linear solid. Springs represent the elastic component and dashpots represent the viscous components of the polymer system.
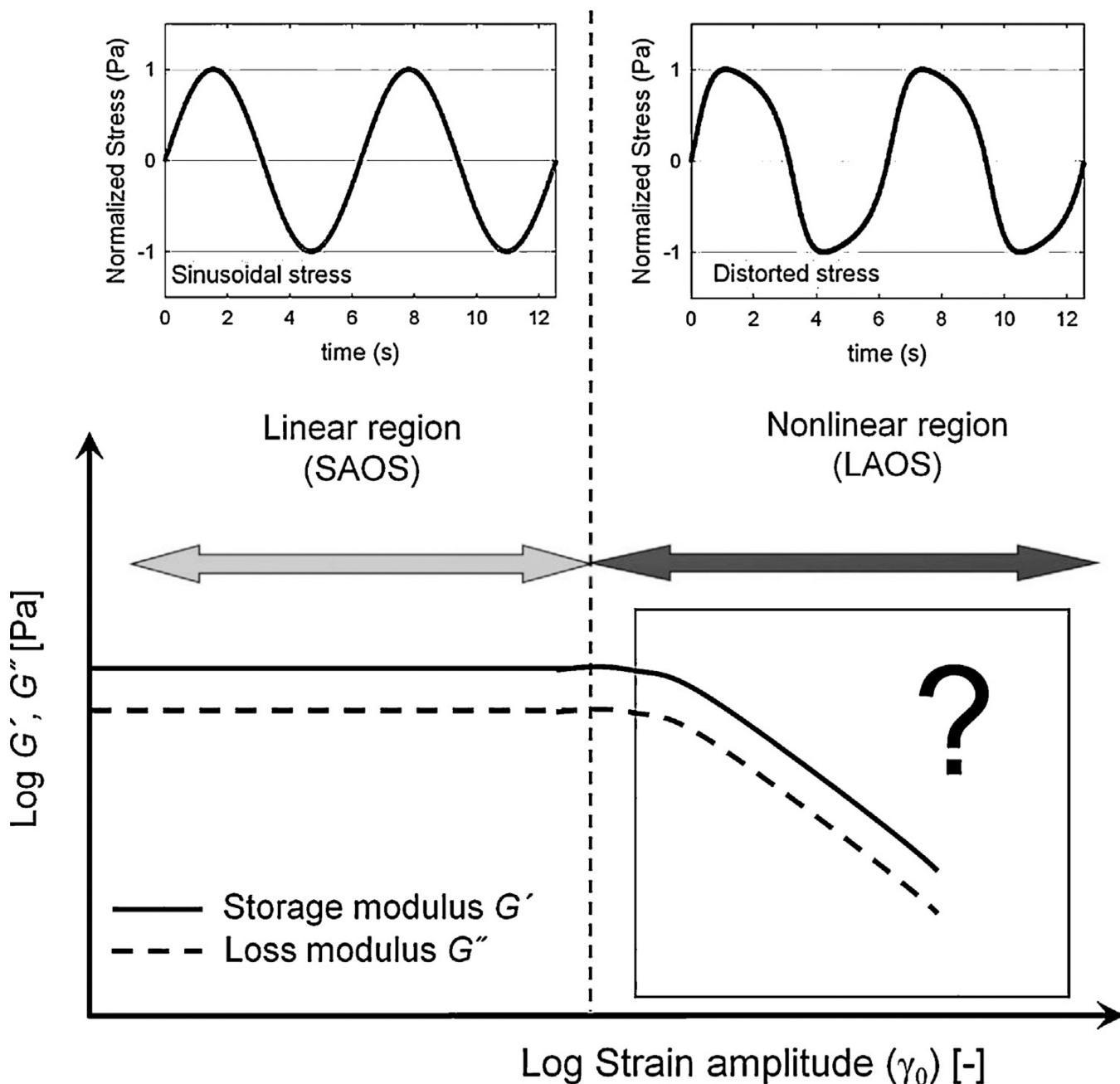
Fig. 23.
Within the linear viscoelastic region (bottom left) the storage and loss moduli, G' and G'', respectively are independent of the applied strain amplitude. The resulting shear stress curve is, therefore, sinusoidal (top left). However, once entering the non-linear region (bottom right), G' and G'' become dependent on shear amplitude, *i.e.* $G'(\gamma_0)$ and $G''(\gamma_0)$, and the shear stress curve is no longer sinusoidal (top right). This illustrates the different behaviors expected from small amplitude oscillatory shear (SAOS) and large amplitude oscillatory shear (LAOS) experiments. As a note, the distortion of the stress curve in the non-linear region can be attributed to the higher harmonics of G' and G''. Reprinted with permission from Hyun et al. [388].
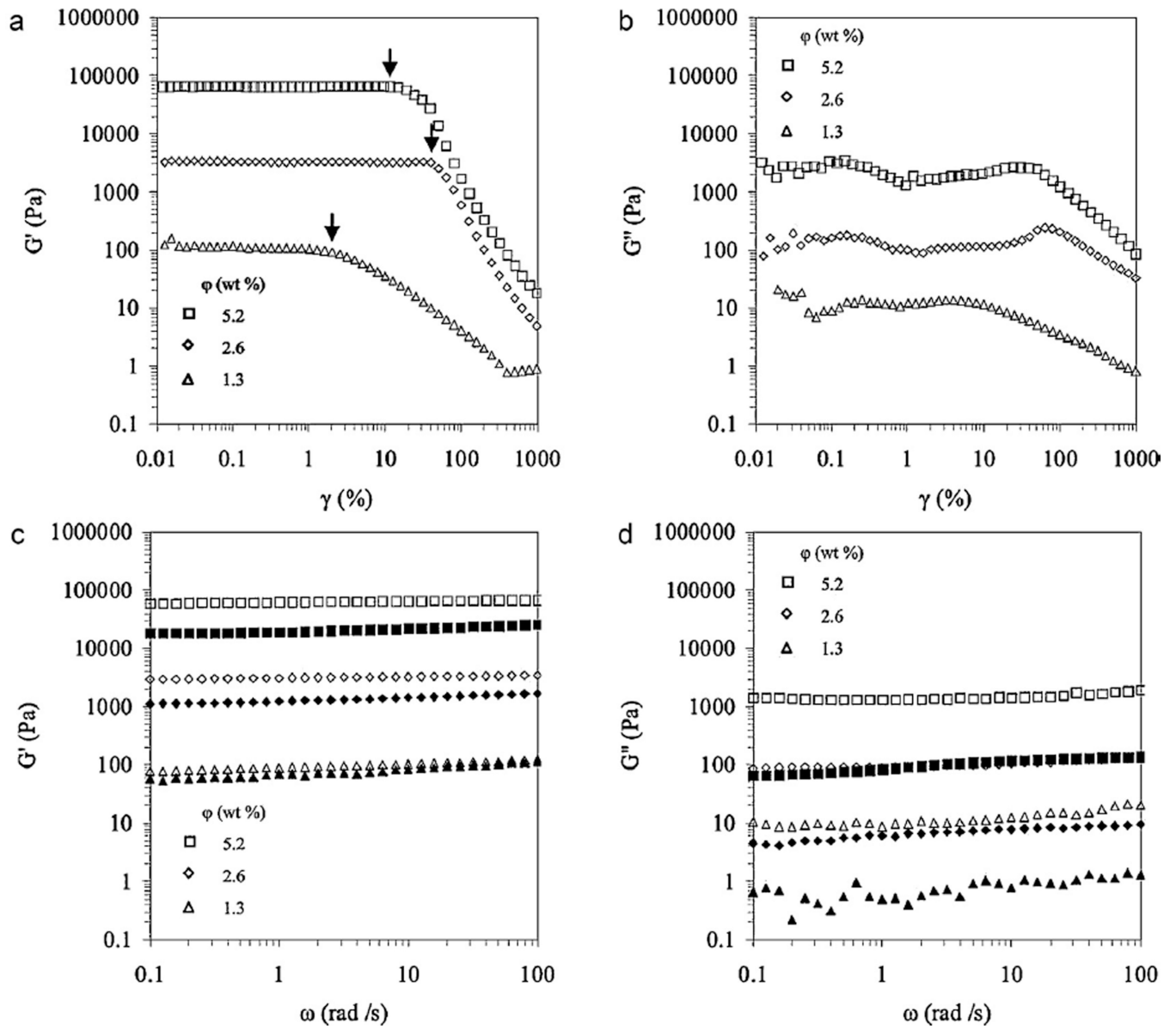
Fig. 24.
(a) and (b) depict strain-sweeps from vortex-induced fibroin hydrogels with varying silk concentrations. The arrows depict yielding/thinning behavior. (c) and (d) show frequency sweeps before (open symbols) and immediately after shear-thinning by injection (closed symbols).
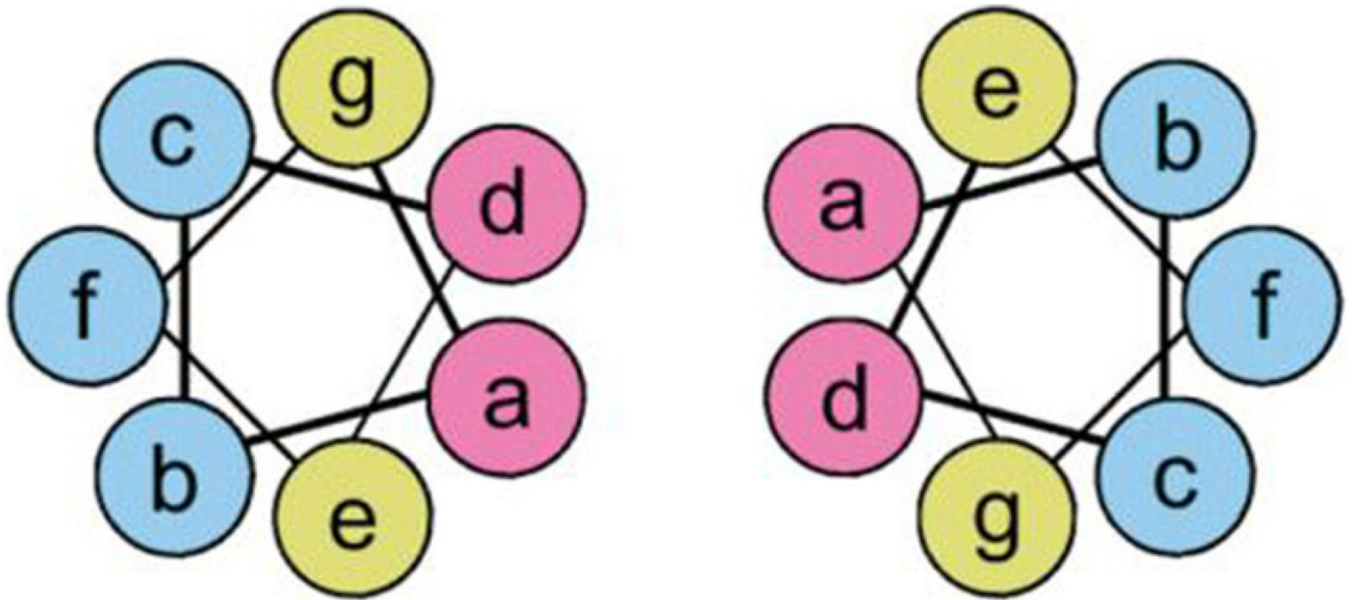
Fig. 25.
A schematic of a coiled–coiled dimer containing the (abcdefg) motif. The 'a' and 'd' residues are typically hydrophobic amino acids, while the 'e' and 'g' residues are charged moieties. The dashed lines represent hydrophobic and charge interactions resulting in the coiled-coil structural motif.
Obtained and modified from Jonker et al. [415].
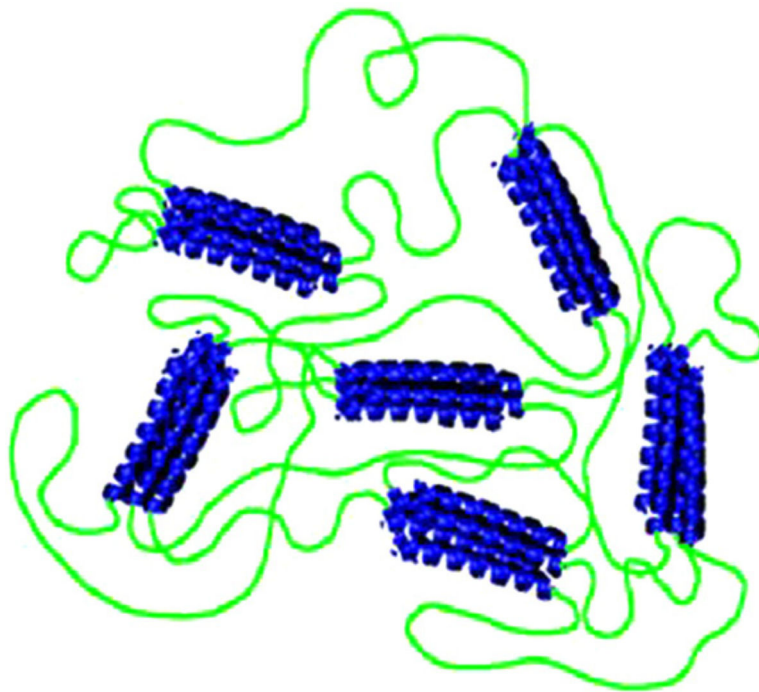
APQMLRE LQETNAA LQDVREL LRQQVKE ITFLKNT VMESDAS

(AGAGAGPEG) n

Fig. 26.
Network formed with a tri-block copolymer consisting of coiled-coil forming end blocks
and a polyanionic linker.
Reprinted with permission from Olsen et al. [413].
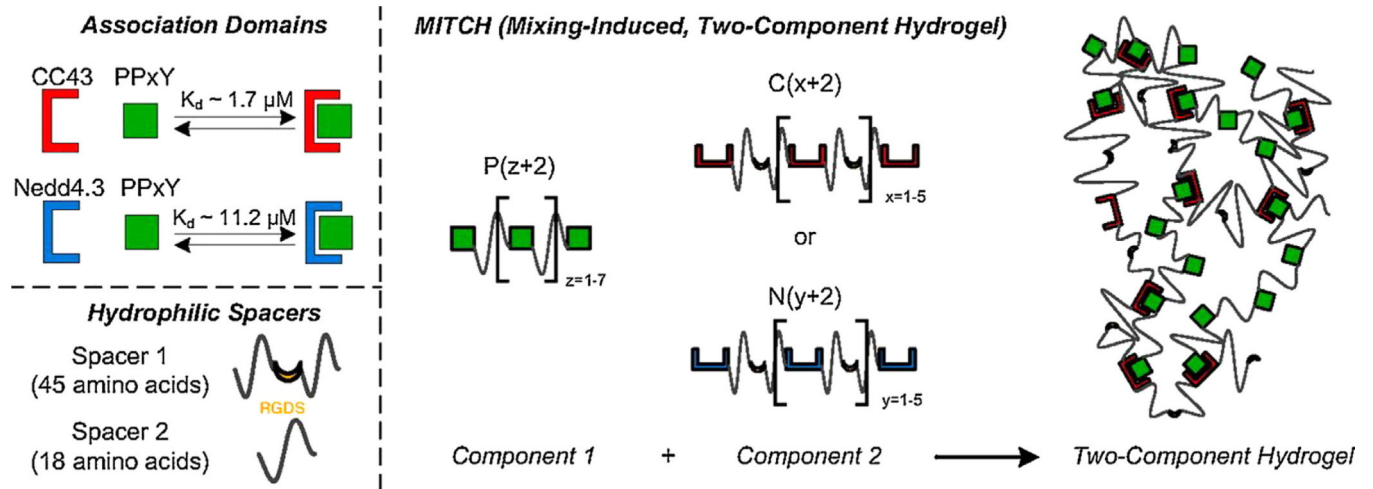
Fig. 27.
MITCH schematic showing (top left) the WW association domains, CC43 and Nedd.3, and the proline peptide (PPxY) and (bottom left) hydrophilic spacers linking repeat units of either the WW domains or proline peptides. (Right) The two-component gel results from the mixing of the WW association domains and the respective proline peptide chains. Reprinted with permission from Foo et al. [448].
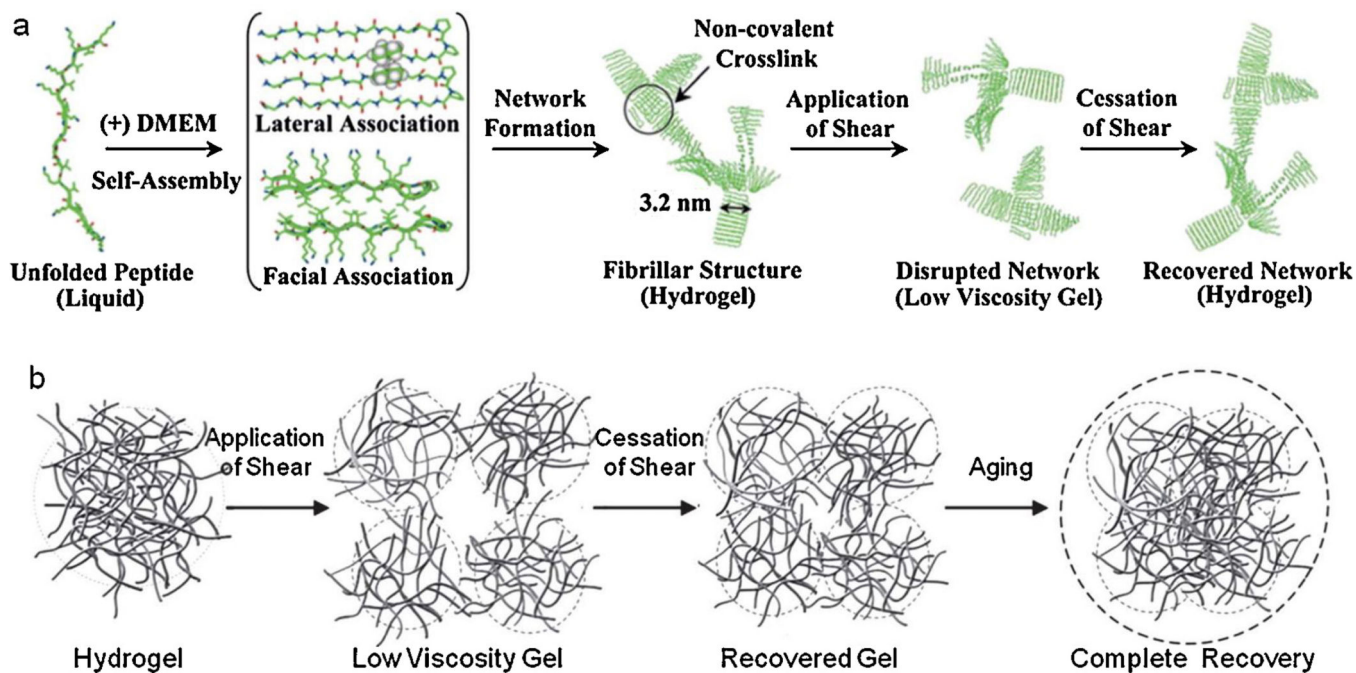
Fig. 28.
(Top) Self-assembly of b-hairpin peptide and their subsequent assembly into fibrillar hydrogels. Also pictured is the reaction of the network to the application of shear force.
(Bottom) Proposed mechanism of the network behavior during shear-thinning and recovery, or self-healing.
Reprinted with permission from Guvendiren et al. [365] (Top) Haines-Butterick et al. [411]. (Bottom) Yan et al. [464].
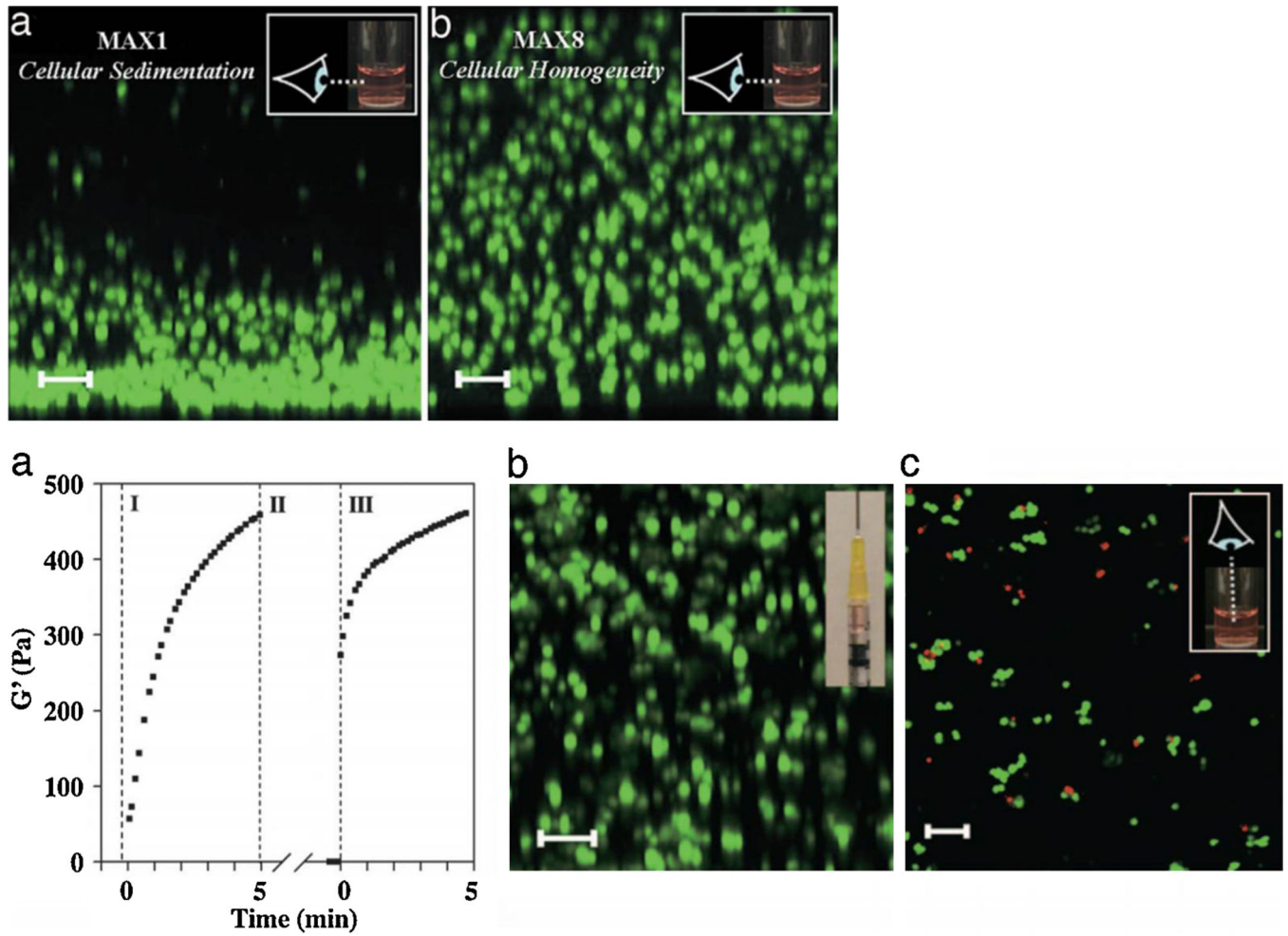
Fig. 29.
(Top) Distribution of fluorescently labeled C3H10t1/2 cells in a MAX1 (left) and MAX8 (right) peptide hydrogel. (Bottom left) G' is being measured as a function of time to observe the properties of the MAX8 hydrogel before, during and after the introduction of shear flow. The cells were stained for viability before (bottom middle) and after (bottom left) being injected through a syringe.
Reprinted with permission from Haines-Butterick et al. [411].
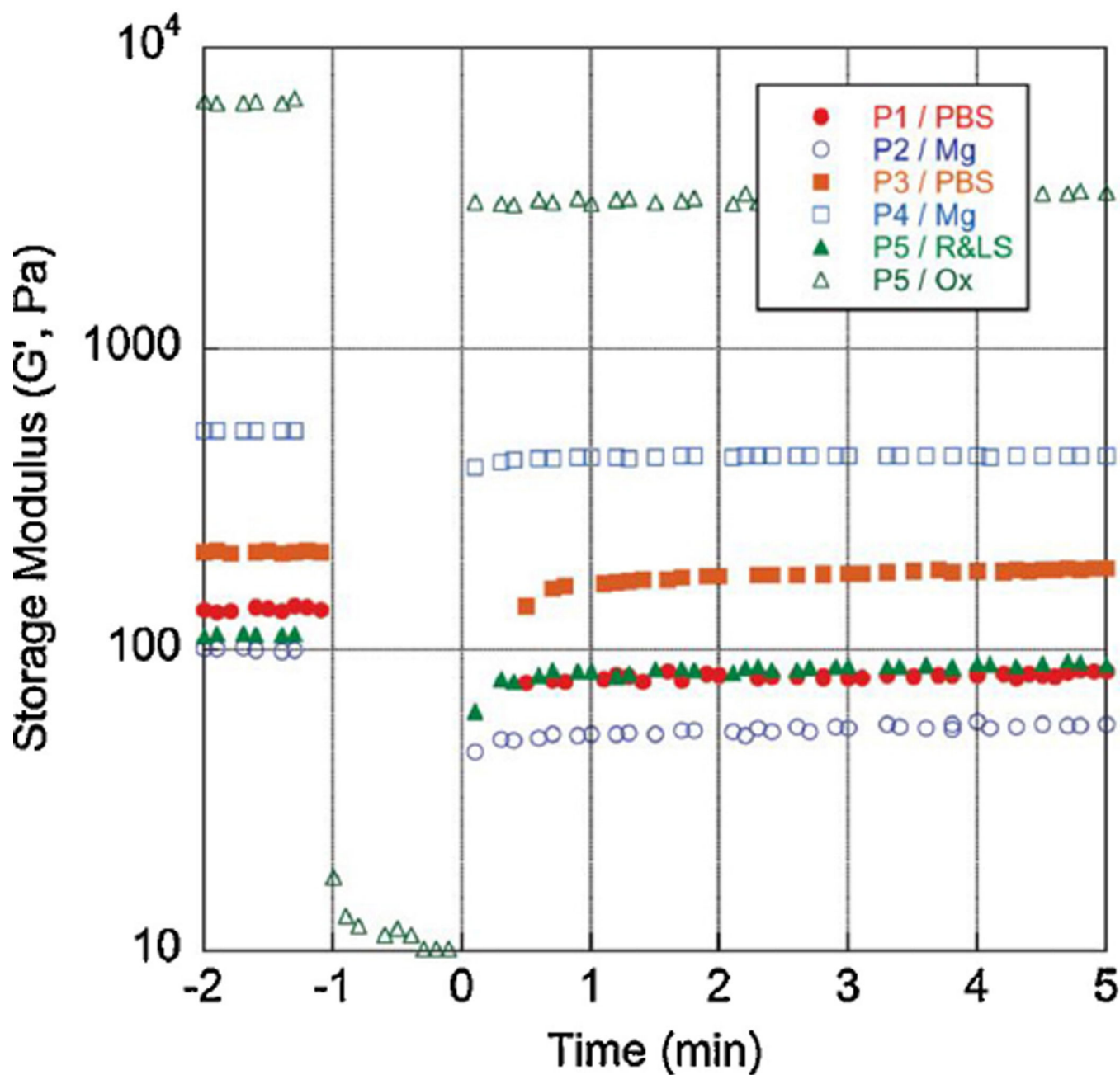
Fig. 30.
Shear-thinning behavior of MDP hydrogels self-assembled in various ionic solutions. Shear
is applied at $t = -1$ and released at $t = 0$. G' is measured as a function of time and as a
response to applied shear.
Reprinted with permission from Aulisa et al. [395].
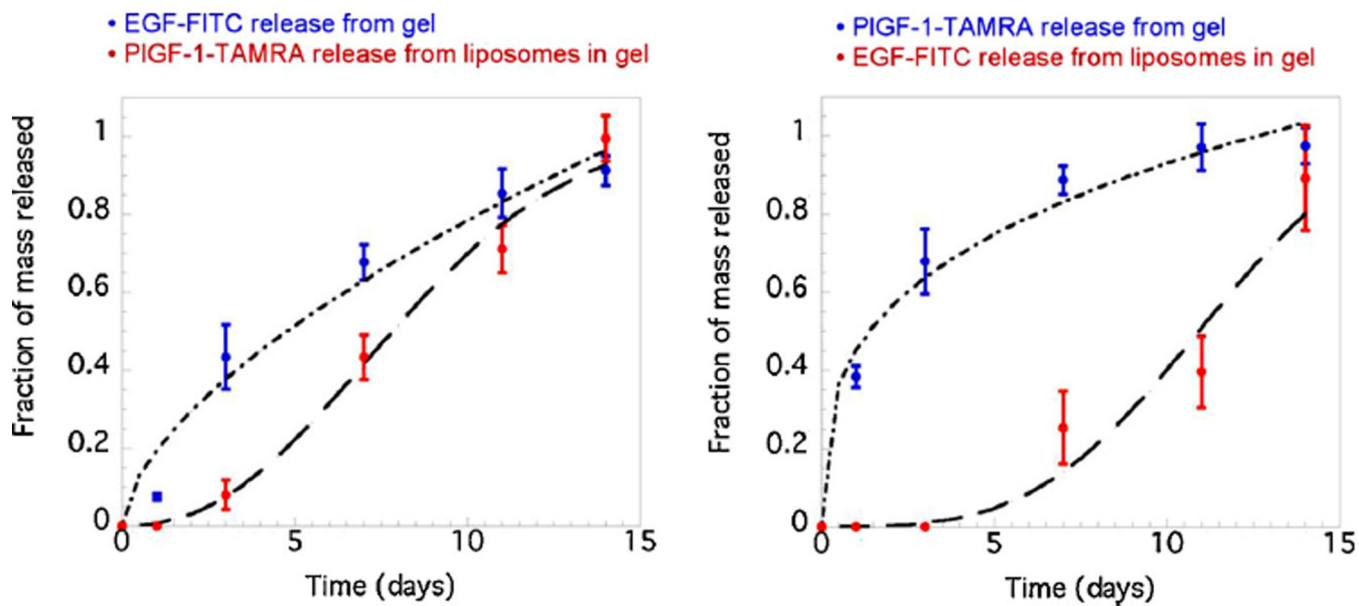
Fig. 31.
Bimodal release of EGF-FITC and PlGF-1-TAMRA from hydrogel alone (blue) or liposome (red). Both drugs show ~100% release over a 15 day period. However, the drug from the hydrogel alone is released much more rapidly, *i.e.* burst release, than the drug that had been encapsulated within the liposome. These systems exhibit temporal control over drug release. (For interpretation of the references to color in this figure legend, the reader is referred to the web version of the article.)

Reprinted with permission from Wickremasinghe et al. [483].
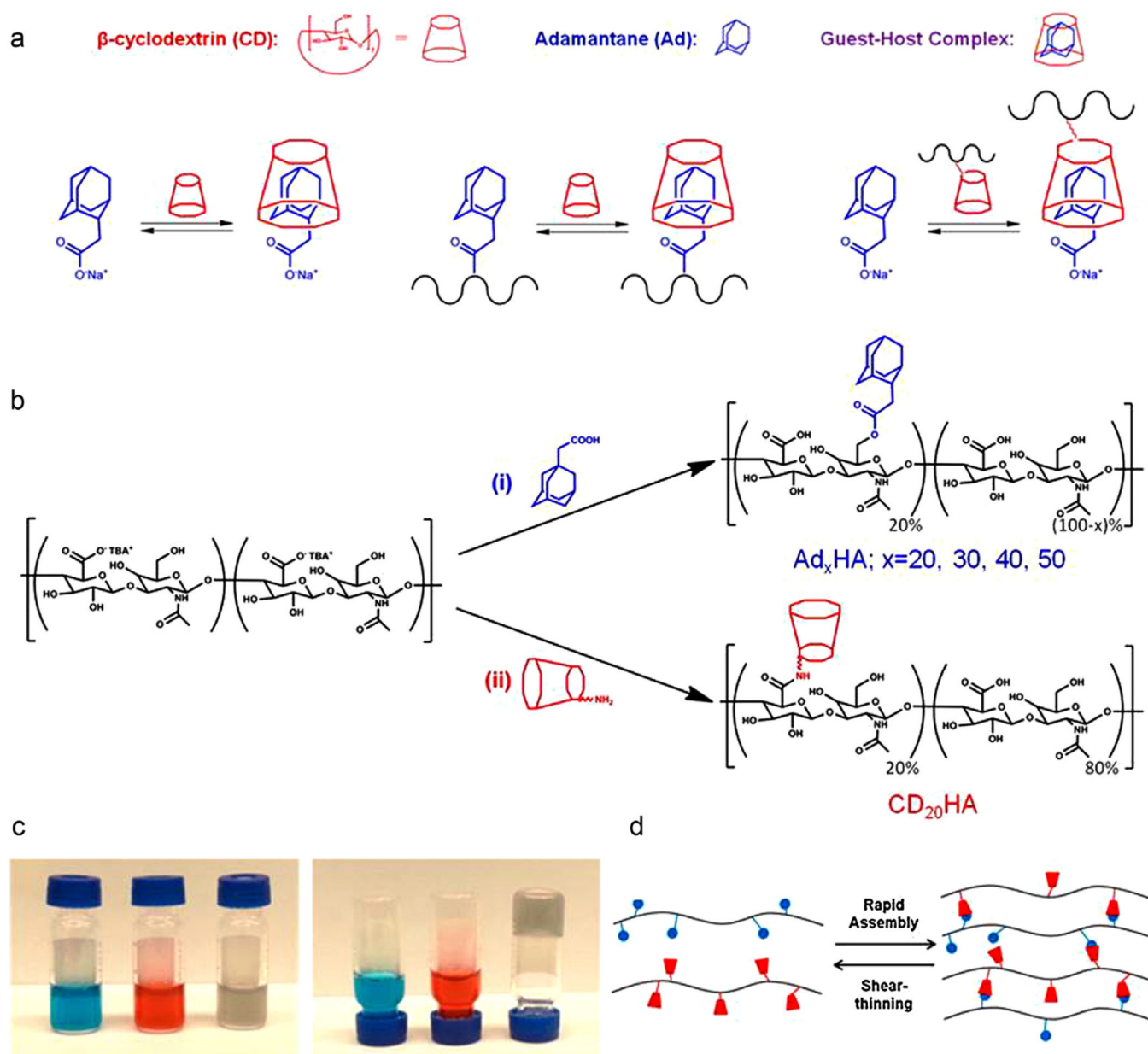
Fig. 32.
(a) Schematic of CD, Ad and the guest host complex, either when alone or when Cd or Ad
are joined to HA. (b) Synthesis of Ad-HA and CD-HA. (c) Inversion test to observe gelation
between Ad-HA and CD-HA. (d) Schematic of guest–host interactions forming reversible
physical crosslinks.
Reprinted with permission from Chen and Jiang [501].
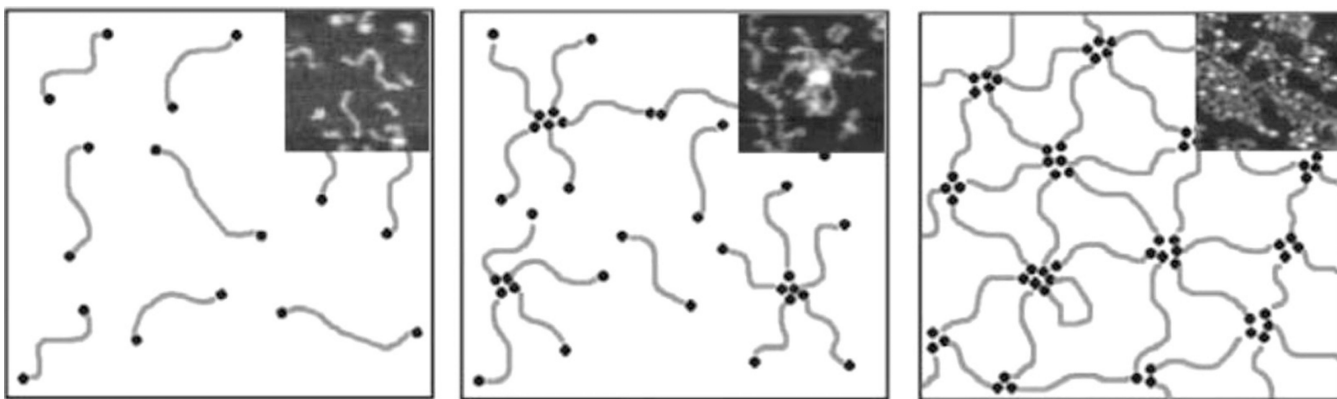
Fig. 33.
The concentration-dependent formation of a network of the cationic telechelic polymer, MMA-DMAEMA-MMA in a salt-free environment. Concentration of polymer increases from left to right.
Reprinted with permission from Bossard et al. [518].

Table 1

Locations within the body that exhibit a dynamic pH range during normal function or as a response to a disease state.

Location	pH
Blood	7.34–7.45
Stomach	1.0–3.0
Upper small intestine	4.8–8.2
Colon	7.0–7.5
Tumor, extracellular	7.2–6.5
Early endosome	6.0–6.5
Late endosome	4.5–5.0
Vagina	3.8–4.5
Inflamed tissue/wound	5.4–7.4

Adapted from Schmaljohann [51].
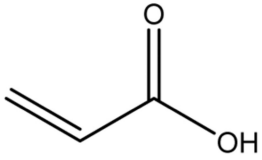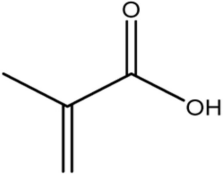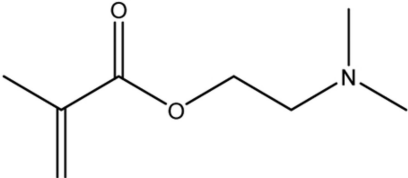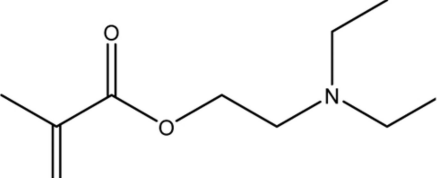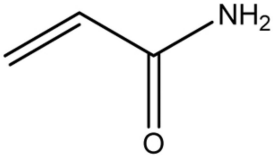
Table 2

Structures of common anionic and cationic pH-responsive monomers.

Table 3

Molar absorptivities (ε) for ortho-nitrobenzene linkers. Apparent rate constants of degradation (k_{app}, $\lambda = 365$ nm) for their fluorescein conjugates. Reprinted with permission from Griffin and Kasko [313]. Copyright 2012 American Chemical Society.

	I	II	III
$k_{app}/I_0 \times 10^4$ (cm²/mW·s)	76.3	9.76	1.47
ε_{365nm} (M⁻¹ cm⁻¹)	2500 ± 93	150 ± 3.6	3400 ± 170
ε_{405nm} (M⁻¹ cm⁻¹)	161 ± 6.0	4.7 ± 0.26	730 ± 42
ε_{436nm} (M⁻¹ cm⁻¹)	2.7 ± 2.1	0.35 ± 0.21	56 ± 3.8
τ_{365nm} (min); $I_0 = 5.53$ mW/cm²	0.395	3.09	20.5
τ_{405nm} (min); $I_0 = 5.53$ mW/cm²	1.58	25.5	24.7
τ_{436nm} (min); $I_0 = 5.53$ mW/cm²	45.3	164	154